Suberin biosynthesis in *O. sativa*: characterisation of a cytochrome P450 monooxygenase

Dissertation

zur

Erlangung des Doktorgrades (Dr. rer. nat.)

der

Mathematisch-Naturwissenschaftlichen Fakultät

der

Rheinischen Friedrich-Wilhelms-Universität Bonn

vorgelegt von

Friedrich Felix Maria Waßmann

aus

Berlin

Bonn, April 2014

Angefertigt mit Genehmigung der Mathematisch-Naturwissenschaftlichen Fakultät der Rheinischen Friedrich-Wilhelms-Universität Bonn.

1. Gutachter: Prof. Dr. Lukas Schreiber
2. Gutachter: Dr. Rochus Franke

Tag der Promotion: 28.07.2014

Erscheinungsjahr: 2015

Contents

List of abbreviations

Physical variables and derived dimensions are abbreviated according to the International System of Units (SI).

Chemical elements will be referred to as their symbols and compounds are abbreviated with their chemical formula. A simplified nomenclature based on lipid numbers will be used for aliphatic compounds, e.g. the monounsaturated omega-9 fatty acid containing 18 carbon atoms, oleic acid (trivial) or (9Z)-Octadec-9-enoic acid (IUPAC) with the formula $C_{18}H_{34}O_2$ will be referred to as C18:1 fatty acid or monocarboxylic acid C18:1, whereas the number for double bonds will be omitted if redundant.

aa	amino acids
ABC-transporter	ATP-binding cassette transporter
ABA	abscisic acid
approx.	approximately
att	flanking recombination sequences (attB, -P, -L, -R)
bp	base pair
BSTFA	bis(trimethylsilyl)trifluoroacetamide
ccdB	control of cell death, lethal DNA gyrase inhibitor
cDNA	complementary DNA
CDS	coding sequence
CI	confidence interval
CoA	coenzyme A
cv.	cultivar
CYP	cytochrome P450 enzyme
d	day
dai	days after imbibition
demin	demineralised
DEPC	diethylpyrocarbonate
DNA	deoxyribonucleic acid

DNase	deoxyribonuclease
dw	dry weight
EDTA	ethylenediaminetetraacetic acid
e.g.	for example (*exempli gratia*)
EMS	ethyl methanesulfonate
EtBr	ethidium bromide
ER	endoplasmic reticulum
FAE	fatty acid elongation
FAME	fatty acid methyl ester
FID	flame ionisation detector
GC	gas chromatography
G3P	glycerol-3-phosphate
GPAT	glycerol-3-phosphate acyltransferase
i.e.	that is (*id est*)
min	minute
MS	mass spectrometry
MS medium	Murashige and Skoog medium
no.	number
OPR	outer part of the root
mOsm	milliosmole
KCS	β-ketoacyl-CoA synthase
KO	knockout (of a gene)
HPLC	high-performance liquid chromatography, here for analytical grade
PAM	pulse-amplitude modulation (fluorometer)
PCR	polymerase chain reaction
PS II	photo system II
PTFE	polytetrafluoroethylene
RNA	ribonucleic acid
RNAi	RNA interference, approach for gene silencing
RNase	ribonuclease
ROL	radial oxygen loss
rpm	revolutions per minute
RT	reverse transcription
SD	standard deviation
SE	standard error

SRS	substrate recognition site
T_a	annealing temperature
T_m	melting temperature
TAE	buffer composed of Tris base, acetic acid and EDTA
TMS	trimethylsilyl ester
var.	variety
VLCFA	very long chain fatty acid ($\geq$ C22)
v/v	volume per volume
w/v	weight per volume
WT	wild type (regarding a specific allele)
Y II	photochemical quantum yield of PS II

1 Introduction

An organism is defined to be *alive* when it features certain characteristics: It has to have the ability to reproduce itself, a metabolism to absorb and convert energy from the environment and to build its own components, it has to be discrete from its surrounding media, and maintain its homoeostasis. The smallest natural units fulfilling these definitions are single cells which are separated from the outside environment by a membrane, consisting mainly of amphiphilic lipids and proteins.

The most abundant component of probably all life forms on earth is water. Since it is not only the essential solvent for nutrients and cell constituents but also involved in a great portion of chemical reactions, maintaining the water content is vital. Organisms of most taxonomic kingdoms form a cell wall surrounding the cell, which increases resistance against mechanical stress, while also supporting the water and ion and via these the pressure homoeostasis, a process which can become a high proportion of the cell's energy consumption, even in aquatic life forms.

1.1 Adaptations of the apoplast to terrestrial life

The colonisation of terrestrial habitats by plants, starting about 480 million years ago (Kenrick and Crane, 1997), required substantial adaptations of the outermost cell layers to the aerial environment, which is characterised by a strong negative water potential. The needs of light capturing and at the same time protection against radiation, of water and nutrient uptake as well as prevention of dehydration without loss of gas exchange, increased selection pressure and led to the evolution of tissues and organs of distinct functionality.

Nearly all multi-cellular organisms are separated from the environment by an outermost layer of tightly connected cells, the epidermis. Peptide polymers, such as keratin in the skin cells of mammals, birds and reptiles, or polysaccharides like chitin, forming the exoskeleton of arthropods in combination with proteins or minerals, or the cell wall of fungi together with glucans, provide mechanical strength. These polymers in combination with solvent extractable lipids also protect living organisms against uncontrolled water

loss and cell damage by radiation.

All above-ground organs of plants in the primary developmental state are equipped with an epidermis which is covered by a lipophilic incrustation of 0.1–10 µm thickness. This cuticle is comprised of waxes, mainly aliphatic with lesser amounts of aromatic components, embedded and deposited atop a polyester matrix, composed of aliphatic compounds and glycerol (Nawrath et al., 2013).

1.1.1 Aromatic and aliphatic polymers in vascular plants

The distribution of nutrients and metabolites depends on concentration gradients and diffusion, which restricts the size of lower plants. The appearance of bigger multicellular organisms required the development of vascular tissues, and along with cell differentiation to organisms of higher complexity, borders of structures and compartments evolved to barriers for solvents and solutes.

The incorporation of lignin into cell walls not only enables terrestrial plants to grow upright, under water facilitated by buoyancy, it also supports vascular tissues to cope with the tremendous tensions build up by the transpiration driven transport of water from ground to the apex. The structural macromolecule lignin is a racemic aromatic heteropolymer of the phenylpropanoids *p*-coumaryl alcohol, coniferyl alcohol, and sinapyl alcohol (monolignols) (Boerjan et al., 2003). It stabilises cell walls in the secondary developmental state and is found specifically localised in Casparian bands. These tight connections between endodermal cells in their radial and transverse cell walls strongly reduce apoplastic transport between cortex and stele. Even though another lipophilic polymer, suberin, was found in isolated Casparian bands of different species (Schreiber et al., 1999), it has been discussed recently that the herbaceous model plant *Arabidopsis thaliana* could only build up lignin during formation of these endodermal cell wall modifications (Naseer et al., 2012). One might suggest that a polymer accumulation in the endodermal cell wall, mainly composed of aromatic components (Schreiber, 1996), mediates or facilitates a connection between the plasma membranes of the endodermal cells in early Casparian strip formation across the dense radial cell wall, and later on, mainly aliphatic suberin is embedded to seal the thickening apoplastic domain.

Another internal suberin accumulation was found in the walls of bundle sheath cells of C_4 plants (Hattersley and Browning, 1981) such as *Zea mays*, limiting diffusion of CO_2 and O_2 and thereby reducing photorespiration by keeping local concentrations high and low, respectively. Suberin or suberin-like polyesters occur on all sites to be sealed against water loss and pathogen infiltration, either wound induced or on abscission sites (Franke et al.,

2009). More commonly known are suberin depositions of up to 50 % in the periderm on aerial plant surfaces during secondary and tertiary developmental stages, especially the phellem, or cork, of the tree *Quercus suber* (Pereira, 1988). Differential expression studies helped to identify enzyme classes and regulatory genes involved in the suberin biosynthsis (Soler et al., 2007). Also, periderms of tubers can be suberised, such as the surface of potato (Kolattukudy and Agrawal, 1974). Due to relatively high amounts of approx. 25 % suberin in the tuber periderm, the crop plant *Solanum tuberosum* is used as a model organism for suberisation (Graça and Pereira, 2000; Serra et al., 2009).

The sealing properties of the lipophilic suberin are known and widely used for a long time, e.g. as cork stoppers for gases and liquids. Additionally, the biosynthesis of suberin is induced by pathogens and it provides a penetration barrier for microbes (Thomas et al., 2007). Even though some wood degrading fungi are capable to decompose suberised tissues and can be cultivated on the polymer (Kolattukudy, 2002), suberin is highly persistent against bio-degradation and can outlast lignified wood by far.

1.2 Structures of the root apoplast

Driven by the pressure of requirements, the root as a designated below ground organ of higher plants evolved to a structure quite different from the shoot derived aerial leaves and stems as well as their subsurface adaptations. Roots serve as anchor for the plant body in the substrate, which is the main storage for water and nutrients. By maximising their surface area with lateral roots and root hairs, they optimised the uptake of water and solutes. The development of internal structures and barriers helped to overcome uncontrolled water loss at drought, uptake of toxic amounts of solutes, oxygen deficiency in hypoxic substrates or pathogen infiltration. A schematic overview of the root structure of higher plants is depicted in figure 1.1 by means of a root cross section of *O. sativa*.

Roots of most plants can be divided into several tissues which are a rhizodermis forming the outermost cell layer, an optional exodermis and lignified sklerenchyma, the cortex and the endodermis surrounding the stele with the vascular bundles. The main uptake of water can be located to young root parts. In this primary developmental state the apoplastic water and solute flow is only limited by the above mentioned Casparian bands, in roots located in the radial and transverse cell walls of the endodermis as well as in the exodermis of some species (Nagahashi et al., 1974). At these border tissues the main water flow is forced along the cell-to-cell pathway (depicted as green arrows in figure 1.1), including both the symplastic and the transcellular (vacuolar) paths (Steudle and Peterson,

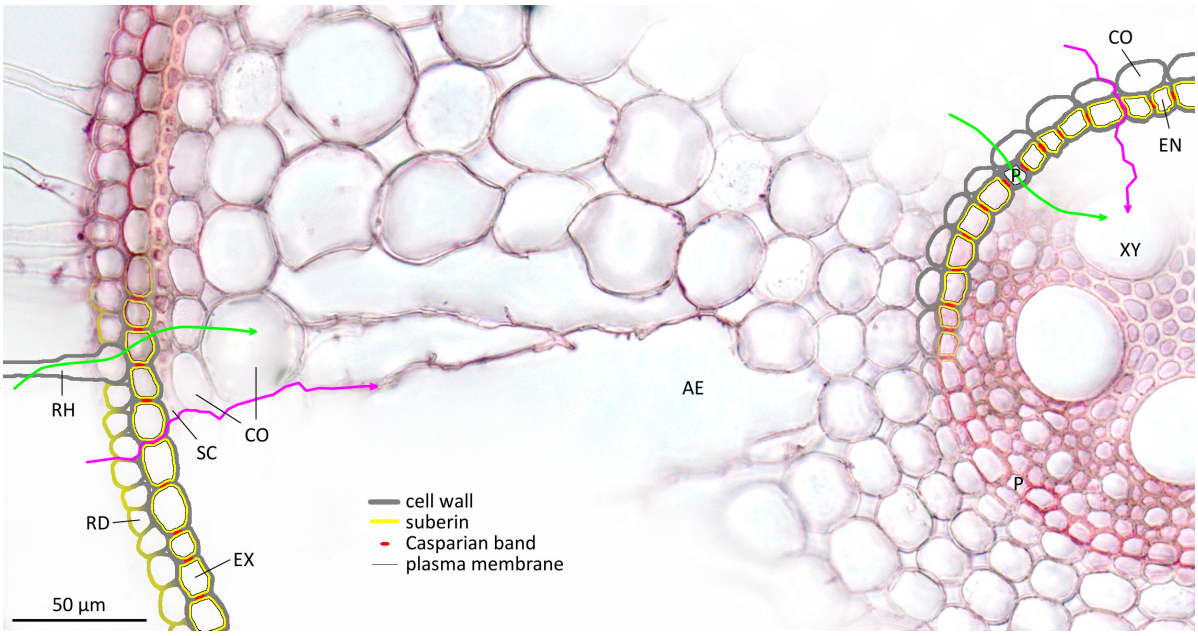

Figure 1.1: Schematic diagram of suberised cell walls in roots (adapted from Ranathunge et al. (2011b)) embedded in a microscopic picture of a free hand root cross section from *O. sativa* stained with Sudan red 7B. Water and solute pathways as proposed by Steudle and Peterson (1998) are depicted as arrows. The cell-to-cell pathway (green) includes both the symplastic and the transcellular path whereas the apoplastic pathway (pink) is restricted to cell walls and intercellular spaces. The outer part of the root comprises (radially towards the root center) root hairs (RH), the rhizodermis (RD) with diffusely suberised cell walls (yellowish), the exodermis (EX) with Casparian bands (red) in the primary developmental state and the suberin lamellae (yellow) in the secondary state, the lignified sclerenchyma (SC), and one cell layer of cortex cells (CO). The formation of aerenchyma (AE) by apoptosis of cortex cells supports the oxygen supply of the apical root. Passage cells (P) in the endodermis (EN), which in contrast to the other cells of this layer do not develop suberin lamellae, facilitate uptake of water and solutes into the central cylinder and finally into xylem vessels (XY).

1998). To enter the cell, water and solutes, such as nutrient ions as well as dissolved other compounds, have to cross the plasma membrane, which enables a selectively limited uptake into the stele.

In the secondary state the suberin lamella is deposited on the inner side of endodermal and exodermal cell walls (Schreiber and Franke, 2011). This restricts the cell-to-cell pathway to a few passage cells in the endodermis, whose cell walls remain unmodified.

Another and even more important function of those apoplastic barriers in roots is the limitation of backflow of water and ions from the stele to the cortex or even soil (Enstone et al., 2003). Since the apoplastic pathway is not selective for water and solutes (low reflection coefficient), only its restriction allows an accumulation of ions in the vascular system and an increased root pressure, facilitated by the negative osmotic water potential. In times of low transpiration rates a positive hydraulic water potential is essential to supply above-ground organs with water. However, with increasing transpiration a negative hydraulic water potential in the photosynthetically active organs will additionally drive water transport, up to the point of solvent drag (Ranathunge, 2005). The main barrier function of suberised tissues is generally attributed to the aliphatic suberin, caused by its high hydrophobicity (Zimmermann et al., 2000; Hose et al., 2001).

In well ventilated soils root tissues receive oxygen for respiration via diffusion in the gas phase. Since the diffusion of gases in the aqueous phase is approx. ten thousand times slower than in air, dissolved oxygen in waterlogged soils can be consumed within hours by micro organisms and plant cells of the rhizosphere (Drew and Lynch, 1980). The formation of aerenchyma by programmed cell death in the root cortex, either as scheduled by the general root morphology development or induced by stagnant growth conditions, is well described (Nishiuchi et al., 2012; Yamauchi et al., 2013). The formation of an effective barrier which reduces radial oxygen loss (ROL) in roots is experimentally proven (Colmer, 2003); though its exact composition is still discussed (Shiono et al., 2011), there is evidence that the barrier properties are facilitated by aliphatic rather than aromatic suberin and ligning (Kotula et al., 2009; Watanabe et al., 2013).

1.3 The lipid polyester suberin

To examine the monomer composition of suberin, chemical transesterification of the polymer is inevitable. Subsequently, the single molecules can be analysed via chromatographic methods like high-performance liquid chromatography (HPLC) and gas chromatography (GC) supported by mass spectrometry (MS) for identification. The non-saponifiable residue

is referred to as suberan, which consists of supposedly crystalline fatty acid derivatives of chain lengths up to C22 that represent approx. 10 % of the mass of *Betula nigra* bark (Turner et al., 2013), to name but one example.

The suberin monomers extracted after methanolysis consist of species dependent proportions of glycerol (3.8 % of the dry mass of cork from *Q. suber* (Pereira, 2013) or 14 % and 22 % of the suberin monomer extracts from *Q. suber* and *S. tuberosum*, respectively (Graça and Santos, 2007)), the hydroxycinnamic acids *p*-coumaric acid and ferulic acid (from 5 % in *A. thaliana* (Franke et al., 2005) to 60–70 % in *Oryza sativa* (Ranathunge et al., 2011a)), and aliphatic compounds of chain lengths from C16 to C32. The latter are mainly ω-hydroxy acids, α,ω-dicarboxylic acids (-diacids) and lesser amounts of monocarboxylic acids and primary alcohols. Some species additionally incorporate mid-chain unsaturated, hydroxylated or oxygenated suberin monomers (Bernards, 2002), which are more typical for cutin (Franke et al., 2005). The composition of the different fatty acid derivatives and the distribution of their carbon chain length are species dependent.

Due to the depolymerising treatment, limited information is available about the linkage of suberin monomers within the polyester and to cell wall carbohydrates. However, non-destructive techniques like Fourier transform infrared spectroscopy and nuclear magnetic resonance spectroscopy in particular revealed the binding of aromatics to cell wall carbohydrates as well as to polyaliphatics (Bernards, 2002). After partial hydrolysis linear acylesters, acylglycerols and feruloyl esters have been identified as components of suberin (Graça and Santos, 2007). Together with alternating layers of different density in transmission electron micrographs of tuber periderm from *S. tuberosum*, these findings led to the model of distinct domains of aliphatic and aromatic suberin (Bernards, 2002). However, this model is based on a predominant proportion of bi-functional aliphatic compounds. A three dimensional polyester built from the described aliphatics requires interconnections via esterified glycerol or hydroxycinnamates.

1.3.1 Suberin biosynthetic pathways

Despite different approaches from chemical analysis and biochemical studies (reviewed three decades ago by Kolattukudy (1981)) to reverse genetics (recently reviewed by Ranathunge et al. (2011b), Beisson et al. (2012) and Molina and Franke (2013)) on various models like the bark of *Q. suber*, the tuber periderm of *S. tuberosum*, green cotton fibres, as well as root endodermal tissue of *A. thaliana*, *Clivia miniata*, *Zea mays* and others, there are still gaps in the understanding of suberin biosynthesis. To synthesise the suberin monomers identified by chemical analysis, certain enzyme classes were postulated

and several corresponding genes could be characterised so far. Nevertheless, questions of specific substrates for these enzymes, transport of monomers within and out of the cell and assembly of suberin building blocks are still unanswered.

Even though the sequential order of enzymatic steps is still unclear, the suberin biosynthesis models for aliphatic suberin (see figure 1.2 or for a highly detailed model see aralip.plantbiology.msu.edu) suggest an initial elongation of monomers in the fatty acid elongation (FAE) complex at the endoplasmic reticulum (ER). Therefore, either a C16 or C18 fatty acid from lipid synthesis in plastids, which has been activated with coenzyme A (CoA) by a long-chain acyl-CoA synthetase (LACS), or an already elongated acyl-CoA molecule is condensed with malonyl-CoA by a β-ketoacyl-CoA synthase (KCS) to β-ketoacyl-CoA, the reaction limiting step in FAE. After the following reduction to β-hydroxyacyl-CoA, dehydration to enoyl-CoA and a second reduction, the carbon chain of the initial acyl-CoA is elongated by two hydrocarbons (Haslam and Kunst, 2013). Subsequent modifications of the CoA-activated pool of very long chain fatty acids (VLCFA) and C16 and C18 fatty acids are expected to occur at the ER as well. Reduction by fatty acid reductases (FAR) leads to primary alcohols, desaturation to unsaturated fatty acids, and ω-hydroxylation produces the major aliphatic suberin monomers ω-hydroxy acids, which can be further oxidised in two steps to α,ω-diacids.

No direct evidence is provided so far, whether suberin precursors are exported as monomers or building blocks, e.g. of acyl-glycerols or ferulate esters. However, lipid transport proteins and ABC-transporters as well as exocytosis are hypothesised to be involved in the export from the cell to the site of suberin polymerisation (Molina and Franke, 2013). Regiospecificity of *sn*-2 glycerol-3-phosphate acyltransferases (GPAT) might be involved in assigning fatty acids and their derivatives to different lipid pathways by producing distinct classes of glycerol-3-phosphates (G3P) and acylglycerols, such as 2-acyl-G3P for suberin and *sn*-2 monoacylglycerols for cutin, in contrast to phosphatidic acid and 1-acyl-G3P for membrane and storage lipids (Yang et al., 2010; Li-Beisson, 2011). An aliphatic suberin feruloyl transferase (ASFT) was found to catalyse the formation of feruloyl esters from primary alcohols and ω-hydroxy acids (Molina et al., 2009).

In analogy to the cuticle synthesis, extracellular enzymes similar to GDSL-lipases (Yeats et al., 2012; Girard et al., 2012) and esterases (Kurdyukov et al., 2006) might be involved in the polyester formation of suberin and peroxidases are expected to initiate polymerisation of the supposed poly-phenolic domain (Bernards et al., 2004).

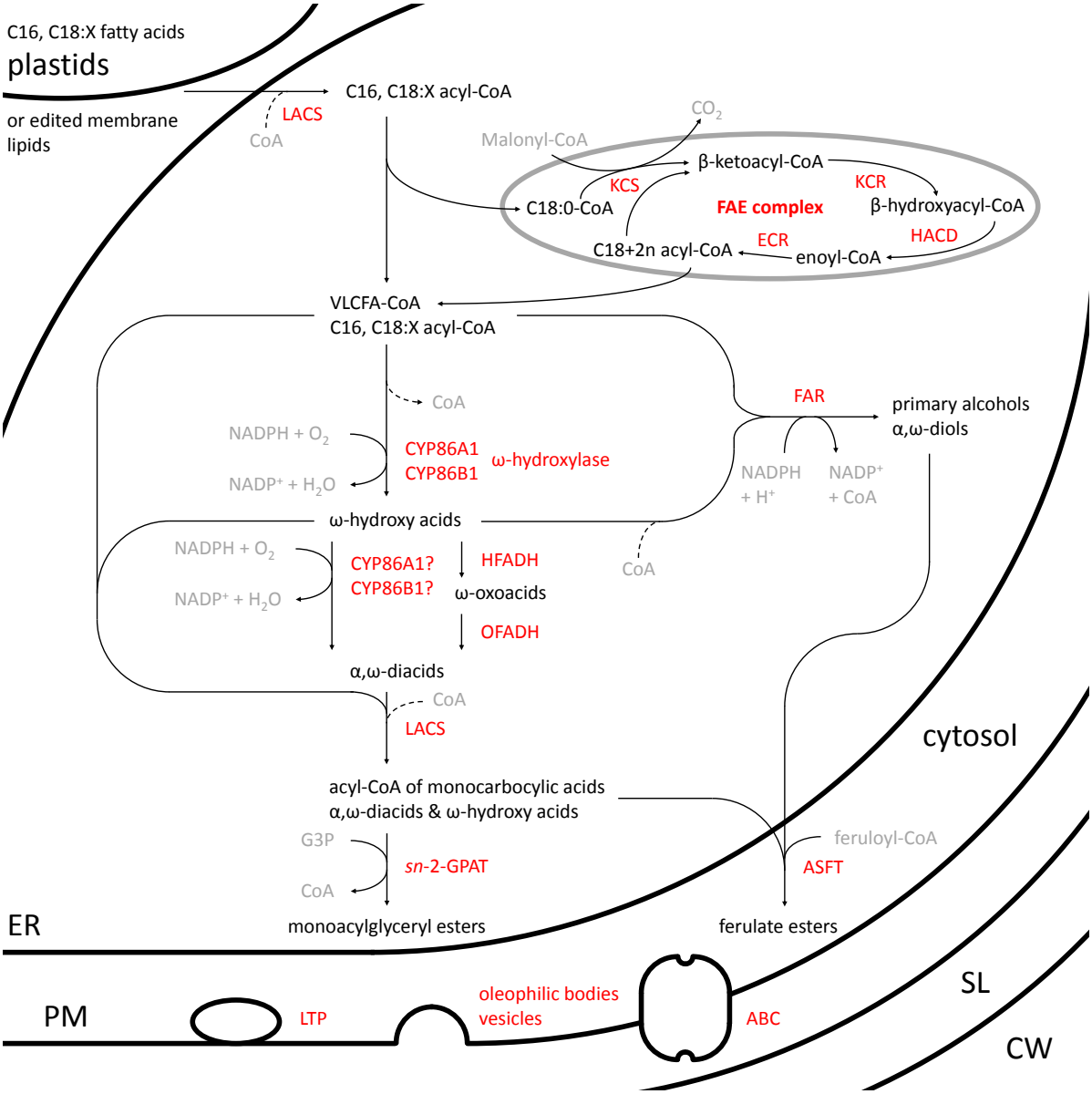

Figure 1.2: Synthesis model of aliphatic suberin monomers in a cell (not to scale), adapted from Molina and Franke (2013) and Pollard et al. (2008). With fatty acid: monocarboxylic acid; CoA: coenzyme A; LACS: long chain acyl-CoA synthase; KCS: β-ketoacyl-CoA synthase; KCR: β-ketoacyl-CoA reductase; HACD: hydroxyacyl-CoA dehydrase; ECR: enoyl-CoA reductase; VLCFA: very long chain fatty acid; FAR: alcohol-forming fatty acyl-CoA reductase; HFADH: ω-hydroxy fatty acyl dehydrogenase; OFADH: ω-oxo fatty acyl dehydrogenase; G3P: glycerol-3-phosphate; GPAT: glycerol-3-phosphate acyltransferase; ASFT: aliphatic suberin feruloyl transferase; LTP: lipid transport protein; ABC: ATP-binding cassette transporter; ER: endoplasmic reticulum; PM: plasma membrane; SL: suberin lamellae; CW: cell wall.

1.3.2 Cytochrome P450

ω-Hydroxylation of fatty acids in the cutin and suberin pathways is catalysed by cytochrome P450 enzymes (CYP). The monooxygenases obtain two electrons from NADPH or NADH and transfer them successively to molecular oxygen which is bound to the heme in the enzyme's catalytic center. This leads to activation and cleavage of the oxygen molecule of which one atom is subsequently inserted into the substrate, the other released as water:

$$\text{R–H} + \text{O}_2 + \text{NADPH} + \text{H}^+ \longrightarrow \text{R–OH} + \text{H}_2\text{O} + \text{NADP}^+ \text{ (Bak et al., 2011)}$$

The name of the enzyme family is derived from the high affinity to bind carbon monoxide, which leads to a shift of the absorption maximum of the pigment to 450 nm. The catalytic center of P450 enzymes in all kingdoms of life comprises a universal cysteine coordinating an iron in the heme iron center. The heme binding motif and tertiary structure of the protein are highly conserved in plants. Even so, the amino acid sequence identity of different CYP can be less than 20 % only in *A. thaliana*. Almost all P450 enzymes in plants are anchored with a single N-terminal transmembrane helix to the cytoplasmic side of the ER membrane and only a few are targeted to plastids (Schuler et al., 2006).

The activation of oxygen, which results in a high reactivity, in combination with the diverse but highly specific substrate recognition leads to a wide range of products formed by the members of one of the biggest enzyme families. Many enzymes hydroxylate their substrates but biochemical processes of P450 enzymes include "aromatic hydroxylations, epoxidations, dealkylations, isomerizations, dimerizations, dehydrations, carbon-carbon cleavages, decarboxylations, nitrogen and sulfur oxidations, dehalogenations and deaminations" (Schuler and Werck-Reichhart, 2003). With the functional diversity members of the group are involved in detoxification of xenobiotics, the synthesis of hormones, pigments, signalling molecules and defence compounds as well as of structural macromolecules such as lignin, cutin and suberin (Schuler et al., 2006; Bak et al., 2011). Especially the CYP86 clan comprises fatty acid ω-hydroxylases which are essential for the plants secondary metabolism contributing to hydrophobic polyesters. The first cytochrome P450 mutant with a phenotype in the polyester composition was *att1* (Xiao et al., 2004). The content of cutin covering the stems was reduced by up to 70 % in these EMS-mutagenised *A. thaliana* plants compared to WT, caused by a mutation in *CYP86A2*. Since then, a number of CYP has been characterised contributing to a better understanding of the biochemical pathways of lipid polyesters in plants.

CYP genes can be found in all phyla and almost all organisms and it is one of the largest gene families known. With about 1 % of all genes, e.g. 244 (and 28 pseudogenes) in the

dicotyledonous *A. thaliana* (Bak et al., 2011) and approx. 328 (and 99 pseudogenes) in the monocotyledonous *O. sativa* (Nelson et al., 2004), a notably high variety is present in higher plants. The appearance of the majority of CYP families in plants before the monocot-dicot divergence approx. 200 million years ago allows a direct comparison of P450 enzymes in both model species (Nelson et al., 2004).

1.4 Aims of this work

Apoplastic barriers in plants and suberin in particular have been studied for many years. Histology, physiology, chemical analysis and enzymatic studies contributed to the knowledge about the polymer, but the completed sequencing of the *A. thaliana* genome in 2000 opened the door to reverse genetic approaches and since then numerous genes of the suberin biosynthetic pathway have been described. *O. sativa* is a major crop plant which is a very important local and global nutrition source, facing a broad range of environmental stress factors on the one hand and a model organism for cereals and a valuable tool to investigate water and solute transport in relation to apoplastic barriers in roots on the other hand. However, the formation of those barriers in *O. sativa* is poorly understood and no genes involved in the suberin pathway are known today.

With the help of genome databases and *in silico* studies, suberin candidate genes in *O. sativa* are intended to be identified by sequence homology to *A. thaliana* orthologues which are known to be involved in suberin formation. Expression analysis should help to select genes which are specifically expressed in tissues undergoing suberisation or after treatments increasing suberin amounts, such as salt and osmotic stress. With the help of *O. sativa* mutant lines, involvement of these genes in suberin biosynthesis should be characterised in an reverse genetic approach by histochemical examination and chemical analysis of their possibly altered suberin phenotype. Furthermore, it is proposed to study water and solute relations and correlate physiological and chemical phenotypes of mutants under different growth conditions.

2 Materials and methods

2.1 Materials

2.1.1 Chemicals

All chemicals used in this work were of analytical reagent grade or higher quality and either purchased from Carl Roth (Karlsruhe), Merck (Darmstadt), Sigma-Aldrich (including Fluka and Supelco; Steinheim; St. Luis, USA) and VWR (Darmstadt) or are indicated with producer or supplier. Kits and materials for molecular biological applications were obtained from Life Technologies (including Invitrogen™; Carlsbad, USA), Macherey-Nagel (Düren, Germany) or PEQLAB (Erlangen, Germany). For all chemical analytical methods water of analytical grade was used, referred to as H_2O_{HPLC}, which was sterilised by autoclaving for all molecular biological applications. Media for microbiology, solutions and buffers were prepared with demineralised water, indicated as H_2O_{demin} in this work and for hydroponic cultures tap water of drinking water standards was used.

2.1.2 Media and solutions

Solutions for plant cultivation

Nutrient solution	90 µmol L^{-1} $(NH_4)_2SO_4$
for *O. sativa*	50 µmol L^{-1} KH_2PO_4
hydroponic culture	50 µmol L^{-1} KNO_3
(Miyamoto et al., 2001)	30 µmol L^{-1} K_2SO_4
	60 µmol L^{-1} $Ca(NO_3)_2$
	70 µmol L^{-1} $MgSO_4$
	110 µmol L^{-1} Fe-EDTA
	4.6 µmol L^{-1} H_3BO_3
	1.8 µmol L^{-1} $MnSO_4 \times H_2O$
	0.3 µmol L^{-1} $ZnSO_4 \times 7\ H_2O$
	0.3 µmol L^{-1} $CuSO_4 \times 5\ H_2O$
Seed sterilisation solution for	167 mL H_2O_{demin}
O. sativa	200 µL Triton X-100
	3.3 mL 12 % NaClO
Seed sterilisation solution for	10.5 mL H_2O_{demin}
A. thaliana	2 mL 12 % NaClO
	12.5 mL 100 % ethanol

Media for microbial cultures

LB medium	10 g L^{-1}	tryptone
for cultivation of *Escherichia coli*	5 g L^{-1}	yeast extract
and *Agrobacterium tumefaciens*	5 g L^{-1}	NaCl
	1 mL L^{-1}	NaOH 1 N
optional	1 % (w/v)	agar
		autoclave
SOB	20 g L^{-1}	tryptone
	5 g L^{-1}	yeast extract
	8.56 mmol L^{-1}	NaCl
	2.5 mmol L^{-1}	KCl
		pH 7
		autoclave
SOC		SOB
	0.01 mmol L^{-1}	$MgCl_2$
		autoclave
	0.02 mmol L^{-1}	glucose, sterile

Solutions for molecular biological applications

6×gel loading buffer	40 % (w/v)	sucrose
	0.125 %	bromophenol blue
	in	H_2O_{HPLC} sterile
agarose gel	1 g	agarose
	100 mL	TAE buffer
	approx. 0.05 %	ethidium bromide
DEPC treated water	0.1 % (v/v)	diethyl bicarbonate
		H_2O_{HPLC}
	2 h	37 °C
		autoclave
50×TAE buffer	242 g L^{-1}	Tris base
	57.1 mL L^{-1}	acetic acid
	0.05 mol L^{-1}	EDTA pH 8

Solutions for stainings and microscopic sample preparation

Fluorol yellow dye	0.01 % Fluorol yellow 088 × mL PEG 400 1 h 90 °C × mL glycerol 90 %
Sudan red dye	0.1 % Sudan red 7B × mL PEG 400 1 h 90 °C × mL glycerol 90 %
Mounting medium	75 % glycerol

Solutions for gas chromatography sample preparation

Enzyme solution for cell wall digestion	2 % (v/v)	cellulase (Novozym 476, Novozymes, Bagsværd, Denmark)
	2 % (v/v)	pectinase (Pectinex 3x, Novozymes, Bagsværd, Denmark)
	10 mmol L^{-1}	citric acid monohydrate
	1 mmol L^{-1}	NaN_3
		H_2O_{demin}
	pH 3	KOH, HCl
Solvents for lipid extraction	50 %	chloroform
	50 %	methanol

2.1.3 Software

MS spectra were interpreted using HP Enhanced Chemstation (Ver. A.03.00, Hewlett Packard, now Agilent Technologies, Santa Clara, USA) and chromatograms from FID analysis were evaluated with GC ChemStation (Rev.B.03.01-SR1, Agilent Technologies, Santa Clara, USA).

For processing of digital still images from scanner, camera and microscope, the GNU Image Manipulation Program (GIMP, open source, available at gimp.org) was used. ImageJ (public domain, available at ImageJ.net) analysis was applied to determine surface areas of plant organs from still images and scans, or colour saturation and size of bands in gel pictures to interpolate nucleic acid abundance. Microsoft Office 2007 professional

(Microsoft Corporation, Redmond, USA) was the basis for all data processing including spreadsheet analysis, statistical analysis and presentation unless otherwise stated. This work was written and edited with the LaTeX editor Texmaker 4.0.4 (open source, available at xm1math.net/texmaker) and the TeX distribution MikTex 2.9 (open source, available at miktex.org).

2.1.4 *In silico* tools and databases

Based on *A. thaliana* protein sequences of enzymes interfering with suberisation of root tissues obtained from arabidopsis.org, BLAST analyses (Altschul et al., 1990) of different databases featuring nucleotide and amino acid sequences of *O. sativa* have been conducted. In this way putative orthologue suberin candidate genes were collected mainly via the Rice Genome Annotation Project BLAST Search provided by the Michigan State University (MSU), available from rice.tigr.org (Ouyang et al., 2007). Since common resources for gene annotations refer to different standards in labelling, the gene ID Converter of the Rice Annotation Project Database (RAP-DB) under rapdb.dna.affrc.go.jp was used to translate gene loci numbers.

Availability of rice mutant lines was assessed via the Rice Functional Genomic Express Database accessible under signal.salk.edu/cgi-bin/RiceGE, the Rice Tos17 Insertion Mutant Database at tos.nias.affrc.go.jp and the aforementioned RAP-DB.

The software Geneious version 6.1.6 (Biomatters, Auckland, NZ. Available from geneious.com) was used for bioinformatic tasks such as sequence comparison, *in silico* cloning and primer design, visualisation and managing of sequences.

Sequence alignments and phylogenetic trees were generated with the software MEGA5 (Tamura et al., 2011) and with the help of the algorithms CLUSTAL and MUSCLE (Larkin et al., 2007; Edgar, 2004) as part of the software Geneious. To investigate and visualise common motifs and highly conserved domains in closely related proteins MEME (Multiple Expectation Maximisation for Motif Elicitation) (Bailey and Elkan, 1994) was used, a web tool which is accessible via meme.nbcr.net.

Tissue specific transcript abundance of suberin candidate genes as detected by microarray analyses was examined via the web tools Genevestigator (Hruz et al., 2008) and the Rice Oligonucleotide Array Database (Cao et al., 2012). To compare expression levels of multiple genes in different tissues, visualisation in form of a heat map was chosen, which was based on a colour range indicating relative expression potential as provided by Genevestigator. For direct comparison with RT-PCR results (method described in chapter 2.3.3) relative expression values of selected genes for different tissues were extracted

from Genevestigator and presented as Excel graphs. The web tool RiceFREND (Sato et al., 2013), available at ricefrend.dna.affrc.go.jp, was used to search for genes co-expressed with LOC_Os10g34480 based on microarray data.

2.2 Plants

2.2.1 Genotypes

All analyses presented in this work were carried out with plants either of the genetic background of *O. sativa* var. japonica cv. Dongjin or *A. thaliana* ecotype Columbia (Col-0 and Col-8). *O. sativa* T-DNA insertion mutants (Jeon et al., 2000) were kindly provided by Gynheung An from the Plant Functional Genomics (PFG) Institute at POSTECH University, Pohang, Korea. Three *O. sativa* lines with mutations in *CYP86B3* were propagated and examined in the course of this work. A map of the insertion locations is depicted in figure 3.5.

- PFG_4A-02646.L, carrying a T-DNA insertion in the intron of LOC_Os10g34480, generated with the help of the vector pGA2715 (Jeong et al., 2002), here referred to as *cyp86b3-1*.
- PFG_1B-19308.L with an insertion only 349 bp upstream of PFG_4A-02646, generated with the vector pGA2717 and in the following named *cyp86b3-2*.
- PFG_2B-30065.R with an insertion 950 bp upstream of the start codon of *CYP86B3*, generated with the vector pGA2707, here referred to as *cyp86b3-3*.

Homozygous seeds of the *A. thaliana* mutants and WT were propagated and kindly provided by Daniela Nosbüsch from the work group Ecophysiology, University of Bonn, Germany. The WT Col-8 served as control.

- SM.37066, a transposon insertion line from the John Innes Centre Sylvestre Marillonnet Line Collection (Department of Molecular Genetics, Norwich, England), was characterised by Diehl (2008). The mutant with defective At5g23190 was described as *cyp86b1-1* or *ralph-1* (Compagnon et al., 2009).
- By crossing of the preceding mutant with the T-DNA insertion line SALK_107454 from the Nottingham Arabidopsis Stock Centre (NASC, Nottingham, England), which is mutated in At5g58860 and was described as *cyp86A1-1* or *horst-1* (Höfer et al., 2008), the double knockout (KO) line *ralph*/*horst* was generated by Diehl (2011).

Both lines served as background for heterologous complementation with *CYP86B3* from *O. sativa* as conducted and summarised in this work.

2.2.2 Cultivation and propagation of *O. sativa*

Seeds of *O. sativa* were incubated on paper tissue soaked with tap water in Petri dishes for up to 10 d. Seeds were sterilised before imbibition in case of fungal infestation. Therefore husks were removed, seeds were rinsed with 70 % ethanol and subsequently with tap water to wet surfaces. Afterwards, seeds were incubated in sterilisation solution (see chapter 2.1.2) on a rotary shaker for maximal 30 min and with subsequent thoroughly fivefold washing with water.

Cultivation in hydroponics

After germination seedlings with a shoot length of at least 1 cm were mounted with polyurethane sponge in holes of approx. 1 cm in diameter in plastic lids covering non-transparent containers with 26.5 L of hydroponic solution for rice (see chapter 2.1.2). 11 days after imbibition (dai) the medium was continuously flushed with air for proper oxygenation and exchanged weekly. Cultivation took place under short day conditions with a 12/12 h day/night cycle with 25/21 °C, a relative humidity of 57/75 % and a photon flux of 130/0 μmol m^{-2} s^{-1}. Alternatively, 3–5 dai very small seedlings were transferred to a mesh with a mesh size of about 1.5 mm, which was floating on hydroponic solution for rice (see chapter 2.1.2). Later on, plants were transferred from the mesh to bigger containers as described above.

Cultivation on soil

For propagation of *O. sativa*, plants which were characterised to be homozygous respective the annotated mutation were transferred to waterlogged soil in a mixture of approx. 5:2:1.5 C-horizon/sand/humus from a local site and cultivated in greenhouses under light intensities in excess of the cultivation conditions of the growth chambers.

2.2.3 Cultivation and propagation of *A. thaliana*

Cultivation on soil

For propagation and floral-dip transformation *A. thaliana* was cultivated on soil in batches of up to 15 pots on trays for irrigation. Therefore, pots with an edge length of 10 cm

were filled with potting soil (Floradur, Floragard, Oldenburg, Germany) and soaked with tap water containing mineral fertiliser (Flory 3 Verde, Planta, Regenstauf, Germany) and insecticide (Confidor WG70; Imidacloprid; Bayer CorpScience, Langenfeld, Germany) in concentrations recommended by the manufacturer. Seeds were kept in tap water for imbibition at 4 °C in the dark for 2 d. Afterwards, either five times 2–5 seeds were sown per pot and thinned out after germination or in a dense coverage for the purpose of floral-dip transformation. Trays were covered with transparent lids to facilitate high humidity for 10 d. The growth chamber was maintained at long day conditions with a 18/6 h day/night cycle with 22/20 °C, a relative humidity of 60 % and a photon flux of 100/0 $\mu mol\,m^{-2}\,s^{-1}$ at the level of rosette leaves. To synchronise emergence and to increase the number of flowers, inflorescence stems of all plants of a batch were cut depending on the intended use. In case of fungal infections plants cultivated in the growth chamber were irrigated with water containing 2.5 $mL\,L^{-1}$ of Proplant (722 $g\,L^{-1}$ Propamocarb-Hydrochlorid, Profiline, Stähler, Stade, Germany).

Cultivation in hydroponics

For root suberin analysis *A. thaliana* was grown in hydroponic culture. Therefore, the commercial Araponics system (Araponics SA, Liège, Belgium) was used with the included Floraseries nutrient solution stocks FloraGro, FloraMicro and FloraBloom according to the manufacturer's instructions for *A. thaliana*. Cultivation took place under the same growth conditions as described for cultivation on soil.

Cultivation on axenic medium

A. thaliana was cultivated on axenic plates to select positive transformants which contained the hygromycin resistance gene. Therefore, seeds were submerged in 500 µL sterilisation solution (see chapter 2.1.2) and incubated in 2 mL Eppendorf caps for 10 min with gentle shaking. The sterilisation solution was subsequently decanted and the seeds were quickly washed three times with denatured ethanol. The remaining ethanol was immediately removed with a pipette and seeds were dried in the caps for a minimum of 2 h on the clean bench. Sterile seeds were stored in closed caps at 4 °C until used.

Sterile seeds were sown on Murashige and Skoog medium (MS, Duchefa, Haarlem, the Netherlands) supplemented with 0.65 % agar and 30 $mg\,L^{-1}$ hyromycin and cultivated in Petri dishes sealed with parafilm under the same temperature and light conditions as described for cultivation on soil.

2.2.4 Stress treatments of *O. sativa*

To induce suberisation of root border tissues in *O. sativa*, an osmotic stress treatment of hydroponically grown plants was chosen. For expression analysis a short term treatment with 200 mmol L^{-1} NaCl in hydroponic nutrient solution was carried out for 2 h with subsequent sampling of tissues from different organs and root parts, immediate freezing in liquid nitrogen and storage at −80 °C until further processing. The osmotic pressure of different solutions was determined using a freezing point osmometer with a commercial calibration standard (Osmomat 030, 300 mOsmol kg^{-1} NaCl/H_2O, Gonotec, Berlin, Germany). Nutrient solution for *O. sativa* hydroponic culture had an osmotic pressure of 6 mOsmol kg^{-1} and 365 mOsmol kg^{-1} when spiked with 200 mmol L^{-1} NaCl for stress treatments. The addition of 400 mmol L^{-1} mannitol to the hydroponic solution led to an osmotic pressure of 433 mOsmol kg^{-1}.

For long term stress treatments with the aim to increase amounts of suberin in root border tissues, cultivation in hydroponic culture was carried out and modified according to the time schedule depicted in figure 3.11.

Cultivation under stagnant growth conditions was established from the 11th dai by exposing plants to a deoxygenated nutrient solution containing 0.1 % agar. The latter had been dissolved by boiling and to remove remaining oxygen the medium was gased with nitrogen.

Salt stress treatment from the 19th dai was carried out in a nutrient solution containing 100 mmol L^{-1} NaCl. Control and salt stressed plants were aerated continuously from the 11th dai. Cultivation took place in 2.4 L thin layer chromatography developing tanks covered with custom made polypropylene lids holding six plants. The glass ware enabled monitoring of root development and was covered to protect roots and medium against light.

2.3 Molecular biological methods

2.3.1 Purification of nucleic acids

DNA extraction

To extract DNA from plant material two different methods were used. Normally, DNA from leaf tissue ground on liquid nitrogen was isolated via DNA binding columns of the peqGOLD Plant DNA Mini Kit (PEQLAB, Erlangen, Germany) according to the manufac-

turer's instruction. For screening of higher numbers of segregating *O. sativa* mutants a quicker method was used to prepare plant tissue for PCR analysis (Wang et al., 1993; Collard et al., 2007) modified according to Alexander Fleck (Institut für Pflanzenernährung, Hannover, Germany, personal communication). Therefore, *O. sativa* leaf tissue was ground in 100 µL of 0.5 mol L^{-1} NaOH. 900 µL of 0.1 mol L^{-1} Tris buffer of pH 8 was added and centrifuged at 15 000 *g* for 2 min. Finally, the supernatant was transferred to a clean reaction tube and stored at −20 °C until application of 1 µL in a 25 µL PCR reaction mix.

RNA extraction

For examination of transcript abundance of selected genes in RT-PCR analyses as well as for cloning of genes containing large introns, RNA was isolated with the help of a kit based on DNase and RNA binding columns. For tissue specific expression analysis approx. 100 mg material of the different plant organs were collected separately in 1.5 mL reaction tubes, frozen in liquid nitrogen and stored at −80 °C until use. To isolate RNA the collected tissue was crushed to fine powder and extracted with the NucleoSpin RNA Plant kit (Macherey-Nagel, Düren, Germany) according to the manufacturer's instructions. Concentration of eluted RNA was determined with a Nanodrop 2000c spectrophotometer (Thermo Scientific, Wilmington, USA) and diluted with RNase free water to a concentration of 70 ng μL^{-1}. Amount and quality of RNA was tested by applying a mixture of 3 µL RNA solution, 3 µL 6×gel loading buffer and 12 µL RNase free water per sample to an agarose gel and subsequent separation by electrophoresis. Degradation of RNA was analysed from the ratio of intensities between the resulting RNA-fragments on the gel. A low degree of RNA degradation is indicated by a ratio of approx. 2:1 of 28S rRNA to 18S rRNA (large and small ribosomal subunit, respectively). RNA was stored up to one week at −20 °C or at −80 °C before further processing.

2.3.2 Gel electrophoresis

Nucleic acids deriving from RNA isolation, restriction digest and PCR were examined by agarose gel electrophoresis, irrespective of the further application. Gels consisted of 1 % agarose (w/v) in TAE buffer with approx. 0.05 % ethidium bromide, see chapter 2.1.2. Unless otherwise specified 5 µL of 6×gel loading buffer were added to 25 µL of nucleic acid solution and loaded onto an agarose gel. Nucleic acid fragments were then separated by size in the agarose matrix by applying an electric potential of 80 V. Nucleic acid bands were visualized under UV light, captured by a digital camera with UV filter (PowerShot

Table 2.1: Protocol for cDNA synthesis with the SuperScript® VILO™ cDNA Synthesis Kit.

RT reaction mix	4 µL 5×VILO Reaction Mix
	2 µL 10×SuperScript Enzyme Mix
	6.5 µL DEPC treated H_2O
525 ng RNA	7.5 µL RNA (70 ng µL^{-1})
Incubation programme	25 °C 10 min
	42 °C 60 min
	85 °C 5 min
	−20 °C until use

G2, Canon, Tokyo, Japan) and compared to either a 100 bp DNA-ladder, extended or 1 kbp DNA-ladder (Carl Roth, Karlsruhe, Germany) depending on the expected fragment size. Images were processed with Gimp 2.6 (GNU Image Manipulation Program, available at gimp.org) and ImageJ (Abramoff et al., 2004) for presentation and quantification of signal abundance.

2.3.3 Semi-quantitative RT-PCR

Semi-quantitative RT-PCR was performed to examine RNA levels of different genes (see table 2.3) in tissues of *O. sativa*. In preliminary tests only one PCR kit led to satisfactory amplification of *O. sativa* exon sequences, presumably as a consequence of the high GC content of approx. 66 %. Therefore, a two-step solution for RT-PCR was chosen. In the first step, first strand cDNA from RNA was generated with the help of the SuperScript® VILO™ cDNA Synthesis Kit (Invitrogen™, Carlsbad, USA) according to the manufacturer's instructions (see table 2.1) in a Primus 96 advanced Thermocycler (MWG-Biotech, Ebersberg, Germany).

During the second step, the PCR was performed with the AccuPrime™ GC-Rich DNA Polymerase (Invitrogen™, Carlsbad, USA) according to the protocol depicted in table 2.2. Quantification of the PCR products was carried out by comparison of respective band intensities after agarose gel electrophoresis.

Primers (see table 2.3) were designed with the help of different tools to find oligonucleotides with equal annealing temperatures (T_a) within a selected region on the DNA and to avoid those sequences tending to form secondary structures decreasing the yield of PCR products. The tools used included the stand-alone software GENtle (Manske, 2006), an online tool available at primer3.ut.ee and the primer design function integrated in Geneious,

Table 2.2: Protocol for PCR with AccuPrime™ GC-Rich DNA Polymerase.

PCR mixture		8.5 µL H_2O_{HPLC} sterile
		5 µL 5×Buffer A
		0.5 µL AccuPrime GC-Rich DNA Polymerase
		5 µL forward primer (1 µmol L^{-1})
		5 µL reverse primer (1 µmol L^{-1})
		1 µL template
Thermal cycler programme		94 °C 3 min
	32×	94 °C 45 s
T_a=T_m−2 °C	32×	55–65 °C 30 s
	32×	72 °C 1 min/kb
		72 °C 10 min
		4 °C until use

based on Primer3 (Koressaar and Remm, 2007; Untergasser et al., 2012).

2.3.4 Identification of knockout mutant lines

Genotyping of T-DNA insertion mutants was conducted via competitive PCR using a set of three primers, two targeting a genomic sequence spanning the annotated T-DNA insertion and a third one annealing to the T-DNA up to 300 bp from the annotated border sequence. Primers are listed in table 2.5 and a scheme including binding sites of the genomic primers used to genotype mutations in *CYP86B3* is depicted in figure 3.5. In case of an insertion the fragments produced by PCR would be significantly shorter compared to those deriving from WT DNA. A PCR on DNA from plants which are heterozygous for the examined location would result in two distinct bands of known sizes for the single sample. Two different PCR kits were chosen depending on the GC content of the targeted genomic DNA. For *A. thaliana* and intron sequences of *O. sativa* the KAPA2G™ Fast ReadyMix with Dye (PEQLAB, Erlangen, Germany) was used as summarised in table 2.4 based on the manufacturer's reference. For PCR targets spanning *O. sativa* exon sequences the AccuPrime™ GC-Rich DNA Polymerase (Invitrogen™, Carlsbad, USA) was used as summarised in table 2.2. The reactions were performed in a Primus 96 advanced Thermocycler (MWG-Biotech, Ebersberg, Germany). PCR products were examined after separation by size in a gel electrophoresis.

Table 2.3: List of primers used for RT-PCR. With for: forward primer; rev: reverse primer; T_m: melting temperature.

no.	**target**	**prediction, amplicon size**	**sequence**	T_m
LS580	Os05g49290	KCS-like, for, 963 bp	CCTCACGCTCTTGCTGCTGCC	65.7 °C
LS581	Os05g49290	KCS-like, rev, 963 bp	GCGTGGCGAAGAAGAGGAGCTG	65.8 °C
LS584	Os10g34480	*CYP86B3*, for, 919 bp	TGGTGGCGGTGTCGATCTTCG	63.7 °C
LS585	Os10g34480	*CYP86B3*, rev, 919 bp	GGCGGGGTTCTTGTTGAGCAG	63.7 °C
LS740	Os04g47250	*CYP86A11*, for, 712 bp	AAGTCCCGGTTCGACAACTA	57.3 °C
LS741	Os04g47250	*CYP86A11*, rev, 712 bp	TGGAGACCAGCCAGAAGAAC	59.4 °C
LS744	Os03g50885	*Actin*, for, 400 bp	CCTCTTCCAGCCTTCCTTCAT	59.8 °C
LS745	Os03g50885	*Actin*, rev, 400 bp	ACGGCGATAACAGCTCCTCTT	59.8 °C
LS748	Os02g44654	*CYP86A10*, for, 644 bp	CGTACATGACGTGGTTCTGG	59.4 °C
LS749	Os02g44654	*CYP86A10*, rev, 644 bp	CAGGTACTCCGGGAAGATGA	59.4 °C
LS846	Os05g38350	GPAT-like, for, 663 bp	CATGTCGCTCGTCATCCTC	58.8 °C
LS847	Os05g38350	GPAT-like, rev, 663 bp	GCGAGTATCCTCTGCACGTAG	61.8 °C
LS884	Os11g37900	KCS-like, for, 502 bp	CAGGTTCACCGGAACTCGTA	59.4 °C
LS885	Os11g37900	KCS-like, rev, 502 bp	GGTTCTTCTCGATGGTGTCG	59.4 °C

Table 2.4: Protocol for PCR with KAPA2G™ Fast ReadyMix with Dye.

PCR mixture		7.75 µL H_2O_{HPLC} sterile
		12.5 µL 2×KAPA2G Fast ReadyMix with Dye
		1.25 µL forward primer (10 µmol L^{-1})
		1.25 µL reverse primer (10 µmol L^{-1})
for competitive PCR		1.25 µL insertion primer (10 µmol L^{-1})
		1 µL template
Thermal cycler programme		95 °C 1 min
	30×	95 °C 15 s
T_a=T_m−2 °C	30×	55–65 °C 15 s
	30×	72 °C 5–15 s/kb
		4 °C until use

Table 2.5: List of primers used for genotyping. With for: forward primer; rev: reverse primer; LB: left boarder; RB: right boarder; T_m: melting temperature.

no.	**target**	**use**	**sequence**	T_m
LS138	At5g58860	genotyping *horst*, for	AAGAACCAGCTCAAGGCCACC	61.8 °C
LS139	At5g58860	genotyping *horst*, rev	AGCAAAAAGCCTAAACCGGGA	57.9 °C
LS347	SALK_107454	genotyping T-DNA, LB	AACACTCAACCCTATCTCGGGC	62.1 °C
LS331	At5g23190	genotyping *ralph*, for	TCCATCAGGAAATACGTCGTC	57.9 °C
LS332	At5g23190	genotyping *ralph*, rev	CCTACTTGCGTGTGGAAGTTC	59.8 °C
LS186	Spm 32	genotyping transposon	TACGAATAAGAGCGTCCATTTTA GAGTGA	62.4 °C
LS590	Os10g34480	genotyping *cyp86b3-x*, for	ACCCGTAGACCACAAAGAGGT	59.8 °C
LS591	Os10g34480	genotyping *cyp86b3-x*, rev	CGTCCGCAATGTGTTATTAAG	61.4 °C
LS943	Os10g34480	genotyping *CYP86B3*, rev	TCAAAGCTTGCTCTTGTCCCT	57.9 °C
LS592	pGA2715	genotyping T-DNA, LB	CGTCCGCAATGTGTTATTAAG	55.9 °C
LS593	pGA2717	genotyping T-DNA, LB	ACGCTGAACTTGTGGCCGTTC	61.8 °C
LS708	Os10g34480	genotyping *cyp86b3-3*, for	AGCTGGGTTAGAAGTTTGAGAA	56.5 °C
LS709	Os10g34480	genotyping *cyp86b3-3*, rev	GAGATCGTGGTGCGTGAAG	58.8 °C
LS594	pGA2707	genotyping T-DNA, RB	GGTGAATGGCATCGTTTGAAA	55.9 °C

2.4 Generation of transgenic *A. thaliana*

The *A. thaliana* mutant *ralph* (*Atcyp86b1*) has been described by Compagnon et al. (2009) and Diehl (2008, 2011) to lack the function of a ω-hydroxylase for VLCFA in suberin. A mutation in the orthologous gene *OsCYP86B3* (LOC_Os10g34480) was shown to cause a corresponding loss of function in the suberin biosynthesis of *O. sativa* as part of this work. To further test whether OsCYP86B3 is the orthologue of AtCYP86B1, which would implicate a homologous role in the suberin pathway, the coding sequence of *CYP86B3* (CDS *CYP86B3*) was cloned into the *A. thaliana* mutant *ralph* and the double mutant *ralph*/*horst* in order to complement their root suberin phenotypes by heterologous expression under control of the *RALPH* promoter.

The commercial Gateway® cloning System (Invitrogen™, Carlsbad, USA) was used according to the Gateway® Technology user guide for the molecular biological part, as described by Diehl (2011) and Nosbüsch (2009). The Gateway® Technology is based on the ability of the bacteriophage lambda for site- and direction-specific recombination facilitated by DNA recombination sequences (att sites). The cloning was conducted in two steps: firstly, an entry vector was produced by a so-called BP reaction, in which the CDS of the gene to be heterologously expressed produced by PCR (adding attB sites) was integrated in a donor vector (containing attP sites). Secondly, the just produced entry vector (featuring attL sites) was recombined in a so-called LR reaction with a destination vector (with attR sites) resulting in the final expression construct. All plasmids were amplified in *E. coli* DH5α and transformation with positive clones was ensured by a *ccdB* (control of cell death) gene coding for a lethal DNA gyrase inhibitor, only present on plasmids which are not positively recombined. Antibiotic resistance genes on entry and expression vectors served as further markers to select positive transformants. The expression vector was transferred into *A. tumefaciens* to finally transform *A. thaliana* via floral dip.

2.4.1 Cloning of an entry vector via Gateway

The schematic structure of *CYP86B3* in figure 3.5 illustrates the intron of 2002 bp expanding the total genomic length to 3685 bp, compared to a length of only 1683 bp of the CDS. Since attempts to clone the full length gene failed, RNA of roots from seedlings of *O. sativa* cv. Dongjin was extracted (chapter 2.3.1) and cDNA was produced (chapter 2.3.3). Since different proofreading DNA polymerases did not produce any PCR product on either genomic DNA or cDNA templates from isolated RNA of *O. sativa*, the AccuPrime™ GC-rich DNA Polymerase (Invitrogen™, Carlsbad, USA) was used to generate a PCR product con-

Table 2.6: Primers used for cloning. Small letters for nucleotides represent attB adapters for the Gateway® BP reaction. With attB1: forward adapter; attB2: reverse adapter; T_m: melting temperature without attB sequence.

no.	target	sequence	T_m
LS919	CDS Os10g34480 with attB1	ggggacaagtttgtacaaaaaagcaggct AACGCCATGAGCGCCACCAT	57.9 °C
LS920	CDS Os10g34480 with attB2	ggggaccactttgtacaagaaagctgggt TCAAAGCTTGCTCTTGTCCCT	61.4 °C

taining attB sites. Primers with attB adapters targeting the CDS of *CYP86B3* are listed in table 2.6. The PCR conditions listed in table 2.2 were changed to 2 min elongation time, 59 s for primer annealing at temperatures decreasing from 60–46.5 °C in steps of 1.5 °C and additional 25 cycles with 50 °C annealing temperature. The PCR was run in triplicate with double volumes and results were examined after separation by size via gel electrophoresis (chapter 2.3.2). Bands with the size of 1727 bp representing the three PCR products were cut out, combined and purified with the NucleoSpin® Gel and PCR Clean-up kit (Macherey-Nagel, Düren, Germany).

The BP reaction was performed according to the manual using the vector pDONR™/Zeo. The total volume was applied in the subsequent transformation of competent *E. coli* DH5α for selection of positive clones and plasmid amplification (see chapter 2.4.2).

Plasmids amplified in *E. coli* were purified with the NucleoSpin® Plasmid preparation kit (Macherey-Nagel, Düren, Germany) according to the manufacturer's instructions and a restriction digest was carried out with the enzymes *Apa*I at 25 °C and *Xho*I at 37 °C for 1 h (New England Biolabs® Inc., Ipswitch, USA). Restriction fragments were examined after separation by size in a gel electrophoresis. Only clones featuring exactly the expected fragment sizes were sent to Eurofins MWG GmbH (Ebersberg, Germany) for sequencing using primers listed in table 2.7.

Since PCR was performed with the AccuPrime™ GC-Rich DNA Polymerase without proofreading capability, none out of the 22 sequenced individual clones was free of mutations. To solve this problem, a different approach was carried out, with the basic idea of combining mutationless sequences of different clones with each other. Therefore, isolated plasmids were digested with different restriction enzymes and selected mutation-free fragments, separated via gel electrophoresis, were ligated with a T4 DNA Ligase (New England Biolabs® Inc., Ipswitch, USA). The resulting entry vector was amplified in *E. coli* DH5α.

Table 2.7: Primers used for sequencing. With for: forward primer; rev: reverse primer; T_m: melting temperature.

no.	target	sequence	T_m
M13uni (-21)	any vector containing lacZ with integrated cloning site, for	GTAAAACGACGGCCAGT	52.8 °C
M13rev (-29)	any vector containing lacZ with integrated cloning site, rev	CAGGAAACAGCTATGAC	63.7 °C
LS585	Os10g34480 first exon, rev	GGCGGGGTTCTTGTTGAGCAG	50.4 °C

2.4.2 Transformation of *E. coli*

For plasmid amplification in *E. coli* competent cells (MAX Efficiency® DH5α™ Competent Cells, Invitrogen™, Carlsbad, USA) were transformed. Therefore, an aliquot was thawed on ice, mixed with the plasmid of choice and incubated for 30 min in iced water. After a 30 s heat shock in a 42 °C water bath cells were again incubated in iced water for 5 min. 950 µL 25 °C warm SOC medium were added to the cells and incubated horizontally at 37 °C on a rotary shaker with 225 rpm for 1 h. Positive clones were selected by plating 10 µL, 100 µL and the remaining volume of cell suspension on LB agar containing appropriate antibiotics, 50 µg mL^{-1} Zeocin™ (Invitrogen™, Carlsbad, USA) in case of the entry clones and 50 µg mL^{-1} Kanamycin in case of the expression clone. Positive clones were picked after 1–3 d of incubation at 37 °C. Liquid LB medium with corresponding antibiotics was inoculated with this cell material and incubated over night at 37 °C.

Aliquots of 700 µL culture were used for long term storage at −80 °C in glycerine stocks after addition of 300 µL 50 % sterile glycerine in H_2O_{HPLC} and freezing in liquid nitrogen. Plasmids were isolated from the remaining culture using the NucleoSpin® Plasmid preparation kit (Macherey-Nagel, Düren, Germany) according to the manufacturer's manual and nucleic acid concentration was determined via a Nanodrop 2000c spectrophotometer (Thermo Scientific, Wilmington, USA).

2.4.3 Cloning of an expression vector via Gateway

An expression construct to be expressed in *A. tumefaciens* for transformation of *A. thaliana* was produced with the entry vector described in chapter 2.4.1 and a destination vector provided by Nosbüsch (2009) comprising LR recombination sites attR1 and attR2 downstream of the promoter region of *AtCYP86B1* on a pMDC vector from Curtis and Grossniklaus

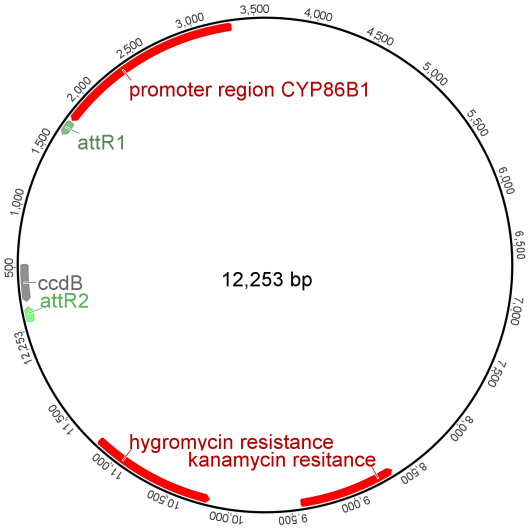

Figure 2.1: Plasmid map of the destination vector featuring the promoter region of *RALPH* (*AtCYP86B1*) and antibiotic resistance genes for selection of positive transformants, based on pMDC99. With attR: recombinase attachment sites for LR reaction and ccdB: control of cell death, a topoisomerase II inhibitor.

(2003), see figure 2.1. The LR reaction was conducted with the Gateway® LR Clonase™ II Enzyme Mix (Invitrogen™, Carlsbad, USA) according to the manufacturer's instructions and the resulting plasmid was selected and amplified as described in chapter 2.4.2.

2.4.4 Transformation of *A. thaliana*

In order to generate transgenic *A. thaliana* plants for heterologous expression of CDS *CYP86B3* under control of the promoter of *RALPH*, *A. tumefaciens* was transformed with the expression vector described in chapter 2.4.3.

Transformation of *A. tumefaciens*

Chemically competent cells of the *A. tumefaciens* strain GV3101pMP90 were thawed on ice and mixed with 1 µg of plasmid. After incubation in iced water and freezing in liquid nitrogen for 5 min each, cells were heat shocked at 37 °C in a water bath for 5 min. 800 µL LB medium were added and the suspension was incubated at 28 °C and 170 rpm for 3 h. Positive clones were selected by plating 20 µL, 200 µL and the remaining volume separately on LB agar containing 50 µg mL^{-1} Kanamycin and 10 µg mL^{-1} Rifampicin and incubation at 28 °C for 48 h. Positive clones were confirmed by colony PCR (data not shown) and glycerine stocks were generated for long term storage as described in chapter 2.4.2.

Floral dip

10 mL of LB medium containing 50 µg mL^{-1} Kanamycin and 10 µg mL^{-1} Rifampicin were inoculated with an isolated clone of transformed *A. tumefaciens* and cultivated at 28 °C and 170 rpm over night in a 500 mL baffled flask as pre-culture. This was used to inoculate 300 mL of the same medium as main culture, which was cultivated in the same way as the pre-culture. Cells were pelleted at 3 000 *g* for 15 min and resuspended in inoculation medium.

Florescences of *A. thaliana* plants grown for five weeks as described in chapter 2.2.3 were dipped for 2×10 s into the inoculation medium. Inoculated plants were kept at maximal humidity for 3 d and were then cultivated under the conditions described in chapter 2.2.3 until harvest of mature seeds. Seeds were dried and positive clones, carrying the corresponding antibiotic resistance gene, were selected in axenic culture on MS agar containing 30 µg mL^{-1} Hygromycin (see chapter 2.2.3).

2.5 Chemical analysis

To prevent contamination of samples of plant lipids and cell wall polyesters for GC analyses, only glass ware which has been rinsed thoroughly with chloroform was used during all steps of sample collection, preparation and extraction. Septa or lids were lined with PTFE and were resistant to organic solvents. All solvents were of analytical purity.

2.5.1 Sample preparation for chemical analysis

For chemical analysis of the root systems, plants were hydroponically grown, for 20 d in case of *A. thaliana* and for four weeks under aeration in case of *O. sativa*. When differential analysis of apical and basal root tissue was intended, root sections of up to six individual plants were separated by relative distance from the root tip. In *O. sativa* apical is referred to the 2–4 cm from root tip and basal to the 3–6 cm from root-shoot junction. In order to analyse suberin contents of *O. sativa* and *A. thaliana* root tissues, reference properties of the collected material had to be examined before further processing. Therefore, root systems were carefully washed in H_2O_{demin} and surface areas of roots were determined in a layer of water using a modified flatbed scanner (CanoScan LiDE, Canon, Tokyo, Japan) with an opaque black cover as background and ImageJ (Abramoff et al., 2004) for picture processing. Samples were weighed out to obtain materials' fresh weight (fw), and after

total lipid extraction and drying to receive the dry weight (dw) to which the results of analysis were referred to finally.

The following protocol for sample preparation is adopted from Zeier and Schreiber (1998) and is based on the method described by Kolattukudy and Agrawal (1974). Except of samples for analysis of solvent extractable fatty acid methyl esters (FAME), all samples were subjected to an enzymatic cell wall hydrolysis with cellulase and pectinase in citric acid buffer, see chapter 2.1.2. After vacuum infiltration, incubation took place for two weeks on a rotary shaker and the enzyme solution was exchanged up to five times. Finally, roots were washed in H_2O_{demin} over night.

For suberin analyses, soluble lipids had to be removed from root samples. Therefore, roots were extracted with chloroform/methanol (1:1 v/v) for up to three weeks, either in Erlenmeyer flasks on a rotary shaker or in 9–20 mL glass vials with PTFE lined lids on roller mixers. The extraction solution was exchanged at least three times. The digested and extracted roots were placed on PTFE sheets for drying and stored over silica gel in an exsiccator for several days after evaporation of organic solvents. Dry weights of samples were determined with a micro balance (MC21S, Sartorius, Göttingen, Germany).

2.5.2 Transesterification with BF_3:methanol

Root samples were cut into small pieces in glass vials, covered with 1.5–3 mL BF_3:methanol (approx. 10 % (1.3 mol L^{-1}) boron trifluoride-methanol solution, Fluka, Sigma-Aldrich, Steinheim, Germany) and transesterified for 16–18 h at 70 °C. After cooling, 10 µg C_{30} alkane were added as internal standard to each sample and the transesterification was stopped by adding 2 mL saturated $NaHCO_3$ solution very slowly. Suberin monomers were extracted in 3×1 mL chloroform by mixing on a vortex mixer and successively collecting the lower phases. Extracts were washed two times with 1 mL H_2O_{HPLC} by mixing and discarding the upper phase. Anhydrous $NaSO_4$ was added to the extract to bind the remaining water as necessary. The solvent volume was reduced by evaporation of the chloroform to less than 100 µL per sample.

2.5.3 Extraction of lipids for FAME analysis

FAME were extracted according to a protocol described by Dethloff (2009). Freshly harvested root tissue was ground on liquid nitrogen in glass vials containing steel spherules and a construction screw with removed head on a vortex mixer. As internal standard 20 µg C_{15} and 5 µg C_{21} fatty acids were added to each sample. The root tissue powder was

Table 2.8: Temperature profiles for GC analyses.

suberin/FAME			acid standard		
change	final	hold	change	final	hold
injection	50 °C	2 min	injection	50 °C	1 min
10 °C min^{-1}	150 °C	1 min	40 °C min^{-1}	200 °C	1 min
3 °C min^{-1}	310 °C	15 min	3 °C min^{-1}	310 °C	15 min

extracted in 4 mL chloroform/methanol (1:2 v/v) for 30 min on a roller mixer and centrifuged at 750 *g* for 10 min. The supernatant was collected in a clean vial and the pellet was extracted in 4 mL chloroform/methanol (2:1 v/v) for 30 min mixing several times on a vortex mixer. After a second centrifugation the supernatants were combined and 3 mL of the solution were transesterified in 2 mL 1 N methanolic HCl for 2.5 h at 80 °C. After cooling the transesterification was stopped by mixing with 4 mL saturated NaCl solution. FAME were extracted in 3×1 mL hexane by mixing on a vortex mixer and successively collecting the upper phases. The solvent volume was reduced by evaporation of the hexane to less than 100 µL per sample.

2.5.4 Analysis with GC-MS and GC-FID

In order to increase volatility of the compounds, analytes were derivatised with bis(trimethylsilyl)trifluoroacetamide (BSTFA) to convert polar functional groups, such as hydroxyl and carboxyl groups, into their corresponding trimethylsilyl-esters (TMS). Therefore, 20 µL of both pyridine and BSTFA were added to all samples and incubated at 70 °C for 40 min with subsequent analysis via gas chromatography (GC).

1 µL of the derivatised samples was injected on-column. Analytes were separated by volatility, depending on molecular size and polarity, on a DB-1 capillary column (30 m×0.32 mm; 0.1 µm poly(dimethylsiloxane) coating; Agilent J&W Scientific, Santa Clara, USA). Helium was used as carrier gas for mass spectrometry (MS) and hydrogen for flame ionisation detector (FID) analyses with flow rates of 2 mL min^{-1}. Gas chromatography (GC 6890N coupled with FID or 5973N Mass Selective Detector; Agilent Technologies, Santa Clara, USA) was performed with the temperature programme depicted in table 2.8.

Identification of substances was carried out on basis of their characteristic mass spectra derived from MS. After gas chromatographic separation molecules were ionized resulting in typical fragmentation patterns, which were determined by a mass selective quadrupole

measuring mass to charge ratios of the molecule's fragment ions. Identified substances in total ion chromatograms from MS analyses were assigned to peaks and to corresponding areas in chromatograms from FID for quantification. Compound masses were calculated based on the internal standard and related to either sample dry weight or surface area of the applied root tissue.

Since non-volatile sample residues, that can accumulate at the on-column-injection end of the GC capillary, decrease detector response of polar analytes with increasing molecular size, the column quality was regularly tested and maintained. For this purpose, a standard solution comprising equal amounts of C_{24} alkane, C_{29}, C_{30} and C_{31} monocarboxylic acids in chloroform, referred to as acid standard, was derivatized and analysed on the system to be tested according to the temperature profile given in table 2.8. The ratio of peak areas deriving from the alkane and the C31 monocarboxylic acid had to be lower than 1.3, otherwise the column was reconditioned to restore analytic quality.

2.6 Histology

Sample preparation

In order to examine suberisation and possible changes in root and cell morphology of mutants, free-hand cross sections of either freshly harvested samples of adventitious *O. sativa* roots or those fixed in methanol were prepared. To hold roots in place while sectioning, extruded polystyrene foam with very small pores was used. Cross sections from 10 mm, 20 mm, 30 mm and 50 mm distance from root tip were produced with a razor blade, collected in water droplets and preselected by section thickness and quality.

Staining procedures

Staining of sample tissues was conducted according to Brundrett et al. (1991). For bright-field microscopy sections thinner than one cell layer were stained with a 0.1 % (w/v) solution of Sudan red 7B, also referred to as solvent red 19, for at least 30 min at 50 °C on microscope slides. To differentially stain suberin lamellae, free hand root cross sections were incubated in 0.01 % (w/v) Fluorol yellow 088 for 2 h in the dark.

Excess dye was washed out thoroughly with water and root sections were mounted in 50 % (v/v) glycerol under cover slips.

Bright field and epifluorescence microscopy

For all microscopic investigations an Axioplan microscope (Carl Zeiss, Jena, Germany) was used with a digital camera (DXM-1200, Nikon, Düsseldorf, Germany) mounted to capture still images.

Stained root cross sections were either examined by bright-field microscopy or by epifluorescence microscopy under UV light (excitation filter: bandpass 365 nm, dichroic mirror: coloursplitter 395 nm, barrier filter: longpass 397 nm). The image manipulation software GIMP was used to arrange, sharpen and convert pictures to different file formats. Brightness and contrast of different pictures were adjusted by maximal 10 %.

2.7 Physiology

2.7.1 Examination of stress response and biomass

Development and morphology of various genotypes (see chapter 2.2.1) under different growth conditions (described in chapter 2.2.4) were documented with the help of a digital camera (PowerShot G11, Canon, Tokyo, Japan). Differences of plant organs in biomass were determined with a balance (AG204, Mettler Toledo, Greifensee, Switzerland) after removal of adherent growth media by plotting between paper tissues, as well as after drying at 50 °C for one week. Surface areas of plant organs were either determined on the basis of still images or scans as described in chapter 2.5.1.

2.7.2 Visualisation of ROL

Observations of radial oxygen loss (ROL) were carried out to explore differences in barrier properties of roots of different *O. sativa* genotypes. Stressed and unstressed plants were stained in deoxygenated agar solution with methylen blue, which is colourless in its reduced form and blue in the presence of oxygen.

After dissolving 0.1 % (w/v) agarose in H_2O_{demin} by boiling and thereby removing dissolved oxygen from the solution, 13 mg L^{-1} methylen blue were added and the solution was further deoxygenated by addition of 130 mg L^{-1} $Na_2S_2O_2$ while mixing gently. The colourless solution was poured in a separation chamber for thin layer chromatography (No. 124162, Desaga, Wiesloch, Germany) and plants to be tested were mounted in a way that roots were totally submerged in the staining solution immediately after cooling. Incubation took place in the dark and the staining process of roots and surrounding medium

was monitored over time. After 80 min the staining result was captured as still image with a digital camera (PowerShot G11, Canon, Tokyo, Japan).

2.7.3 Solute uptake monitoring via PAM

To assess the solute uptake of *cyp86b3-1* in comparison to the WT, retention of the herbicide Metribuzin (4-amino-6-tert-butyl-3(methylthio)-1,2,4-triazin-5-on; Bayer, Leverkusen, Germany) was measured indirectly via decrease of photosynthesis rates. Metribuzin prevents binding of electron acceptors to the D1 protein of PS II, and thus inhibits electron transport, as reviewed in Draber et al. (1991).

Plants grown for four weeks in aerated hydroponics were mounted with the roots completely submerged in cultivation medium with 100 µmol L^{-1} Metribuzin. The basic chlorophyll fluorescence yield (F') was recorded with the software WinControl-3 using a pulse-amplitude-modulation (PAM) chlorophyll fluorometer (JUNIOR-PAM, Heinz-Walz GmbH, Effeltrich, Germany) emitting a low energetic pulsing light of 450 nm wavelength and 5 Hz to keep PS II reaction centers open. To fully reduce electron acceptors of PS II and herewith close its reaction centers, saturating pulses of 10 000 µmol m^{-2} s^{-1} were applied for a duration of 0.6 s at a rate of 1 min^{-1}. The saturating pulse led to a maximum in chlorophyll fluorescence yield (F'_M), subsequently terminated by illumination with far red light. This activated PS I again and thus reopened reaction centers of PS II by a withdrawal of electrons from the electron transport chain. The effective photochemical quantum yield of PS II (Y(II)) was calculated by the software WinControl-3 based on the formula (Genty et al., 1989):

$$Y(II) = \frac{F'_M - F'}{F'_M}$$

The raw data was processed with Excel (Microsoft, Redmond, USA) and times between application and half maximal inhibition were calculated from curves of decreasing Y(II), based on a sigmoid asymmetrical five-parameter logistic dose response model in Prism5 (GraphPad Software Inc., San Diego, USA).

3 Results

3.1 Genome and expression analyses

Based on a selection of *A. thaliana* amino acid sequences of proteins, which were identified to be involved in suberin biosynthetic pathways, BLAST analyses on rice databases have been conducted. The candidates were then reassessed with regard to sequence homology to *A. thaliana* suberin genes and temporal and spatial expression which was consistent with tissues undergoing suberisation.

3.1.1 Protein alignments

To confirm the results and to reduce the high number of genes found in the databases by BLAST analysis, multiple alignments have been conducted via CLUSTAL and MUSCLE algorithms. The results were visualised in tree form via MEGA for better accessibility and neighbor-joining phylograms with bootstrap values are depicted in the supplemental including potentially suberin involved members of the protein classes cytochrome P450 (figure 8.1), β-ketoacyl-CoA synthases (figure 8.2), peroxidases (figure 8.3), glycerol-3-phosphate acyltransferases and ABC-transporters (figure 8.4). *A. thaliana* proteins which were used initially for BLASTp analysis are underlined in red and closest related suberin candidates in *O. sativa* in blue. The length of the branches reflect the genetic distance between the sequence and the last node.

The phylogenetic tree in figure 3.1 comprises the protein sequences of *A. thaliana* and *O. sativa* members of the CYP86 group. The orthologue of AtCYP86B1 (RALPH) in *O. sativa* is CYP86B3 (LOC_Os10g34480), the only candidate on this subclade, and closest relatives to AtCYP86A1 (HORST) are CYP86A9 (LOC_Os01g63540), CYP86A10 (LOC_Os02g44654) and CYP86A11 (LOC_Os04g47250).

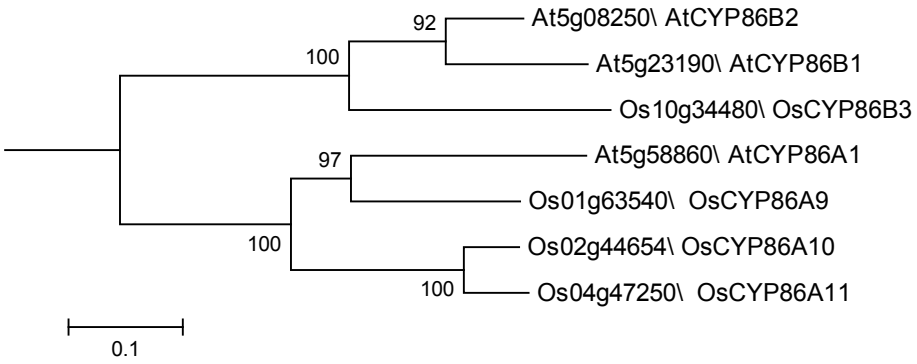

Figure 3.1: Neighbor-joining phylogram of protein sequences from members of the CYP86 subclade with bootstrap values.

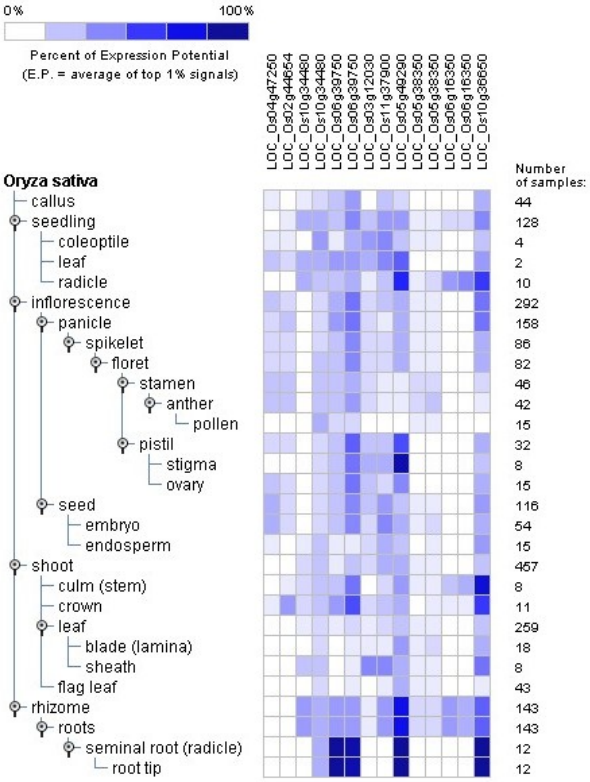

Figure 3.2: Organ expression heatmap of suberin candidate genes based on microarray data via Genevestigator. Genes were selected according to closest amino acid sequence homology to genes from *A. thaliana*, known to be related to suberin biosynthesis.

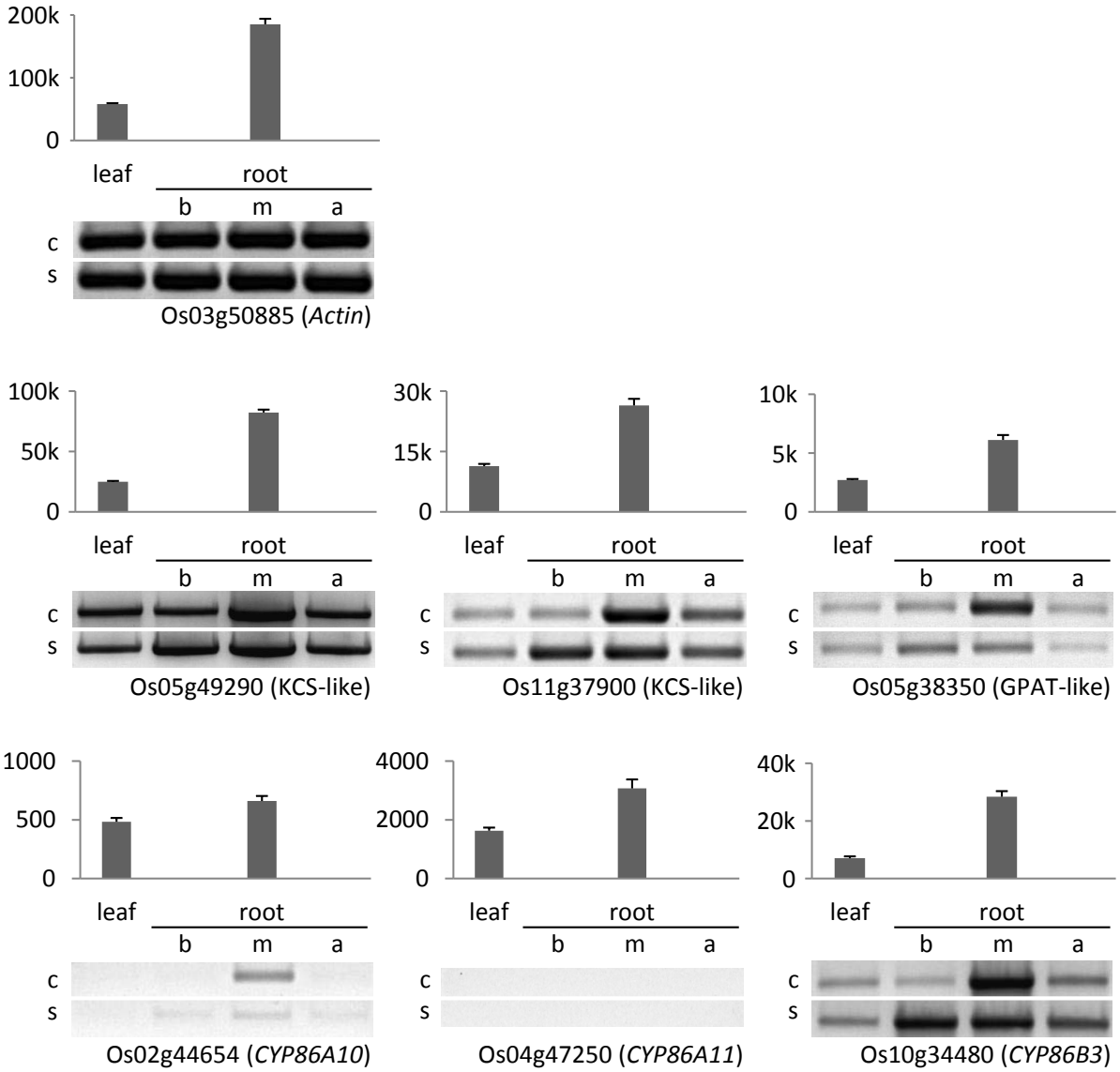

Figure 3.3: Organ expression of *Actin* and suberin candidate genes in *O. sativa* selected by sequence homology to *A. thaliana* suberin genes: relative expression in leaves and roots based on Genevestigator microarray database (grey bars reflect arithmetic means of signal intensities on Affymetrix OS_51K: Rice Genome 51K arrays with SE) and semi-quantitative RT-PCR analysis of tissue specific expression in four week old plants of *O. sativa* var. japonica cv. Dongjin grown in aerated hydroponic culture and after salt stress of 200 mmol L^{-1} NaCl for 2 h. With: k: kilo (1000×); b: basal, 2 cm from root-shoot junction; m: middle, 4–7 cm from root tip; a: apical, 2 cm from root tip; c: control; s: salt stress.

3.1.2 Tissue specific gene expression

Expression studies were conducted to verify the selection of suberin candidate genes. In *in silico* studies microarray databases such as Genevestigator (Hruz et al., 2008) and ricearray.org (Cao et al., 2012) were screened for expression patterns, which are consistent with locations of suberin biosynthesis. In figure 3.2 organ specific expression of a selection of rice genes is visualised in a heatmap with colours white, representing no expression, to dark blue, for the highest relative expression levels. Values are extracted from 101 studies with almost 2000 data sets and sample numbers vary with the different tissues.

Most of the tested genes show an increased relative expression in roots (third line from bottom) and some in parts of flowers and seeds in comparison to other organs and to the reference gene *Actin* (rightmost column). Except of LOC_Os06g39750, a gene predicted to code for a β-ketoacyl-CoA synthase by sequence homology to corresponding genes in *A. thaliana*, no selected genes were expressed stronger in shoot parts than in the root; only the crown, which is the basis of adventitious roots, and sheath, including the crown, were organs with slightly elevated expression in cytochrome P450 and putative β-ketoacyl-CoA synthase genes.

To further examine genes which are potentially involved in suberin biosynthesis, organ specific differential expression was explored before and after osmotic stress treatments with mannitol or NaCl, which has been shown to induce suberisation (Krishnamurthy et al., 2009). The exact osmolalities of different solutions used for the stress experiments were determined with a freezing point osmometer (Osmomat 030, Gonotech, Berlin, Germany).

The osmolality of the hydroponic solution which was used for the cultivation of *O. sativa* was 3 mOsmol kg^{-1}, which is near the detection limit of the osmometer. After one week of plant cultivation the osmolality was 4–6 mOsmol kg^{-1} in three repeated measurements each. When 200 mmol L^{-1} NaCl or 400 mmol L^{-1} mannitol were added, the osmolality was 366 mOsmol kg^{-1} and 432 mOsmol kg^{-1}, respectively. Plants treated with mannitol formed white crystals on the surface of sheaths and leaves and did completely lose turgor. They were not further examined.

In figure 3.3 relative gene expression values in leaves and roots based on Genevestigator (grey bars) are opposed to results of a semi-quantitative RT-PCR on four week old plants, cultivated in aerated hydroponics, and after stress treatment for 2 h with 200 mmol NaCl. Tissues examined were collected from leaves and 8–15 cm long roots, subdivided into basal, 2 cm from root-shoot junction, middle, 4–7 cm from root tip, and the most apical parts, 2 cm from root tip. *Actin*, here referred to the gene LOC_Os03g50885, served as reference and was uniformly strong expressed in all examined tissues, whereas microarray

based relative expression was three times higher in roots than in leaves.

RT-PCR on all suberin candidate genes indicated much higher expression levels in roots than in leaves. Expression was highest in the middle part of the root (4–7 cm from root tip), except of *CYP86A11* for which no expression could be detected in any tissue samples. Highest expression was found for both KCS-like genes and *CYP86B3*, which was reflected in relative expression values from the database as well. After 2 h of salt stress, expression of all selected genes was increased in the basal root and to a smaller extend in the most apical 2 cm at the expense of expression in the middle part.

3.2 CYP86B3

3.2.1 Motif search

In order to compare amino acid sequences deriving from the *in silico* translated CDS of the three genes in subclade *CYP86B* from *A. thaliana* and *O. sativa*, a motif search via MEME (Bailey and Elkan, 1994) has been conducted. Three MEME motifs of the arbitrary length of 50 amino acids (aa) in the putative protein sequence comprising most of the highly conserved CYP motifs known in plants (Bak et al., 2011) were found. To take the general size of sequence motifs into account another search with the maximum length of seven amino acids was conducted, resulting in ten hits (data not shown) of which only two comprised the above mentioned highly conserved plant cytochrome P450 motifs.

Parts of the amino acid sequence of CYP86B3 including the above mentioned MEME motifs of 50 aa sequence length are illustrated in figure 3.4. A sequence logo represents the consensus sequence of the CYP86B-cluster aligned via MUSCLE (Edgar, 2004) with amino acid letters sized relative to their frequency. The three aligned sequences share 339 identical sites, 49.9 % of the code, whereas AtCYP86B1 and OsCYP86B3 have 62 % in common. Located in MEME motif 1 are the PERF/W consensus sequence, part of the E-R-R triad, and the F-G-C heme binding motif of the heme-binding loop conserved in all P450 enzymes in plants. MEME motif 2, though sharing 82 % identical sites in the *CYP86B*-subclade in *A. thaliana* and *O. sativa*, does not contain any conserved plant P450 domains. This was tested on an alignment with 69 protein sequences identified to have a query coverage (percentage overlap of query and subject) of higher than 70 % in a BLAST analysis with P450 enzymes known to be involved in suberin or cutin biosynthesis in *A. thaliana*. In MEME motif 3, in which the sequences share 75.5 % identical sites, AGxDT was identified, the P450 signature for oxygen binding and activation, situated in the I-helix

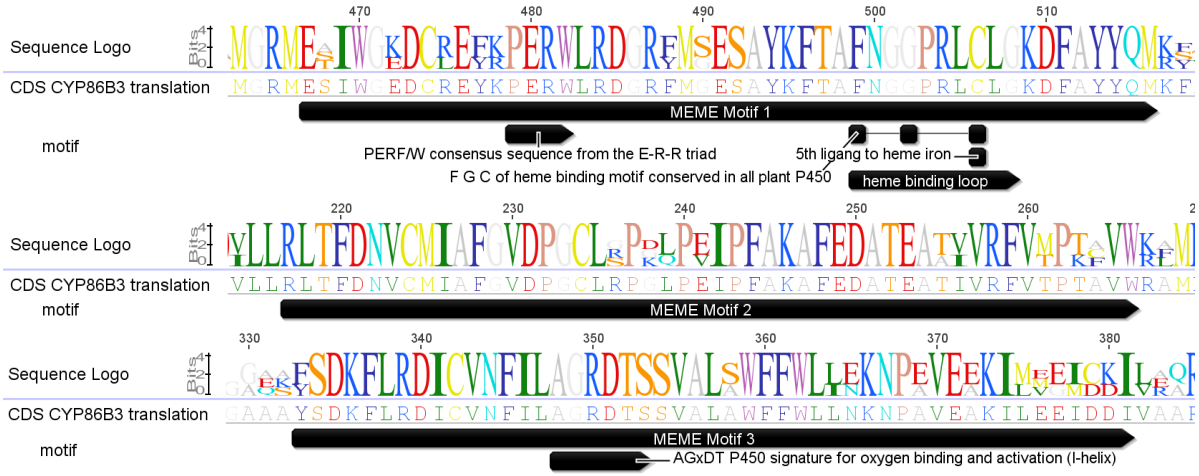

Figure 3.4: Amino acid sequence alignment of the *CYP86B*-cluster. Displayed are selected 50 bp long sequences of high similarity (MEME motifs 1–3). The sequence logo represents the consensus sequence of the MUSCLE alignment with amino acid letters sized relative to their frequency and in colours indicating traditional side chain properties. Numbers above the letters mark distances from the start codon and below the corresponding *in silico* translated CDS of *CYP86B3*. Highly conserved cytochrome P450 motifs are illustrated as black blocks and arrows.

of the folded enzyme. The ExxR pattern of the KETLR P450 motif, part of the K-helix of the tertiary structure, is represented by the amino acids SEALR, located between MEME motifs 3 and 1 (not shown). Additionally, only found in the rice gene, the putative protein ends with SKL, the peroxisomal targeting sequence PTS1.

3.2.2 Selection of mutant lines

As described in chapter 2.2.1 seeds of T-DNA insertion lines in *O. sativa* cv. Dongjin have been obtained from the PFG, Pohang, Korea. Before further propagation and characterisation of the grown plants, genotyping via PCR for selection of homozygous KO has been carried out. In figure 3.5 a schematic representation of *CYP86B3* illustrates the three different T-DNA insertions, represented by black triangles, and binding sites of primers used for genotyping, indicated by narrow triangles. In the following the different alleles PFG_4A-02646, PFG_1B-19308 and PFG_2B-30065 are referred to as *cyp86b3-1*, *-2* and *-3*, respectively. Results of the genotyping to identify homozygous T-DNA insertion lines are collected in figure 8.5. The primer sets used are listed in table 2.5. The second generation of the seeds, which have been received from the stock center, produced uniform

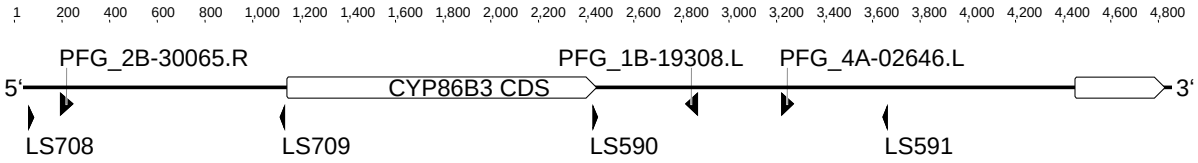

Figure 3.5: Schematic structure of the different alleles of *CYP86B3*. Wide triangles typify T-DNA insertions, narrow triangles represent binding sites of gene-specific primers or those specific to the inserted T-DNA sequence. Lengths of genomic sequences correspond to the scale in bp above.

homozygous plants for *cyp86b3-1* and the segregated WT (figure 8.5 A). In a competitive PCR with a set of three primers (LS590 and LS591 targeting the intron of *CYP86B3* and LS592 binding to the inserted T-DNA left border), WT DNA produced a single band with the expected size of 1238 bp, whereas DNA of *cyp86b3-1* led to a single band of 510 bp confirming the mutation. For all following studies of *cyp86b3-1*, the progeny of plant 3 (*cyp86b3-1*) and plant 25 (Dongjin WT) was used (see figure 8.5 A).

To genotype plants segregating for *cyp86b3-2* the same set of gene-specific primers was used resulting also in a fragment size of 1238 bp for *CYP86B3*, see figure 8.5 B 1, 4, 7 and 12. The third primer LS593, targeting the inserted T-DNA left border, led to an additional band of 802 bp in the PCR with DNA from the heterozygous plants 6 and 9, as well as to a single band of the expected size for plants which are homozygous for *cyp86b3-2* in case of the plants 2, 3, 5, 8, 10 and 11. Chemical characterisation of the suberin phenotype of *cyp86b3-2* and its WT background was performed based on these results with roots of the respective plants and corresponding results will be described in chapter 3.2.4.

To determine the genotype of segregating plants of the mutant line *cyp86b3-3*, primers LS708 and LS709 were used to target the promoter region spanning the T-DNA insertion site. To avoid interactions between the primer pairs a separate PCR was performed with the primers LS594 and LS709 to identify the insertion. Based on results shown in the upper line of figure 8.5 C, plants 3, 5 and 6 were identified to carry the allele *CYP86B3*, whereas plants 1, 2, 4, 9, 10 and 12 were only carrying the mutated allele *cyp86b3-3*, as shown in the lower line of the same figure. No definite results were obtained for plants 7 and 8, and plant 11 was identified to be heterozygous for *CYP86B3*/*cyp86b3-3*.

The effect of the T-DNA insertion on expression of *CYP86B3* was tested by RT-PCR analysis of *cyp86b3-3* plants 1, 2, 4 and 12 as well as of WT plants 3 and 6 and the heterozygous plant 11. The quality of RNA used in RT-PCR had been examined before by separation of

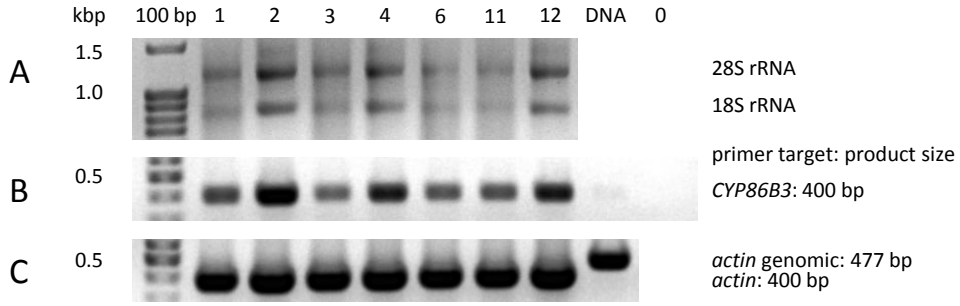

Figure 3.6: Expression of *CYP86B3* in segregating plants of *cyp86b3-3*. Test gel with 400 ng of isolated RNA (A). Expression of *CYP86B3* in roots grown in aerated hydroponics for three weeks (B) and expression of *actin* as reference (C). With kbp: kilo base pairs; 100 bp: 100 bp DNA-ladder, extended; 1–12: templates from respective plants; DNA: control; 0: negative control (H_2O_{HPLC}).

400 ng isolated RNA via agarose gel electrophoresis. As depicted in figure 3.6 A, the two characteristic bands of the highly abundant 28S rRNA of the large, as well as the 18S rRNA of the small ribosomal subunit could be observed. The ratio of approx. 2:1 indicates a low degree of RNA degradation. The RT-PCR with primers targeting an intron spanning part of the CDS of *CYP86B3* revealed expression in all samples independent of the T-DNA insertion in *cyp86b3-3*, see figure 3.6 B. The homozygous mutants identified by PCR (see figure 8.5 C) did not differ in abundance of *CYP86B3* transcript compared to the heterozygous plant 11 or the WT plants 3 and 6. The control gene *actin* was uniformly strong expressed in all tissues sampled, see figure 3.6 C.

3.2.3 Histological survey of *cyp86b3-1*

Root suberin of the mutant *cyp86b3-1* was examined by histochemical microscopic studies. Fluorescence microscopic pictures of freehand cross sections stained with Fluorol yellow 088 are presented in figure 3.7. The microscopic pictures visualize the different root tissues, which are from outside of the root to its central cylinder: the faint outermost epidermis, the yellowish exodermis, the sclerenchyma cell layer autofluorescent in bright blue to white and the cortex cells in blue, with formation of aerenchyma visible by disintegrated cell structures in the older root parts. Developing suberin in the exo- and endodermis about 20 mm from root tip is indicated by a faint yellowish stain of the cell walls in the

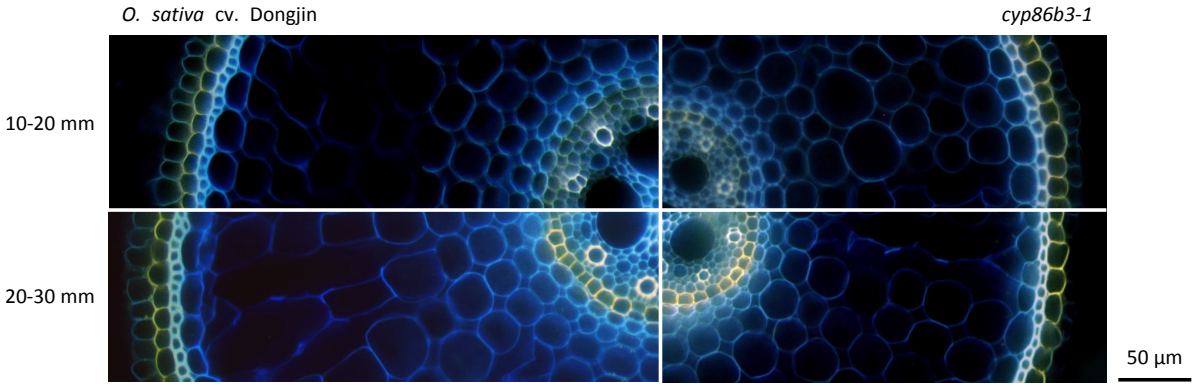

Figure 3.7: Sections of adventitious roots of *O. sativa* cv. Dongjin and the mutant *cyp86b3-1* grown in aerated hydroponics for three weeks. Freehand cross sections of the apical root, 20 mm (top) and 30 mm from the root tip (bottom) stained with Fluorol yellow 088 before fluorescence microscopic examination (excitation filter: bandpass 365 nm, dichroic mirror: coloursplitter 395 nm, barrier filter: longpass 397 nm). Autofluorescent cell walls can be recognised by blue (cortex) to bright blue colour (sclerenchyma) and the suberin lamellae in endodermis and exodermis are specifically stained yellow.

upper pictures. In the bottom row sections of approx. 30 mm from the root tip are shown. The suberised outer tangential cell walls of the exodermis and radial cell walls of the endodermis are intensely yellow, whereas the radial and tangential cell walls appear to be stained to a lesser extend in the exo- and endodermis, respectively. One cell layer away from lignified vessels, which can be recognised by bright white walls inside the central cylinder, are the passage cells in the endodermis which are not suberised. No difference in staining pattern could be found between roots of the WT, on the left, and the mutant, on the right. In contrast to the pictures in figure 3.7, the average root diameter was similar in both lines. Despite the lacking phenotypic evidence chemical analysis of the root suberin was conducted.

3.2.4 Chemical analyses

Apical and basal root suberin of *cyp86b3-1*

To examine the monomer composition of the suberin polyester of *cyp86b3-1* and *-2*, roots grown for 4–5 weeks in hydroponic culture have been prepared according to the method described in chapter 2.5.1. Chemical transesterification and subsequent GC-MS and GC-FID analysis of the isolated suberised root tissues revealed seven different substance classes. The extracted aromatics coumaric acid and ferulic acid constituted the major compo-

nents with 88–93 % in all samples. The main aliphatic constituents were ω-hydroxy acids present in chain lengths of C16 and from C24 to C30. Furthermore, monocarboxylic acids, primary alcohols and α,ω-diacids of the chain lengths C18, C24 or both could be found in traces in most samples. α-Hydroxy acids accounted for up to 62 % of the extractable aliphatic compounds of root tissue after total lipid extraction and transesterification. In contrast to that, this substance class composed only 20 % of the aliphatic fraction in samples which did undergo enzymatic digestion of cell wall carbohydrates first.

The root suberin composition of homozygous KO plants *cyp86b3-1* and their Dongjin background is depicted in figure 3.8. The chemical analysis revealed a complete loss of ω-hydroxy acids with chain length of C24 and higher in the suberin of *cyp86b3-1* of all root parts with different ages. For *cyp86b3-1* and the corresponding WT the suberin of apical (figure 3.8 A) and basal (figure 3.8 B) root sections was analysed separately. The total amount of suberin in the apical 2–4 cm from the root tip was 6.12±1.48 µg cm^{-2} root surface area in Dongjin WT and 2.56±1.56 µg cm^{-2} in *cyp86b3-1* (table 8.2). As long as not expressed otherwise, all values in this section reflect arithmetic means of four or more replicates from individual plants with standard deviation (SD) and significance of difference, based on an unpaired *t*-test with a two-tailed distribution and a significance level of 0.01, is indicated by underlining of the denoted *p*-value.

All suberin monomers were detected in significantly smaller amounts in apical roots of *cyp86b3-1* compared to WT, except of the primary alcohol octadecanol (C18). This effect was reversed for most compounds in the analysis of basal suberin in *cyp86b3-1*. In the 3–6 cm from root-shoot junction total suberin amounts ranged from 17.44±5.07 µg cm^{-2} in Dongjin to 21.64±8.64 µg cm^{-2} in *cyp86b3-1* (table 8.3). Coumaric acid was the only extracted aromatic compound found in significant higher amounts in the basal root parts of *cyp86b3-1*, tested with an unpaired *t*-test with two-tailed distribution and a significance level of 0.1. All aliphatic substances with a portion of more than 5 % to the total suberin were either significantly increased in the mutant or, in case of the ω-hydroxy acids C24–C30, completely absent.

Root suberin of *cyp86b3-2*

Results of the root suberin analysis of *cyp86b3-2* are displayed in figure 3.9. The second investigated allele of *CYP86B3* was characterised by the same suberin phenotype as *cyp86b3-1*. All ω-hydroxy acids with chain lengths of C24 and higher occurring in WT roots were lacking in the KO line.

Heterozygous plants of *O. sativa CYP86B3-2*/*cyp86b3-2* did show the exact root suberin

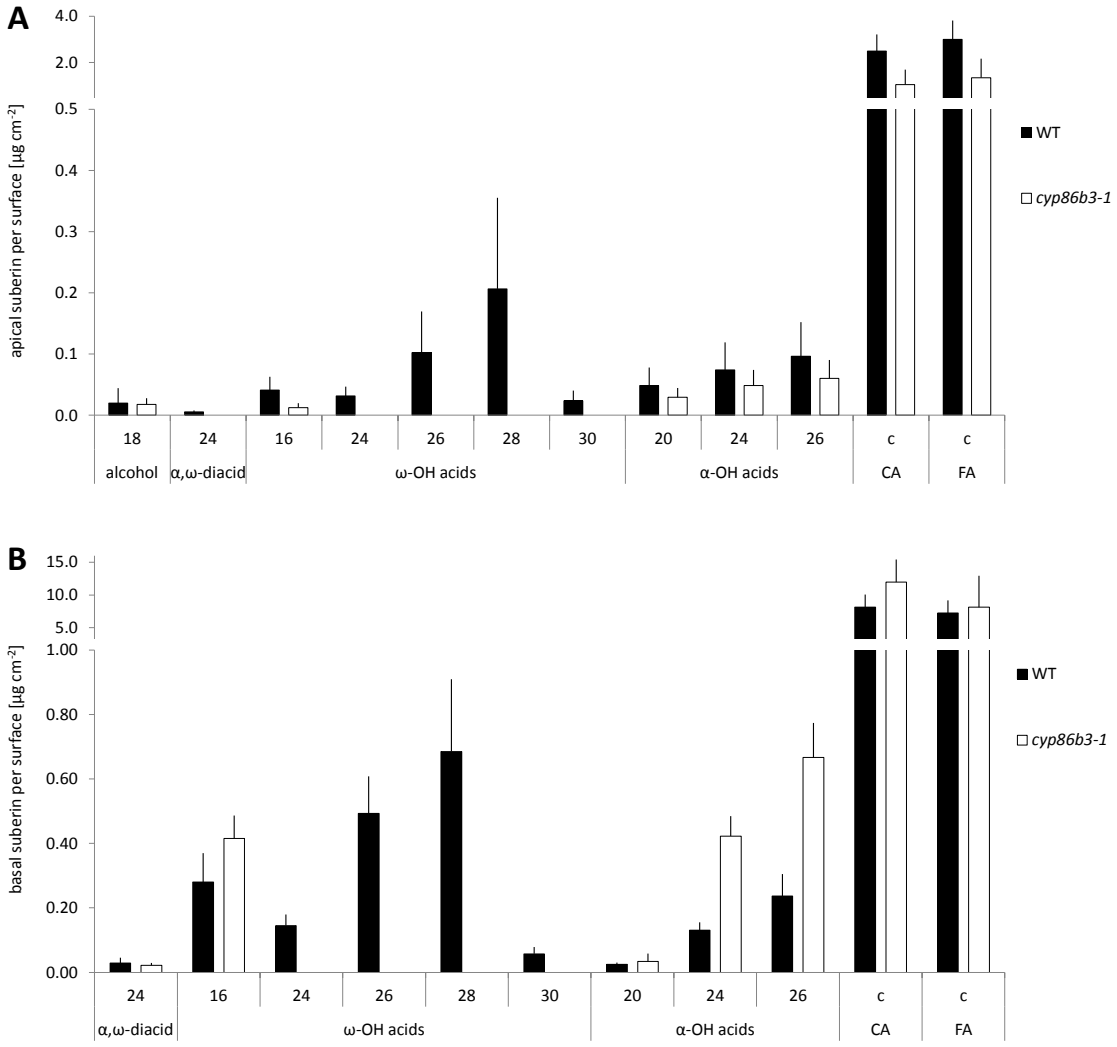

Figure 3.8: Apical (A) and basal (B) root suberin composition of homozygous KO plants *cyp86b3-1* and their Dongjin background. Depicted are amounts of suberin monomers arranged according to substance class and carbon chain length. Bars reflect arithmetic means of four (A) and five (B) replicates respectively from individual plants with 95 % CI in µg cm^{-2} root surface area. Sampling of the most apical 2–4 cm from the root tip without lateral roots (A) and the basal 3–6 cm from the root-shoot junction (B) was conducted after cultivation in aerated hydroponics for 33 d. With α,ω-diacid: α,ω-dicarboxylic acid; ω-OH: ω-hydroxy; α-OH: α-hydroxy; c: cyclic/aromatic substance; CA: coumaric acid; FA: ferulic acid. Absolute values are presented in table 8.2 for A and table 8.3 for B. For the suberin amounts of *cyp86b3-1* related to root dw see figure 8.6.

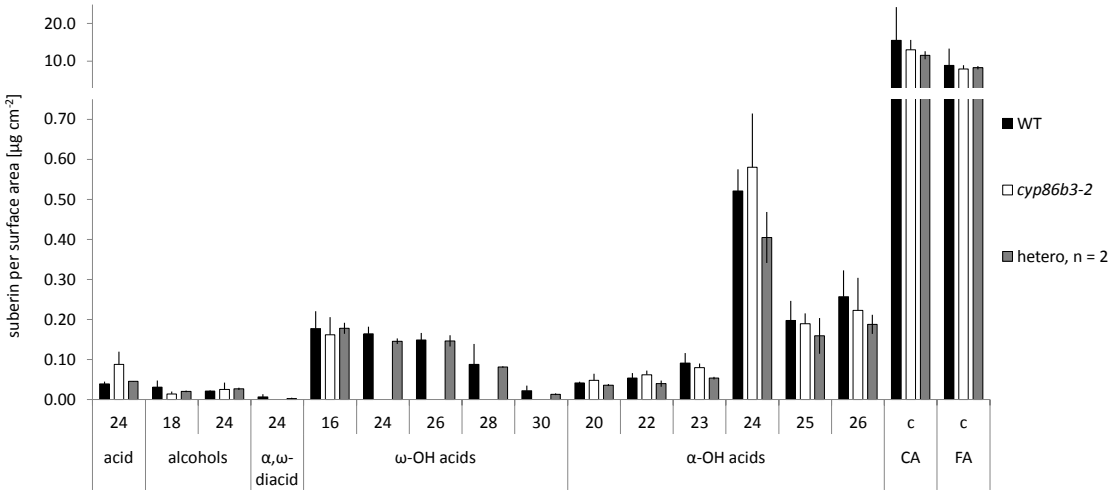

Figure 3.9: Whole root suberin composition of homozygous KO plants *cyp86b3-2* and their Dongjin background. Bars reflect arithmetic means of four (WT), three (*cyp86b3-2*) and two (hetero) replicates from individual plants with 95 % CI and upper/lower value respectively in $\mu g\,cm^{-2}$ root surface area. Sampling was conducted after cultivation in aerated hydroponics for 27 d. With α,ω-diacid: α,ω-dicarboxylic acid; ω-OH: ω-hydroxy; α-OH: α-hydroxy; c: cyclic/aromatic substance; CA: coumaric acid; FA: ferulic acid; hetero: heterozygous for *CYP86B3*/*cyp86b3*. Absolute values of suberin monomer amounts are presented in table 8.4.

phenotype as WT plants. Total amounts of suberin from whole roots (26.27±11.96 µg cm^{-2} in WT and 22.42±3.35 µg cm^{-2} in *cyp86b3-2*, see table 8.4) did not differ from amounts found in basal roots of WT and *cyp86b3-1*. Even though ω-hydroxy acids appeared in increasing amounts from chain lengths of C24 to C28 in samples of the genetic background of *cyp86b3-1*, this pattern could not be observed in the WT samples analysed with *cyp86b3-2*. Here, all extracted ω-hydroxylated fatty acids with chain lengths C16 to C26 were within the range of 0.16±0.02 µg cm^{-2} and amounts of those with higher carbon chain length decreased with increasing molecular size.

Amounts of α-hydroxy acids were increased in all samples processed according to the protocol to collect all extractable free fatty acids. Those root samples were not subjected to enzymatic digestion of cell wall polysaccharides (chapter 2.5.1). The most abundant α-hydroxy acid C24 composed 27 % of the total aliphatic fraction and therefore occurred with a more than three-fold higher amount compared to samples prepared according to the standard protocol. In addition, monomers with three further chain lengths could be detected, even including odd-numbered derivatives of VLCFA (C22, C23 and C25).

Free FAME from roots of *cyp86b3-1*

In order to address the question whether the mutation in *CYP86B3* only causes changes in ω-hydroxy acids of the suberin polyester or as well in lipids upstream in the biosynthetic pathway, a total lipid extraction with subsequent transesterification and analysis via GC-MS and GC-FID was carried out. Besides ferulic acid and six different derivatives of the phytosterol β-sitosterol, which are not specified further in this work, 38 free fatty acid methyl esters and derivatives (FAME) could be extracted and identified and are listed in table 8.5. These aliphatics ranged from chain length of C14 to C30 and were related to the methyl esters of (in order of abundance) monocarboxylic acids, α-hydroxy acids and ω-hydroxy acids, as well as unsubstituted monocarboxylic acids and primary alcohols. In total 8.28±3.56 µg cm^{-2} FAME could be identified related to the surface area of the extracted WT roots. With 8.38±3.56 µg cm^{-2} equal amounts were found in *cyp86b3-1*. The predominant substances were C18 polyunsaturated and C16 monocarboxylic FAME and the whole substance class represented 84.5±7.7 % of the free aliphatics in WT roots, plotted in figure 3.10 in black.

Amounts of the substances already detected in root suberin appeared to be in the same order of magnitude in the solvent extractable lipid fraction. Every single ω-hydroxylated FAME reflected almost exactly the corresponding amount in suberin and in *cyp86b3-1*, depicted in figure 3.10 in white, ω-hydroxy acids C24–C30 were completely reduced in

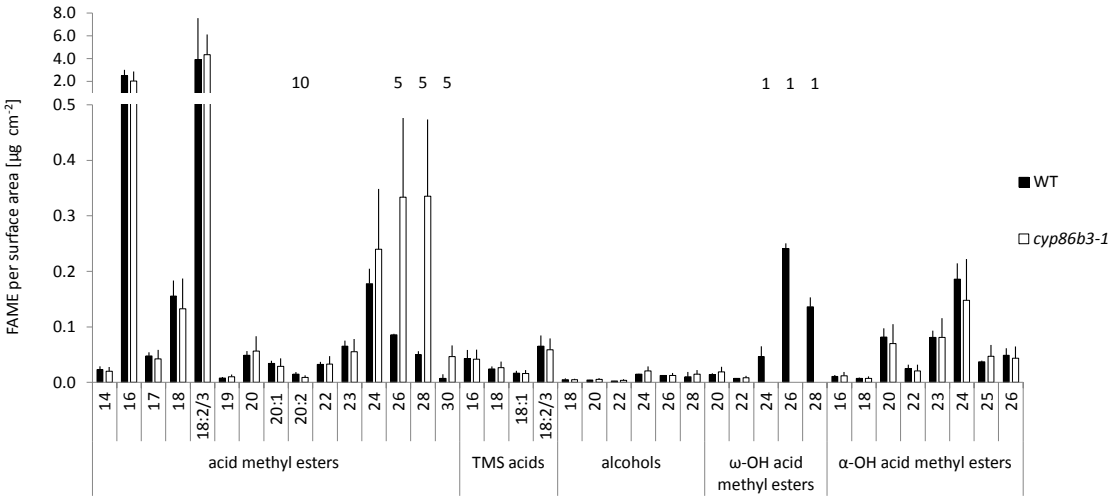

Figure 3.10: Solvent extractable fatty acid methyl esters (FAME) per surface area from roots of homozygous KO plants *cyp86b3-1* and their Dongjin WT background. Depicted are amounts of FAME, deriving from total lipid extracts of ground roots, from plants grown in aerated hydroponics for 33 d. Extracts were transesterified, analysed by GC-FID and are arranged according to substance class and carbon chain length with number of double bonds if applicable. Bars reflect arithmetic means of three (WT) and four (*cyp86b3-1*) replicates from individual plants with 95 % CI in µg cm^{-2} and numbers above bars indicate the significance levels of difference in per cent (unpaired *t*-test with two-tailed distribution). With FAME: fatty acid methyl ester; TMS: trimethylsilyl; ω-OH: ω-hydroxy; α-OH: α-hydroxy. Absolute values of FAME amounts are presented in table 8.5.

the same manner. However, monocarboxylic FAME increased significantly (for $\alpha = 0.05$) in the mutant and to the same extent as the amounts of ω-hydroxy acids of the corresponding chain length decreased.

3.2.5 Effects of the altered suberin in *cyp86b3-1* on root physiology

To approach the question of the physiological impact caused by the total loss of ω-hydroxylated VLCFA in *cyp86b3-1*, various stress treatments and tracer experiments have been performed.

For investigations presented in this work rice seeds were either incubated for germination on moistened tissue paper for 10 d before transfer of the seedlings to aerated hydroponics, or transferred to unaerated nutrient solution shortly after germination at the fifth day after imbibition with start of aeration at around day 11. Both procedures led to plants

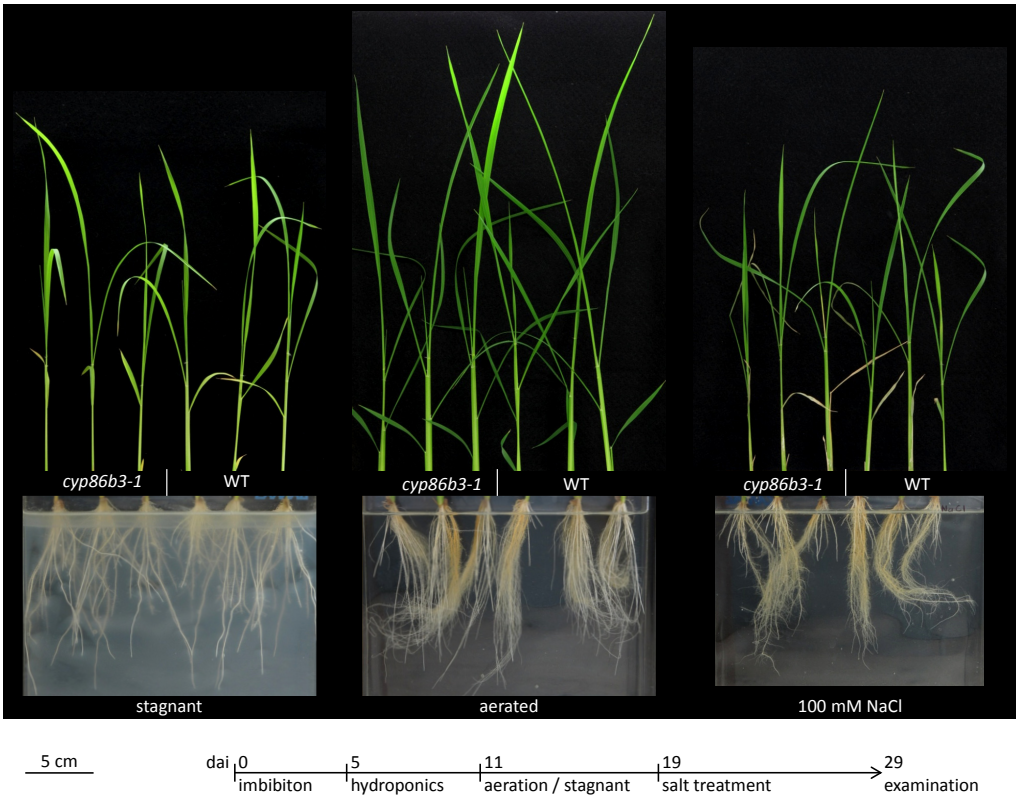

Figure 3.11: Phenotype of *cyp86b3-1* and Dongjin rice plants (WT) after cultivation for 29 d under different conditions. After initial cultivation under equal conditions, plants were either grown for 18 d in aerated hydroponic culture, deoxygenated 0.1 % agar solution (stagnant) or 10 d in 100 mmol L^{-1} NaCl solution. With dai: days after imbibition.

not different in phenotype at time of examination around 4–5 weeks after germination. Germination rates of seeds were seed quality dependent and could not be related to the genotype of the examined lines.

Stress treatments

Aeration of nutrient solution or, in case of the stagnant treatment, cultivation in deoxygenated 0.1 % agar solution was started 11 dai. For the salt stress treatment aerated hydroponics were spiked with 100 mmol L^{-1} sodium chloride eight days later. A scheme of these growth conditions is represented in figure 3.11 together with the resulting phenotypes of *cyp86b3-1* and the genetic background Dongjin four weeks after germination. Three plants are shown for each treatment. Plants grown under stagnant condition were smaller, de-

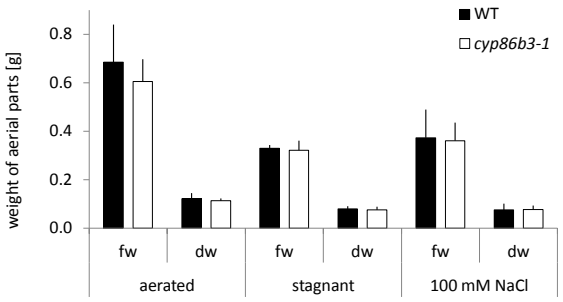

Figure 3.12: Weights of aerial parts of *cyp86b3-1* and Dongjin rice plants after growth in either aerated hydroponics, deoxygenated 0.1 % agar solution (stagnant) for 18 d, or 100 mmol L^{-1} NaCl containing nutrient solution for 10 d, both at time point of harvest (fw) and after drying (dw). With fw: fresh weight; dw: dry weight.

veloped less and yellowish leaves and less but thicker roots compared to control plants grown with aeration, which had longer, healthy green leaves and developed much longer seminal roots. Salt stressed plants had the same number of leaves as control plants, but leaves 1–3 (in order of emergence) were wilted severely and whole plants were considerably smaller; seminal roots had the same length whereas adventitious roots in particular were only about half as long as the roots of the control plants.

Plants of *cyp86b3-1* did not show any growth or development related visible phenotype under the conditions examined. Leaves and roots of the mutant and its background WT looked exactly alike under aerated and stagnant conditions. Even under the salt stress, which was applied for 10 d, no significant difference was observable. Only some leaves of the WT appeared less wilted, though this effect was considered to be in the range of overall variation. This result is reflected in both fresh weight and dry weight of leaves of all plants. Arithmetic means of the weight of whole green parts of three plants of each line and treatment, represented with standard deviation in figure 3.12, did not differ between both lines. Leaf weights of the WT and mutant plants which were grown under standard conditions (0.69±0.16 g and 0.60±0.09 g, respectively) were twice as high as those of the plants cultivated in stagnant medium (WT: 0.33±0.01 g, *cyp86b3-1*: 0.32±0.04 g) or under salt stress, which were at least 40 % smaller (WT: 0.37±0.12 g, *cyp86b3-1*: 0.36±0.07 g).

Visualisation of ROL

Roots of the stressed as well as of control plants were stained in deoxygenated agar solution with methylen blue to visualise radial oxygen loss (ROL) into the surrounding medium. In figure 3.13 representative selections of roots or, in case of the salt stressed plants, whole root systems are depicted after incubation for 80 min in the dark. In zones comprising lateral roots, those and the main root were stained, as well as the surrounding medium. An intermittent stain pattern occurred in apical roots of plants grown under stagnant conditions, which was not apparent in control roots. The basal root zone always remained unstained

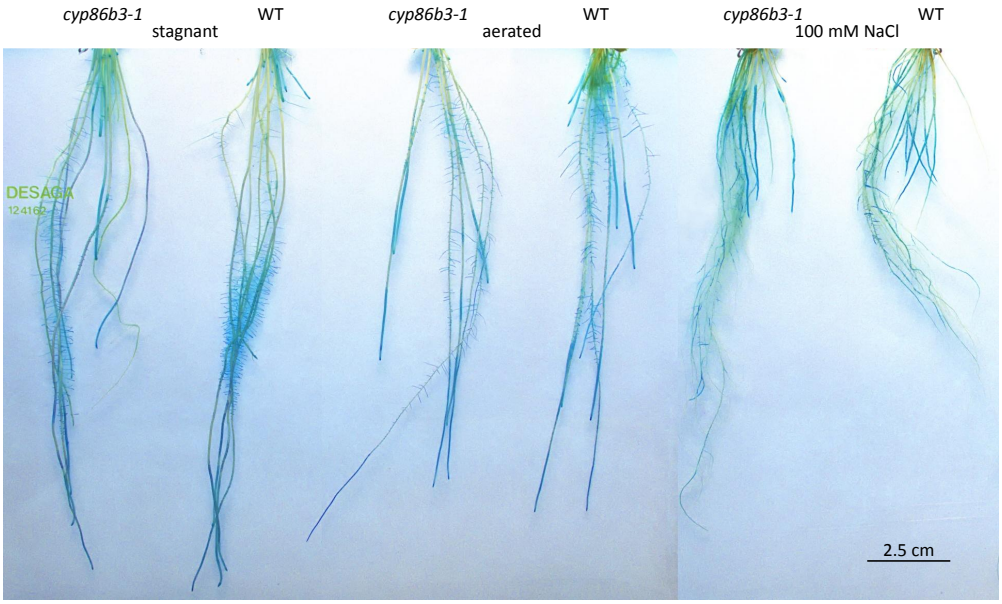

Figure 3.13: Methylen blue stain indicating radial oxygen loss from roots of *cyp86b3-1* and Dongjin WT plants after growth in either aerated hydroponics, deoxygenated 0.1 % agar solution (stagnant) for 18 d or 100 mmol L^{-1} NaCl containing nutrient solution for 10 d. Depicted are representative selections of roots or whole root systems (NaCl treatment) stained for 80 min in the dark.

with exception of roots shorter than 2 cm. Except of the furthermost root tips of some of the salt stressed plants, all apical root parts were stained up to a certain length, which is evaluated in figure 3.14. Besides the bars, reflecting arithmetic means of continuous methylen blue stain from root tip in mm with 95 % CI, numbers of replicates are provided in the bars and above those the significance levels of difference in per cent are given, based on an unpaired *t*-test with two-tailed distribution. Apical parts of roots grown in aerated hydroponic culture were stained 20 % more in the mutant *cyp86b3-1* (21.18±3.07 mm from root tip) than in WT roots (17.61±1.51 mm), whereas in roots grown under stagnant conditions the stain in WT exceeded that in the mutants significantly by 35 % (with 24.63±5.82 mm and 15.89±2.47 mm, respectively). No significant difference was found between mutant and WT in the extent of apical root stain after the salt stress treatment.

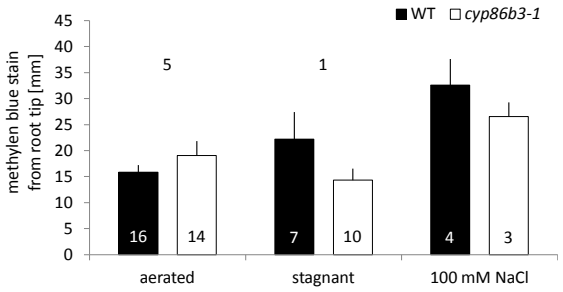

Figure 3.14: Quantification of ROL from *cyp86b3-1* and WT roots longer than 30 mm grown under standard, stagnant and salt stress conditions. Bars reflect arithmetic means with 95 % CI of continuous methylen blue stain from root tip in mm, with numbers of replicates in the bars and above the significance levels of difference in per cent (unpaired *t*-test with two-tailed distribution).

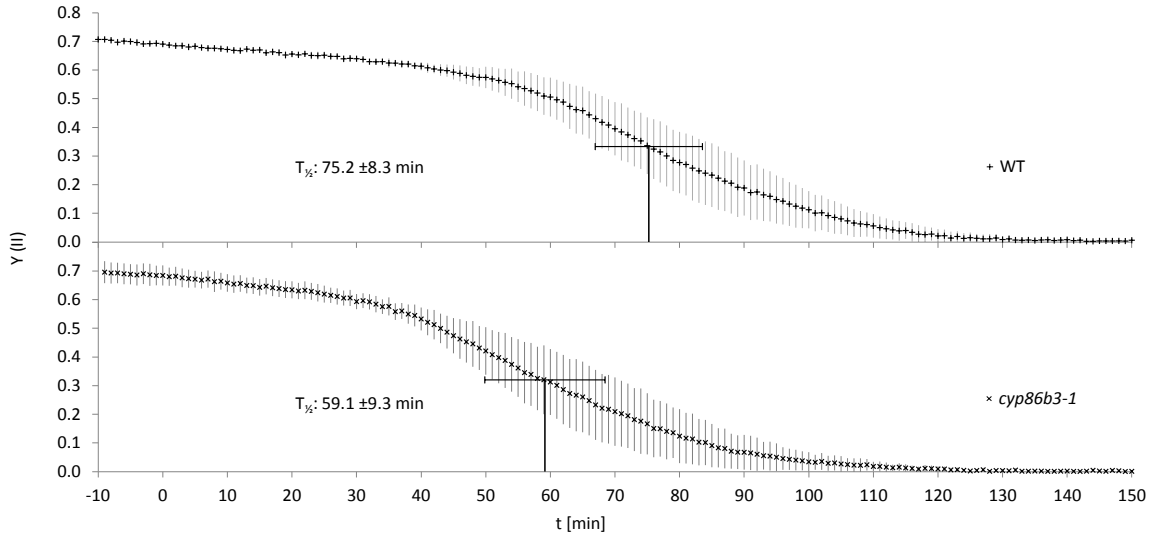

Figure 3.15: Inhibition of photosynthesis by Metribuzin applied via hydroponic solution in leaves of *cyp86b3-1* and the Dongjin background. Treatment was conducted after cultivation in aerated hydroponics for 27 d. Plotted are arithmetic means of photochemical yields monitored via PAM fluorometer of 7 individual plants against time after treatment in minutes. Black vertical lines mark half times of total inhibition. Error bars reflect 95 % CI. With Y(II): photochemical yield of photosystem II; t: time after start of treatment; $T_{\frac{1}{2}}$: half time of total inhibition.

Monitoring of Metribuzin uptake via PAM

Beside the attempts to measure hydraulic conductivity of roots directly via root pressure probe and pressure chamber (data not shown), the herbicide Metribuzin was used as a tracer to characterise altered root barrier properties in *cyp86b3-1*. Photosynthetic yields of the photosystem II (Y II) were monitored via pulse-amplitude modulation (PAM) fluorometers in leaves at equal distances from the root-shoot junction, as described in chapter 2.7.3. The herbicide was applied to roots with hydroponic solution and the resulting decrease of photosynthetic yield was monitored and plotted against time after initiation of treatment, see figure 3.15. At this point all plants had a Y II between 0.60 and 0.74. Half times of total inhibition (arithmetic means of time from application to point of half-maximal inhibition, with 95 % CI) of photosynthesis revealed a faster uptake of Metribuzin in plants carrying the mutation in *CYP86B3* in comparison to WT, with 59.1±9.3 min and 75.2±8.3 min, respectively. An unpaired t-test with two-tailed distribution and a significance level of 0.05 gave statistical evidence. The mean time from start of treatment to maximal inhibition recorded (less than 1 % of initial photosynthetic yield) was 120.6±9.7 min in WT and with 104.6±13 min in the mutant significantly different (for $\alpha = 0.1$). Thus, the half time of total inhibition is 13 % shorter in *cyp86b3-1* compared to control plants, which indicates a loss in barrier properties.

3.3 Heterologous expression of *CYP86B3* in *A. thaliana*

3.3.1 Cloning

In order to further examine the function of *CYP86B3* in plant lipid metabolism, the gene was cloned and heterologously expressed in *A. thaliana* plants mutated in the closest sequence related cytochrome P450 genes, which featured severe suberin phenotypes. As described in chapter 2.4.4 the Gateway® system was used to clone the coding sequence (CDS) of *CYP86B3* under control of the promoter of *RALPH*, known to be specifically expressed in roots. A template was established via RT-PCR on Dongjin root RNA amplifying CDS *CYP86B3*, and cloned into the donation vector pDONR™/Zeo in a recombinating BP reaction. The resulting entry vector was amplified and selected in *E. coli* before confirmation via restriction digest and sequencing. A scheme of the resulting entry vector is depicted in figure 3.16. Only three out of 22 selected entry clones had solely minor point mutations in the inserted CDS *CYP86B3* without causing frame shifts. Those errors, indicated in yellow in figure 3.16, were eliminated by recombining two entry constructs with

restricted enzyme digestion and ligation of the respectively selected fragments.

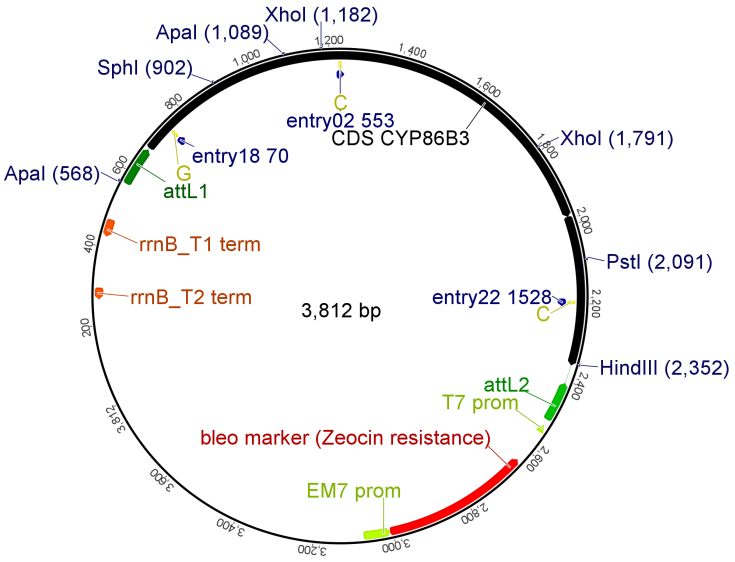

Figure 3.16: Vector map of the entry construct resulting from the BP reaction cloning CDS *CYP86B3* into pDONR™/Zeo. With CDS *CYP86B3* in black, PCR mutations labelled with entry clone identifier and bp from start codon in blue and point mutation in yellow, as well as restriction sites of enzymes used in this work outside of plasmid.

To express the gene of interest specifically in *A. thaliana* root tissue undergoing suberisation, an expression vector was needed. Therefore, the CDS of *CYP86B3*, placed on the entry vector, was cloned into a destination vector downstream of the promoter region of *AtCYP86B1* via the LR reaction of the Gateway® system as described in chapter 2.4.3. A scheme of the resulting expression construct is depicted in figure 3.17. Its overall size and *in silico* predicted locations of restriction sites on both, the destination vector part and the inserted CDS were confirmed via restriction digest before transformation of *A. tumefaciens*. Clones of transformed *A. tumefaciens* were positively tested by cultivation on selection medium containing rifampicin and kanamycin as well as by colony PCR with primers targeting both, the CDS *CYP86B3* and a part of the sequence of the destination vector pMDC99 on the expression vector. This positively transformed strain was then used to transform *A. thaliana* plants via floral dip as described in chapter 2.4.4.

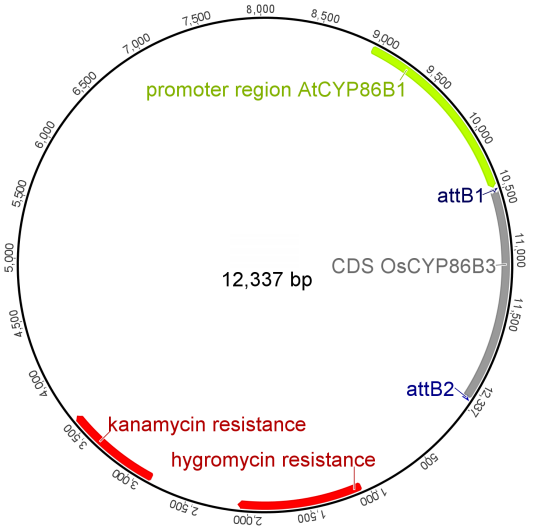

Figure 3.17: Vector map of the expression construct p*Ralph*:CDS *CYP86B3* featuring the coding sequence of *OsCYP86B3* downstream of the promoter region of *AtCYP86B1* and antibiotic resistance genes for selection, as used for *A. tumefaciens* mediated transformation of *A. thaliana*.

3.3.2 Transformation of knockout mutants *ralph* and *ralph*/*horst*

In figure 3.18 graphical representations of the *A. thaliana* alleles *horst* (A) and *ralph* (B) are depicted. Shown are CDS of the genes and binding sites of primers, which are listed in table 2.5. Black triangles represent sites of T-DNA and transposon insertions, in the *A. thaliana* KO lines SALK_107454 and SM.37066, in A and B respectively.

To confirm homozygous *A. thaliana* mutants *ralph* and *ralph*/*horst* as well as their successful transformation with the construct p*Ralph*:CDS *CYP86B3* (figure 3.17), a competitive PCR with DNA extracted from leaf tissue was performed. To amplify genes of interest, two gene specific primers and one primer addressing the corresponding inserted T-DNA or transposon sequence were used. Results are depicted in figure 3.19. Combination of the primers LS331, LS332 and LS186 (A) led to a product of approx. 474 bp when used in a PCR with template DNA from *A. thaliana* mutants *ralph* (templates 2, 3 and 5) and *ralph*/*horst* (templates 1 and 4). This size was expected for alleles carrying the transposon insertion SM.37066. However, the PCR with WT DNA, which served as positive control, produced the expected amplicon of 1030 bp which could not be found in PCR products based on DNA from homozygous mutants. The use of the primers LS138 and LS139 which are specific for the genomic sequence of *CYP86A1*, resulted in a band of 970 bp in all samples from *ralph* and WT plants. Though, in combination with LS347, targeting the T-DNA insertion left border region in *horst*, a single band of approx. 485 bp was produced in the reaction with DNA from double KO *ralph*/*horst* (B). A PCR with the primers LS590 and LS943, which target the CDS of *CYP86B3*, and the templates 1

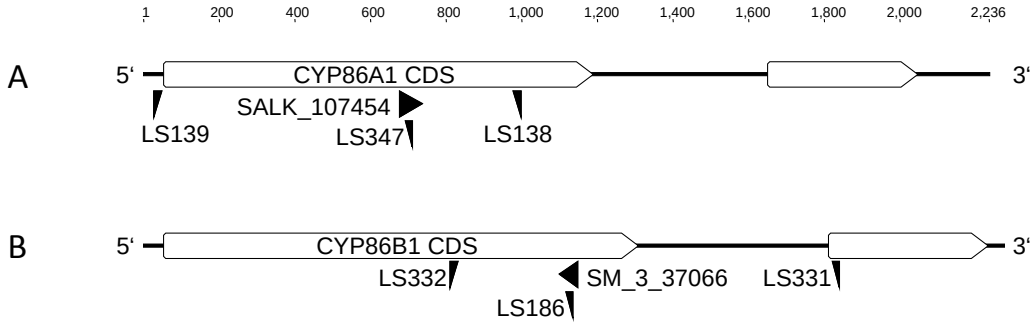

Figure 3.18: Schematic structure of the alleles *horst* (A) and *ralph* (B). Wide triangles typify T-DNA (A) or transposon insertions (B), narrow triangles represent binding sites of gene-specific primers or those specific to the inserted DNA sequence. Length of genomic sequences are proportional to the scale in bp above.

(*ralph*/*horst*::p*Ralph*:CDS *CYP86B3*), 2 (*ralph*::p*Ralph*:CDS *CYP86B3*) and the entry vector used as positive control did result in a single band of the expected corresponding size of 400 bp (see figure 3.19 C). For further propagation and examination of the heterologous expression lines, the positively tested plants 1 and 2 were selected.

3.3.3 Root suberin of *ralph* and *ralph*/*horst* with p*Ralph*:CDS *CYP86B3*

To examine suberin phenotypes of the *A. thaliana* mutants *ralph* and *ralph*/*horst*, which were positively tested to be transformed with p*Ralph*:CDS *CYP86B3*, in comparison with their respective genetic backgrounds, roots grown in hydroponic solution for 20 d were harvested, scanned and prepared according to chapter 2.5.1. Chemical analysis of the root suberin via GC-MS and GC-FID revealed a partial complementation of the mutant phenotypes. Arithmetic means of suberin monomers per root dry weight (dw) are depicted in figure 3.20 with 95 % CI and in table 8.6 and table 8.7 values with standard deviation are provided. 25 different aliphatic monomers of chain lengths from C18 to C26 could be identified. Amounts of total suberin ranged from 5.71±0.18 µg mg^{-1} dw in Col-8 to 3.43±0.62 µg mg^{-1} dw in the complemented *ralph*/*horst* double KO mutant. Most abundant monomers in WT roots were α-hydroxy acid C24, mono unsaturated ω-hydroxy acid C18:1 and α,ω-diacid of the same chain length. α-Hydroxy acids constituted a major part in all samples and comprised up to 57 % of the total aliphatic fraction in case of the

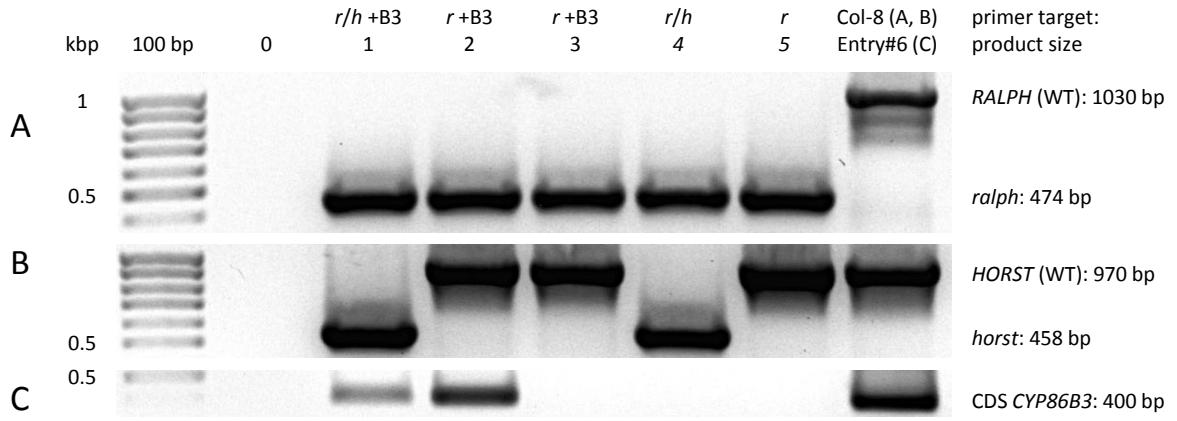

Figure 3.19: Genotyping of the heterologous expression lines complementing *ralph* (A) and *ralph*/*horst* (A and B) with p*Ralph*:CDS *CYP86B3* (C). With kbp: kilo base pairs; 100 bp: 100 bp DNA-ladder, extended; 0: negative control (H_2O_{HPLC}); 1–5: DNA templates of respective plants; *r*/*h*: *ralph*/*horst*; *r*: *ralph*; B3: p*Ralph*:CDS *CYP86B3*; Col-8 and Entry#6: positive control with WT DNA and the entry clone plasmid, respectively.

double KO. Amounts of ω-hydroxylated VLCFA were significantly reduced in roots of the KO mutant *ralph* in comparison to WT plants, monomers of chain length C22 and C24 in particular with a total loss of the latter. On the contrary, monocarboxylic acids C20–C24 were increased.

Since only one plant of the complemented single mutant could be analysed, no statistical evidence can be provided. Nevertheless, in *ralph*::p*Ralph*:CDS *CYP86B3* root suberin contained nearly the exact amounts of ω-hydroxy acids C22 and C24 of the WT, whereas the increased amount of the fatty acid C22 resembled that of the uncomplemented mutant *ralph*, as visualised in figure 3.20 A.

A total reduction of the ω-hydroxy acids C22 and C24 was observed for the double KO *ralph*/*horst* as well. Additionally, the quantities of ω-hydroxy acids of all chain lengths were strongly reduced. ω-Hydroxy acids C16, C18 and C18:1 constituted only 25–30 % of the amounts observed in WT plants. α,ω-Dicarboxylic acids C18, C18:1 and 20 were also significantly reduced. After transformation with p*Ralph*:CDS *CYP86B3* the double KO phenotype was only partially complemented. As in the complemented single KO mutant, amounts of ω-hydroxy acids C22 and C24 were increased in comparison to *ralph*/*horst*, but did not resemble the WT. Amounts of monomers with the chain lengths C16 to C20, both ω-hydroxy acids and α,ω-diacids, were equal in *ralph*/*horst* and *ralph*/*horst* complemented with p*Ralph*:CDS *CYP86B3* and significantly less compared to the WT Col-8.

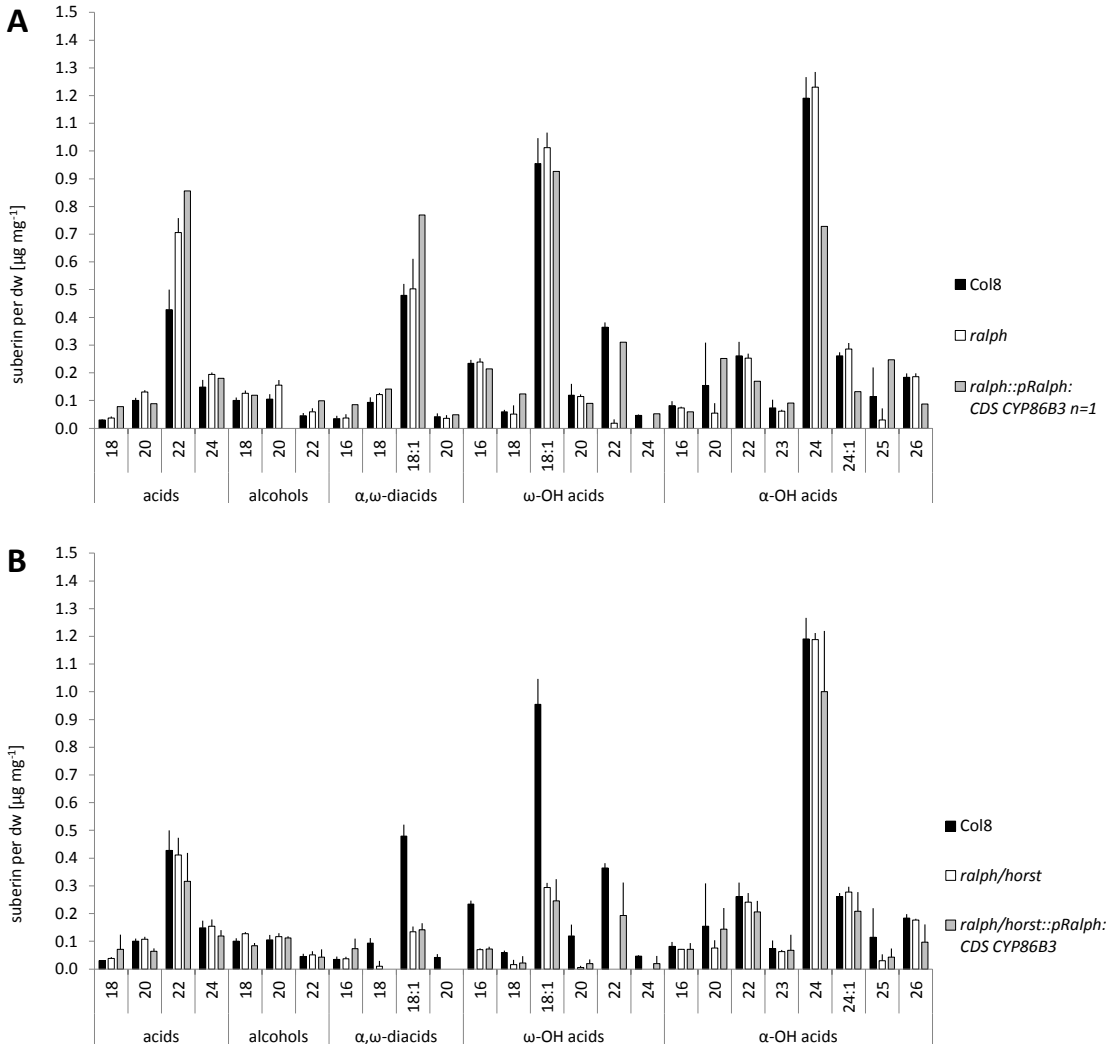

Figure 3.20: Root suberin composition of *A. thalina*, KO plants *ralph* (A) and *ralph*/*horst* (B) as well as their corresponding lines complemented with CDS *CYP86B3*. Depicted are amounts of suberin monomers arranged according to substance class and carbon chain length with number of double bonds if applicable. Bars reflect arithmetic means of four replicates from individual plants (three for Col-8, one for *ralph*::p*Ralph*:CDS *CYP86B3*) with 95 % CI in $\mu g\,mg^{-1}$ dw. With α,ω-diacids: α,ω-dicarboxylic acids; ω-OH: ω-hydroxy; α-OH: α-hydroxy; Col8: *A. thaliana* WT Columbia (Col-8). See table 8.6 and table 8.7 for lists of values.

Summary of results

A number of suberin candidate genes in *O. sativa* were identified in *in silico* studies as putative orthologues of *A. thaliana* genes involved in suberin biosynthesis. One candidate, the cytochrome P450 enzyme *CYP86B3* was characterised with the help of T-DNA insertion lines. Plants mutated in *CYP86B3* were altered in root suberin composition by a loss of ω-hydroxy acids with chain lengths from C24 to C30 in particular. Heterologous complementation of the suberin phenotype of the *A. thaliana* knockout mutant *ralph* indicated a role of CYP86B3 as ω-hydroxylase of very long chain fatty acids with carbon chain lengths from C24 to C30 in the root suberin of the native organism *O. sativa* and of substrates of chain lengths C22 and higher in *A. thaliana*. The lack of ω-hydroxy acids C24–C30 in the root suberin of *O. sativa* mutants *cyp86b3* led to an increased solute uptake into the plant indicating decreased suberin barrier properties.

4 Discussion

4.1 Selection of suberin candidate genes in *O. sativa*

During the last years many attempts were made to elucidate the pathway of suberin biosynthesis. Results of analytical studies of suberin monomer composition implied certain needs in biochemical pathways to obtain the substance classes and chain lengths found within the aliphatic polymer. First biochemical approaches gave insights into enzymes involved as summarized by Kolattukudy (2002). Though lipid biosynthesis mutants with altered composition of cuticular waxes or of the cutin polymer often have distinct phenotypes, such as glossy surfaces or organ fusions, changes in the secondary metabolism interfering with the formation of suberin rarely lead to phenotypes which are easy to screen. Thus, recent studies focused more on reverse genetic approaches than classical genetics and helped to picture a refined model of the biosynthesis pathway of suberin in *A. thaliana* (Molina and Franke, 2013; Franke et al., 2012). Based on the suberin pathway enzymes which have already been characterised, databases were explored and closest sequence related genes in *O. sativa* could be named. The results are depicted in neighbor-joining phylograms in figure 8.1 to figure 8.4. The protein classes considered here comprised cytochrome P450 enzymes (CYP), β-ketoacyl-CoA synthases (KCS), glycerol-3-phosphate acyltransferases (GPAT), ABC-transporters and peroxidases. Their relevance in the suberin biosynthetic pathway will be discussed in the following paragraphs.

4.1.1 β-Ketoacyl-CoA synthases

The neighbor-joining phylogram in figure 8.2 depicts sequence relations of β-ketoacyl-CoA synthases (KCS) of *A. thaliana* and *O. sativa*, putatively involved in root suberin synthesis. Only *A. thaliana* KCS involved in suberin monomer elongation and closest sequence related *O. sativa* genes were selected.

KCS2 and *KCS20* (At1g04220 and At5g43760 respectively) are both expressed in the endodermis of *A. thaliana* roots (Franke et al., 2012) and code for functionally redun-

dant enzymes (Lee et al., 2009). Though *KCS20* is expressed in all organs and strongest in seedlings, leaves and flowers, *KCS2*, the gene encoding the docosanoic acid synthase (*DAISY*) is mainly expressed in roots besides flowers and siliques. In *daisy* roots fatty acids and their derivatives with chain length exceeding C20 were significantly decreased in suberin, C22 monocarboxylic acid in particular with only 46 % of the amounts found in WT, whereas shorter aliphatics accumulated (Franke et al., 2009). The decrease of VLCFA was relatively small, which might be caused by the redundant function of KCS2 and KCS20. This assumption is in line with the finding that the chain length dependent effect of decreased amounts of VLCFA is greater in double KO mutants.

The closest related genes in *O. sativa* are LOC_Os05g49900, LOC_Os02g11070 and LOC_Os06g39750 (described as Wax Crystal-Sparse Leaf1 (*WSL1*) by Yu et al. (2008)), as depicted in figure 8.2. However, their expression pattern, as provided by microarray data, did not indicate that these genes could be involved in suberin metabolism and at time of acquisition either no mutation lines were listed in the databases provided by MSU, Salk Institute and RAP or mapping turned out to be incorrect. LOC_Os11g37900, which is located on a separate branch of the *DAISY* subclade in the neighbor-joining phylogram, was expressed in all tissues of adult plants with highest transcript levels in the sheath and basal roots according to Genevestigator. The organ specific expression pattern was similar to that of the cytochrome P450 gene *CYP86B3* but expression rates were significantly higher (data not shown). Stagnant growth conditions, shown to induce suberisation (Kotula et al., 2009), led to a twofold increase of LOC_Os11g37900 transcript level in outer part of roots (OPR, see figure 1.1) of hydroponically grown *O. sativa* examined by laser microdissection and microarray (personal communication, Katsuhiro Shiono, Fukui Prefectural University, Japan). In figure 3.3 tissue specific expression of LOC_Os11g37900 is visualised and opposed to that of other suberin candidate genes. The expression pattern resembles the spatial distribution of tissues undergoing suberisation. Genevestigator data (bars in figure 3.3) showed a higher transcript abundance in root compared to leaf tissue. The semi-quantitative RT-PCR revealed highest expression of LOC_Os11g37900 in root parts 4–7 cm from tip, corresponding to mid-length of the root, followed by the most apical 2 cm, those tissues which are still developing suberin under aerated control conditions. Lowest expression was monitored in leaves and the most basal 2 cm of roots. A stress treatment with 200 mmol L^{-1} NaCl for 2 h increased expression in the basal root parts. These exact conditions were used before to induce expression of suberin metabolism related genes (Krishnamurthy, 2008) in *O. sativa* and Krishnamurthy et al. (2009) proved that 25 % and 50 % of the NaCl concentration used here, increased the abundance of both

aromatic and aliphatic suberin in the outer part of the root (OPR) as well as in the endodermal tissue of apical and basal root segments. Besides the inducibility by salt stress and an organ specific expression widely consistent with that of KCS2 (Franke et al., 2009), LOC_Os11g37900 shares 66.5 % identical amino acids based on an alignment via MUSCLE and 67.2 % with KCS20, the other of the two closest related *A. thaliana* KCS. Considering this, the gene LOC_Os11g37900 is the best candidate for a *DAISY* orthologue but no T-DNA or transposon insertion mutant lines could be acquired to evaluate its role in suberin, cutin or wax metabolism. Meanwhile, RNA interference (RNAi) lines as well as overexpression lines targeting LOC_Os11g37900 have been established by Nishiuchi Shunsaku in the work group of Mikio Nakazono (Laboratory of Plant Genetics and Breeding, Nagoya University, Japan) and will be matter of thorough investigation in future.

Different kinds of osmotic stress treatments induced the ubiquitous expression of *KCS1* (At1g01120) in *A. thaliana* (Joubès et al., 2008), which was highest in reproductive organs, stems and least in roots, where it could be located to the endodermis (Franke et al., 2012). In *kcs1-1* T-DNA KO plants all wax components with chain length from C20 to C30 were decreased in above ground organs, whereas most FAME extracted from roots accumulated, with doubled amounts of dicarboxylic acids in particular (Todd et al., 1999). LOC_Os03g14170 and LOC_Os10g07010 represent the *O. sativa* genes with sequences closely related to this KCS which is potentially involved in suberin metabolism. Expression of both genes is strongest in sheath and roots with medium and low signal intensity respectively on Rice Genome 51K array according to Genevestigator. Additionally, LOC_Os03g14170 and LOC_Os10g07010 were induced by either salt stress (Genevestigator) or under stagnant conditions (personal communication, Katsuhiro Shiono, Fukui Prefectural University, Japan), exhibiting both as good suberin candidate genes. Unfortunately no positive mutant lines could be acquired for this study.

Based on sequence homology to *FAE1* (James et al., 1995), a condensing enzyme involved in fatty acid elongation from C20 to C22 in seeds of *A. thaliana*, Millar et al. (1999) found and described *CUT1* (At1g68530), a gene expressed in *A. thaliana* stem epidermal cells, coding for a VLCFA condensing enzyme, which led to waxless male sterile plants when suppressed with a 35S-sense construct of the same gene. Mutants of the identical *CER6* were significantly altered in the composition of aliphatic wax of stem and of leaf cuticles by a strong decrease of all compounds with chain length exceeding C28 and the male sterility could be attributed to the same effect on pollen surface (Fiebig et al., 2000). Besides the fact that *CER6*, also referred to as *KCS6*, is not expressed in roots and specifically elongates wax components of *A. thaliana* the putative orthologue in *S. tuberosum* (shar-

ing 94 % amino acid sequence similarity) is necessary for elongation of fatty acids and their derivatives contributing to the suberised phellem, which is part of the potato tuber periderm (Serra et al., 2009). Amounts of suberin and associated waxes were significantly decreased in compounds with chain length of C28 and higher in all substance classes when *StKCS6* was silenced by RNAi, whereas all shorter VLCFA derivatives accumulated. *StKCS6* was expressed mainly in the tuber periderm, about ten times less in leaves and to an even smaller extent in roots of *S. tuberosum*. It has to be mentioned that tubers of *S. tuberosum* are terminal thickenings of stolons, horizontally or downwards growing stems. Thus, the expression of the closest related KCS in *O. sativa*, LOC_Os03g12030, which was discovered by Krishnamurthy et al. (2009) to be specific for stem and leaf tissues, is consistent with that of *AtKCS6* and *StKCS6*. In comparison, the transcript level in roots was very low but peaked 30 min after application of 200 mmol L^{-1} NaCl.

Based on the mentioned results of previous studies, focus was laid on the next closest related gene in this work, LOC_Os05g49290 (see figure 8.2). As depicted in figure 3.3 the KCS-like gene is almost equally expressed in all tissues tested, except for the middle root section, where a peak of expression coincides with the highest rate of suberin accumulation under control conditions in aerated hydroponic solution. The salt stress treatment induced only a slight increase of the already strong expression in basal roots under control conditions. In contrast, all other genes tested were expressed more root specific and were strongly inducible by salt stress. The strong ubiquitous expression of LOC_Os05g49290 points to a more general role of of the gene in the lipid metabolism of the whole plant and an involvement in wax or even cutin biosynthesis. Though this effect seems quite clear and special care was taken to create primer pairs specific for the target genes, one has to keep in mind that the big number of KCS genes within one species share high sequence identity, which could cause mispriming during PCR and thus could lead to falsified results.

According to the RiceGE database, three lines mutated in the gene LOC_Os05g49290 are available, of which PFG_3A-07289 could not be obtained at time of acquisition and PFG_2D-10814 most probably was mapped to a wrong location since a BLAST with three different right border flanking sequences led to a number of different loci with high sequence identities other than LOC_Os05g49290.

However, seeds of the line PFG_3A-17504 could be obtained, which is annotated to feature a T-DNA insertion in the CDS of LOC_Os05g49290. Besides relatively high numbers of seeds which did not germinate and of dying seedlings, plants of this mutant line were significantly smaller compared to Dongjin WT and produced mainly empty panicles either in growth chamber or green house. Whether this was actually caused by the mutation

itself or by other factors such as plant pathogenic infected stock seeds, could not be determined. However, now a small amount of segregating seeds is available and potential lipid phenotypes of the line mutated in LOC_Os05g49290 will be investigated.

4.1.2 Glycerol-3-phosphate acyltransferases

Glycerol-3-phosphate acyltransferases of *A. thaliana* and *O. sativa* with potential involvement in suberin metabolism are depicted in the neighbor-joining phylogram in figure 8.4 according to their sequence similarity. When *GPAT5*, normally expressed in roots, seeds and strongest in flowers of *A. thaliana*, was knocked out, polyester bound lipids of seeds were reduced by 50 %, with almost total reduction of fatty acids, their hydroxylated derivatives and diacids with chain lengths from C20 to C24 in particular (Beisson et al., 2007). The changes in the plants lipid pathway caused a higher seed coat permeability for tetrazolium stain but storage lipids in seeds were not altered in *gpat5*. A preference of GPAT to transfer acyl-CoA to the *sn-2* position of glycerol-3-phosphate is responsible for this pathway selectivity. It was proposed that this results in a pool of glycerol *sn-2*-acyl esters, lysophosphatidic acid in case of GPAT5, which are incorporated in apoplastic polyesters and excluded from lipids predetermined for storage (Yang et al., 2010). In roots of *gpat5* seedlings grown for one week on vertical agar plates the same compounds were reduced as in seeds, though to a lesser extent and except of diacids. However, after three weeks nearly all substance classes and chain lengths of root suberin were affected, primary alcohols in particular (Beisson et al., 2007). In *A. thaliana* over-expressing both *GPAT5* and *CYP86A1*, the typical suberin monomers C20–C22 ω-hydroxy acids and α,ω-diacids occurred in stem cutin, whereas the separate over expression of these genes did not alter the native composition (Li et al., 2007).

GPAT7 had characteristics widely similar to GPAT5, but a more specific role in biosynthesis of wound suberin was proposed (Yang et al., 2012). Enzymes involved in polyester synthesis of both seed coat and root suberin, have been described before, such as the P450 enzyme RALPH (Compagnon et al., 2009).

The GPAT-like gene in *O. sativa* with highest amino acid sequence homology to members of the GPAT5/7 subclade in figure 8.4 is LOC_Os05g38350. The gene is expressed almost ubiquitously at very low levels according to Genevestigator (figure 3.2), but RT-PCR analysis (figure 3.3) revealed strongest expression in tissue undergoing suberisation in mid-length of roots. The salt stress treatment for 2 h increased expression of LOC_Os05g38350 in basal roots with lesser transcript abundance in the middle root parts. The expression pattern was similar to that of other suberin candidate genes tested from different enzyme

classes, but tissue specificity was less pronounced.

In a co-expression analysis with the web tool RiceFREND (Sato et al., 2013) based on microarray data, LOC_Os05g38350 was identified to be co-expressed with *CYP86B3*, which was shown in this work to be essential for ω-hydroxylation of VLCFA in root suberin, see figure 4.1. The spatial distribution of the expression of LOC_Os05g38350 within tissues undergoing suberisation, its stress inducibility as well as its sequence identity of 60.8 % to AtGPAT5 indicate a role in the suberin pathway as glycerol-3-phosphate acyltransferase. Meanwhile homozygous seeds of the mutant line PFG_2C-30271, carrying a T-DNA insertion in the only intron of LOC_Os05g38350, could be selected and propagated and will be basis for KO characterisation in future studies.

4.1.3 ABC transporters

In a comparative expression study aiming at genes involved in the suberin lipid metabolism, an ABC transporter was found to be 32 times stronger expressed in cork of *Q. suber* compared to wood tissue, which was highly homologous to At5g13580 (ABCG6) (Soler et al., 2007). This ABC-2 type transporter family gene is co-expressed with known suberin genes in *A. thaliana*, suggesting an involvement in suberin biosynthesis. Together with two other closely sequence related uncharacterised *A. thaliana* genes, At3g55090 (ABCG16) and At1g53270 (ABCG10), it clusters with LOC_Os03g17350 (see figure 8.4), frequently referred to as RCN1 (reduced culm number) or OsABCG5 in recent literature (Yasuno et al., 2009; Ureshi et al., 2012), which is, according to Genevestigator, differentially expressed in *O. sativa* roots and upregulated under heavy metal stress as well as treatment with abscisic acid (ABA). Additionally, it is co-expressed with the root suberin ω-hydroxylase *CYP86B3* indicating a role in the suberin pathway (see figure 4.1). Another suberin candidate in *A. thaliana* is At1g53270 (ABCG10), with high homology to the dimerising ABC transporters ABCG11 and ABCG12, which are required in cuticle formation and are therefore expected to be involved in the corresponding lipid transport (McFarlane et al., 2010). At1g53270 is differentially expressed in *A. thaliana* roots and within those, in the endodermis in particular. Its putative orthologue in *O. sativa* is LOC_Os01g42900, which has highest transcript abundance in nodes, stigma, crowns and roots according to Genevestigator.

None of the ABC transporters which are potentially involved in suberin biosynthesis were further investigated in this work, due to either overlapping interests with collaborating scientists or lack of appropriate plant material.

4.1.4 Peroxidases

Besides findings of transferases mediating ester bonds between acyl-CoA and either glycerol or ferulic acid (Yang et al., 2012; Molina et al., 2009), peroxidases are expected to initiate polymerisation of the poly-phenolic domain in suberin (Bernards et al., 2004). In co-expression analyses two putative peroxidase genes were co-regulated with *RALPH*, a monooxygenase of suberin monomers described by Compagnon et al. (2009), At1g68850 on a high level and At5g15180 still significantly (Diehl, 2011). Both genes were specifically expressed in apical and At1g68850 additionally in basal root parts. Based on amino acid homology, their orthologue peroxidases in *O. sativa* can be expected to be LOC_Os06g16350 and either LOC_Os03g36560 or LOC_Os07g34710 as visualised in the phylogenetic tree in figure 8.3, which provides a selection of peroxidases closely related to the two aforementioned *A. thaliana* candidates. The expression pattern of LOC_Os07g34710, with highest transcript abundance in pollen tissues, indicated a role other than in root suberin formation. LOC_Os03g36560 was expressed in roots with a peak in the tip and inducible by bacterial pathogens as revealed by microarray data collected by Genevestigator. Expression of LOC_Os06g16350 was highest in root tissues and 3.3-fold increased by stagnant growth conditions (personal communication, Katsuhiro Shiono, Fukui Prefectural University, Japan) and treatment with ABA (Garg et al., 2012). The result of a co-expression analysis, which was carried out via the RiceFREND web tool (Sato et al., 2013) and based on the suberin involved ω-hydroxylase *CYP86B3*, is depicted in figure 4.1. The aforementioned putative peroxidase LOC_Os06g16350 appears at the third level from the guide gene, indicating a connection between the roles of both genes in the plants metabolism. The expression pattern and the co-expression with *CYP86B3* suggests a function of LOC_Os06g16350 in tissues undergoing suberisation.

4.1.5 Cytochrome P450 monooxygenases

The gene At2g27690, coding for CYP94C1, was chosen because the enzyme was demonstrated to metabolize a range of fatty acids with chain lengths C12 to C18, by exclusively hydroxylating the ω-postition, when heterologously expressed in *Saccharomyces cerevisiae* (Kandel et al., 2007). According to Genevestigator the gene was ubiquitously expressed at low levels in *A. thaliana*, and was wound and methyl jasmonate activated in tests by Kandel et al. (2007) thus being a candidate to build up wound suberin. Heitz et al. (2012) reported an important role of CYP94C1 in the turnover of the wound-induced phytohormone jasmonoyl-isoleucine, but not in apoplastic polyesters as cutin. Used as an outgroup

in the amino acid alignment, CYP94C1 did not cluster with suberin candidates in *O. sativa*, see figure 8.1, and was not further investigated.

In roots of five week old *A. thaliana* plants with mutated *CYP86A1*, amounts of ω-hydroxy acids and α-ω-diacids of chain lengths C16 to C18 mainly were sharply decreased, reducing the total amount of suberin by approx. 60 % (Höfer et al., 2008). Together with preceding studies (Benveniste et al., 1998), CYP86A1 could be declared as *ω-hydroxylase of root suberized tissue* (HORST) of fatty acids with chain lengths smaller than C20. CYP86A9 (LOC_Os01g63540) was the closest sequence related CYP in *O. sativa*. Krishnamurthy (2008) reported an increased expression of *CYP86A9* in root tissues sampled after 30 min of treatment with 200 mmol L^{-1} NaCl. This effect was strongest in the salt stress tolerant *O. sativa* cultivar Pokkali, which accumulated more root suberin under control conditions than other cultivars tested. Examination of *CYP86A9* was not continued since unpublished microarray data revealed upregulation under the suberin inducing conditions of deoxygenated hydroponic medium of all candidate genes except for the corresponding LOC_Os01g63540 (personal communication, Katsuhiro Shiono, Fukui Prefectural University, Japan).

In the phylogenetic tree, see figure 3.1 and figure 8.1, CYP86A10 (LOC_Os02g44654) and CYP86A11 (LOC_Os04g47250) formed a separate subclade but shared 58.3 % and 57.3 % identical amino acids respectively with HORST. Expression data, based on beforementioned so far unpublished microarray, was promising. Although the expression of LOC_Os02g44654, as depicted in the heatmap in figure 3.2 based on Genevestigator, was weak and restricted to the crown (the part of the culm where adventitious roots develop), it was 2.4 times higher after exposure to oxygen deficient medium according to microarray data (personal communication, Katsuhiro Shiono, Fukui Prefectural University, Japan). As can be seen in figure 3.3, the expression level was low in comparison to other candidate genes tested. However, with highest transcript abundance in samples taken from around 50 % of the entire root length and an increase in the whole root after salt stress, the expression was specific for tissues undergoing suberisation. Meanwhile, RNAi lines as well as overexpression lines targeting CYP86A10 were established by Nishiuchi Shunsaku in the work group of Mikio Nakazono (Laboratory of Plant Genetics and Breeding, Nagoya University, Japan) which provides the opportunity for thorough investigation in future.

Although only weak activity of LOC_Os04g47250 was monitored in reproductive organs by Genevestigator, see figure 3.2, and no signal was detected via RT-PCR, see figure 3.3, expression of the gene in roots which have been exposed to stagnant conditions, increased by the factor 3.2 in comparison to samples from control conditions in a microarray (per-

sonal communication, Katsuhiro Shiono, Fukui Prefectural University, Japan). However, no mutant lines could be obtained to investigate the role of LOC_Os04g47250 in suberisation.

The discrepancy between different *in silico* expression data evaluations shown in this work can be explained by different datasets used by Genevestigator. The organ expression heatmap in figure 3.2 relies on all microarrays in the database providing any information about different tissues, whereas the bars opposed to RT-PCR results in figure 3.3 are based on a subset of the data originating from a certain treatment.

The 23 times higher transcript abundance of a gene in cork compared to wood of the tree *Q. suber* (Soler et al., 2007) provided good evidence that the closely sequence related *A. thaliana* gene *AtCYP86B2* is involved in suberin biosynthesis. *A. thaliana* members of the CYP86B subclade shown in figure 3.1 were first described by Diehl (2008). Tissue specific transcript information collected by Genevestigator revealed expression in all tissues tested, strongest in roots and approx. 35–65 % less in silliques, flowers, stems and leaves. Its corresponding mutant line *cyp86b2* was not significantly altered in root suberin. Since CYP86B1 and CYP86B2 share 67.3 % identical sites in amino acid sequence, and furthermore a highly similar genetic structure with a congruent intron position and location on the same arm of chromosome 5, one most probably is the product of a relatively recent copy event of the other and functional redundancy might account for the missing effect in the single mutant. The double KO mutant with the allele *horst*, *cyp86a1*/*cyp86b2*, did not differ from the *horst* single mutant in suberin composition and the double KO mutant with *ralph*, *cyp86b1*/*cyp86b2* could not be generated due to the contiguous location of both genes on the chromosome (Diehl, 2011).

In contrast to the CYP86A subclade, which comprises one *A. thaliana* and three *O. sativa* members, only one *O. sativa* enzyme belongs to the CYP86B subclade, as can be seen in figure 3.1. This suberin candidate, CYP86B3, corresponds to the orthologue CYP86B1 in *A. thaliana*, as listed by Nelson et al. (2004), who predicted the following orthologues based on sequence comparison, leaving CYP86A7 and CYP86A8 related to pseudogenes in *O. sativa*: AtCYP86A1 (At5g58860)/OsCYP86A9; AtCYP86A2 (At4g00360)/OsCYP86A10; AtCYP86A4 (At1g01600)/OsCYP86A11. According to Bak et al. (2011) there are five CYP86A and two CYP86B in *A. thaliana*, whereas in *O. sativa* there are four CYP86A and one CYP86B. One explanation for this distribution might be that HORST, as a member of the CYP86A sublclade, is a monooxygenase which is specific for substrates of shorter carbon chain length, which are more common in the plants lipidome, in waxes and in cutin in particular. Assuming that a high sequence homology of enzymes correlates with their

specificity for substrates with similar characteristics, such as carbon chain length, a wider variety of enzymes might be required in lipid pathways to provide a wide range of fatty acid derivatives of chain length less than C22 in different tissues. In contrast, the occurrence of VLCFA and their distinct derivatives which are characterised by carbon chain lengths of C22 and higher, is limited to only a few tissue types which implies a smaller number of the corresponding enzymes such as the members of the CYP86B subclade.

CYP86B1 (RALPH) was described as a monooxygenase of VLCFA involved in biosynthesis of ω-hydroxy acids of chain lengths C22 and higher in *A. thaliana* (Compagnon et al., 2009; Molina et al., 2009). Since CYP86B3 was the only *O. sativa* enzyme in the CYP86B subclade, this enzyme could easily be assigned to the orthologoue representative CYP86B1.

According to Genevestigator *CYP86B1* was strongly expressed in roots, to a lesser extent in flowers and siliques and least in stems and leaves. The expression in roots was confirmed by Diehl (2008) via RT-PCR, highest in the middle part and least in the tip, but no transcript was detected in aforementioned organs listed by Genevestigator. *CYP86B1* promoter activity was visualised using a promoter-GUS construct and mainly corresponded to the tissues affected in polyester composition in the mutant *ralph*; the suberised root endodermis, and seed coat in particular. Expression of LOC_Os10g34480 (*CYP86B3*) is visualized in figure 3.2 and figure 3.3. As far as tested *CYP86B3* is expressed in the same tissues in *O. sativa* as *CYP86B1* is expressed in *A. thaliana*. The expression pattern correlates with tissues expected to be undergoing suberisation: strongest at mid-length of roots, here 4–7 cm, where the suberin lamellae is formed under aerated control conditions (Kotula et al., 2009; Ranathunge et al., 2011a) and strongly increased in basal and apical root sections after a treatment with 200 mmol L^{-1} NaCl for 2 h. Although this salt concentration was shown to be lethal to *O. sativa*, it activated the expression of genes which are expected to be involved in suberin biosynthesis (Krishnamurthy, 2008). However, when only 100 mmol L^{-1} NaCl were applied for one week, amounts of suberin were increased in whole roots (Krishnamurthy et al., 2009).

24.5 % amino acid sequence identity was observed when all seven members of the CYP86 subclades A and B from *A. thaliana* and *O. sativa* were aligned with MUSCLE; amino acid sequences of the CYP86B subclade shared 50 % and CYP86B1 and CYP86B3 shared 62 % identical sites. As mentioned in chapter 1.3.2 CYP are characterised by a high variability in amino acid sequence, enabling their diverse substrate specificity, but they are very similar in overall protein structure and their highly conserved motifs. On the one hand this indicates the high homology of cytochrome P450 putatively involved in plant lipid biosynthesis in general, on the other hand the double amount of identical sites gives a hint at the

common role of CYP86B1 in *A. thaliana* and CYP86B3 in *O. sativa*.

4.2 Suberin of *O. sativa*

The substance classes and chain lengths of aliphatic suberin monomers in roots of *O. sativa*, which were identified in the course of this work, basically reflect the results of previous studies on the matter (Schreiber et al., 2005; Ranathunge et al., 2011a). Main components are C16 and C24–C30 ω-hydroxy acids and varying lesser contents of α,ω-dicarboxylic acids, monocarboxylic acids, α-hydroxy acids and alcohols. However, total amounts per root surface area were smaller by a factor of two but the amounts of aromatics were equal compared to the above mentioned results of Ranathunge et al. (2011a). Some differences might be attributed to the different varieties tested.

In all root samples from *O. sativa* tested in this work the fraction of extracted aromatic suberin, comprising coumaric and ferulic acid (Schreiber et al., 1999), represented the main part with 88–93 % of the total suberin. This is in line with previous studies of suberin in *O. sativa* (Schreiber et al., 2005). In the grass *Hordeum marinum* significantly higher amounts of aliphatic suberin were found in the basal half of roots compared to the apical half, but this was not found for the aromatics (unpublished data, not shown) extracted under comparable conditions as described in chapter 2.5.2 and used in this work. The same effect was found in *Z. mays*, where the aliphatic suberin strongly increased with maturation from the apical root zone I to the basal root zone II, whereas the aromatic fraction of zone I was already equal in mass to the aliphatic fraction of zone II and did not increase any further (Schreiber et al., 2005). Even though this differs in *O. sativa*, it provides an indication that the high amounts of coumaric and ferulic acid extracted together with the aliphatic suberin from Graminean roots at least partially derive from tissues other than exodermis and endodermis, assuming that the aliphatic suberin develops later. As visualised under UV light (see figure 3.7), cell walls of the sclerenchyma and the central cylinder in *O. sativa* are strongly autofluorescent (blue to white in contrast to the yellow fluorescence of the Fluorol yellow stain), which is caused by the aromatic components of lignin. Additionally to these strongly lignified tissues, the unmodified walls of cortical cells are autofluorescent, those of the first cell layer behind the sclerenchyma and the last before the endodermis in particular, indicating aromatic cell wall components. However, this might be due to indirect illumination by the autofluorescence signal of adjacent cell walls and does not necessarily reflect the existence of lignin. When digested root tissues were separated to the OPR on the one hand, composed of rhizodermis, exodermis, scle-

renchyma and one layer of cortex cells, and the central cylinder including the endodermis on the other hand, the ratio of aromatic to aliphatic suberin was approx. 2:1 (Ranathunge et al., 2011a), significantly lower than in this work, where no tissue separation was conducted. This supports the hypothesis of an aromatic fraction derived from cortex cell walls. However, since the main part of cortex including aerenchyma was removed, an increase under stagnant conditions of both aliphatic and aromatic compounds by the same factor strongly suggests a change in the suberised barriers exodermis and endodermis and that the hydroxycinnamic acids coumaric and ferulic acid, highly abundant in the Gramineae, are significantly contributing to those structures.

The compound class of α-hydroxy fatty acids was found to be highly variable depending on sample preparation (see chapter 2.5.1). In suberin fractions of the present work these fatty acids hydroxylated on the second carbon constituted up to 62 % from solvent extracted and transesterified root samples of undigested root tissue and only 20 % after a precursory enzymatic digestion of cell wall carbohydrates (compare figure 3.9 and figure 3.8, respectively). A high variability was also found between previous studies. In extracted *O. sativa* suberin monomers only C18 and C20 α-hydroxy acids (referred to as 2-hydroxy or 2-OH acids) were found, either contributing minor to the total suberin (Schreiber et al., 2005), or were prominent components in the root polyester extract (Ranathunge et al., 2011a). *A. thaliana* leaf cutin comprised 13.93 % α-hydroxy acids, whereas only 0.12 % were found in root suberin (Franke et al., 2005). A comparison of cutin monomers which were solvent extracted either from isolated cuticles or from whole leaves, revealed significantly higher amounts solely of α-hydroxy acids in leaves. This indicates, that α-hydroxy acids are either retained during total lipid extraction by the undigested cell wall due to the size of their esters, or somehow linked to the cell wall carbohydrates, which would also explain the differences between amounts released from digested and undigested root tissues in this work. In contrast to lignified cell walls, the suberin lamellae are deposited between plasma membranes and cell walls. Even though the differences are obvious, the cuticle is deposited on outer walls of epidermal cells alike and one can only speculate about a role of α-hydroxy acids in the connection of the hydrophobic polymer matrices cutin and suberin to the cell wall carbohydrates or in impregnation of the latter as lipophilic embedding. More plausible indeed is the reasoning, why this substance class was excluded from cutin and suberin models (Pollard et al., 2008): Molina et al. (2006) expected the moiety of α-hydroxy acids in transesterified lipid extracts from *Brassica napus* seeds to derive mainly from sphingolipids, which add to storage lipids as well as to membranes in cells but not to the cell wall polymers cutin, suberin or the seed coat polyester.

4.3 The role of CYP86B3 in the suberin biosynthesis of *O. sativa*

4.3.1 *In silico* analyses of the CYP86B subclade

Although one of the biggest gene families, with 244 genes only in *A. thaliana*, all cytochrome P450 enzymes share certain characteristic motifs which were localised in CYP86B3, see figure 3.4 and described in detail in chapter 3.2.1. The motif search at MEME for sequences of a user-defined length of maximal 50 aa, resulted in three sequence sections of which two contained nearly all P450 motifs. However, MEME motif 2 did not include any of the general P450 motifs (Bak et al., 2011) and seemed to be more specific for the subclade CYP86B. Comparing a slightly extended selection of 57 amino acids (including MEME motif 2) in all CYP86B sequences of *A. thaliana* and *O. sativa*, 82.5 % of the sites are identical, whereas only 47.4 % of the residues of all members of the CYP86 clade are the same. Members of the subclade CYP86A share 66.7 % identical amino acids of this sequence. The very high sequence similarity of the MEME motif 2 indicates a common functionality within CYP86B members. One such function could be substrate recognition, although in alignments including CYP86A1 and CYP84A1, for which substrate recognition sites (SRS) were published (Duan and Schuler, 2005; Nelson et al., 2008), only SRS2 falls into MEME motif 2, one out of six SRS.

In Schuler and Rupasinghe (2010) subclade CYP86B members of the cytochrome P450 enzymes in *A. thaliana* and *O. sativa* were compared on the basis of sequence alignments. In this context 62–79 % of pairwise identical amino acids were observed over the whole sequences, similar to the results described in chapter 3.2.1. The comparison of SRS "with absolute conservation in SRS4 (20 aa) and SRS5 (9 aa), high conservation in SRS2 (0–2/7 differences) and SRS6 (1/7 differences), moderate conservation in SRS1 (5–6/23 differences) and somewhat less conservation in SRS3 (1–4/8 differences)" is even more interesting. Furthermore, according to protein models which were compared, the catalytic site is unusually large, with only 3/22 differences in between CYP86B1, -B2 and -B3. These highly conserved predicted substrate binding structures and sequences suggest that the orthologues *CYP86B1* and *CYP86B3* specifically accept the identical substrates.

The co-expression network depicted in figure 4.1, which was constructed via the RiceFREND web tool (Sato et al., 2013) under the use of *CYP86B3* as guide gene, displays genes that are probably functionally related because of their common spatial and temporal expression pattern as well as inducibility by certain treatments. The appearance of

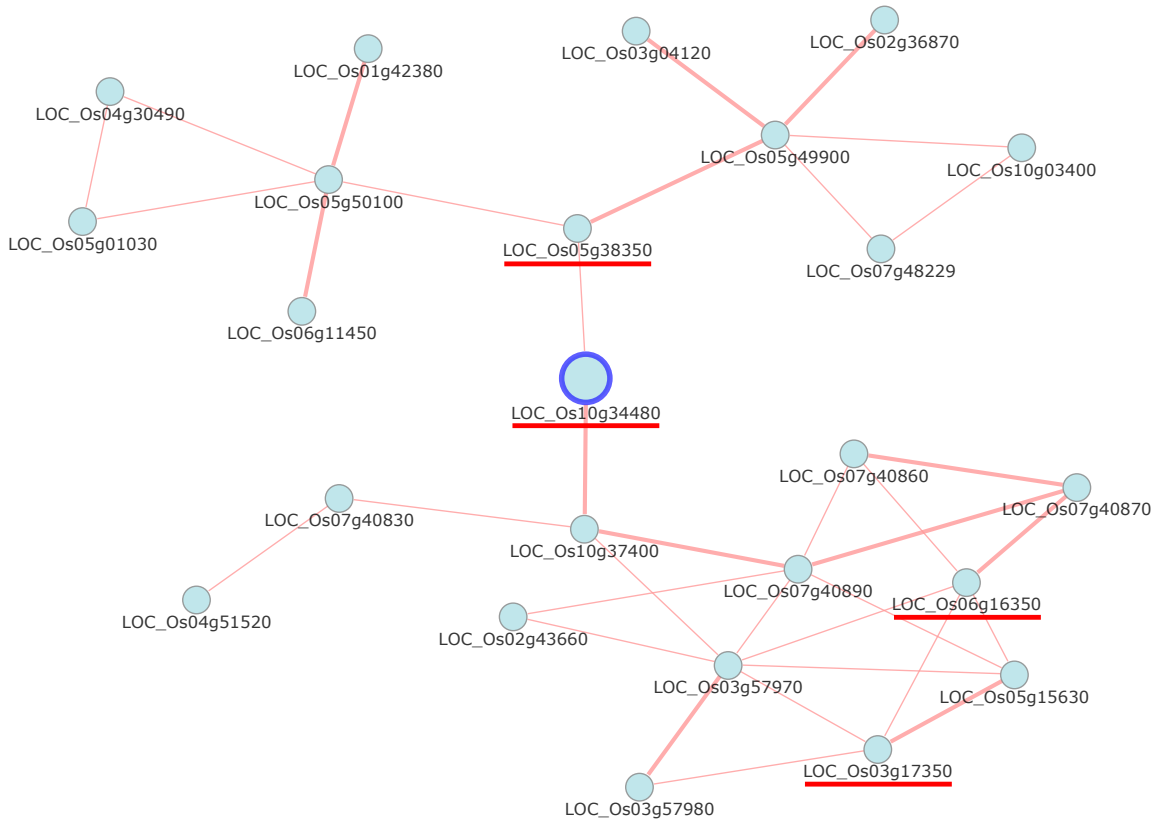

Figure 4.1: Network of genes co-expressed with LOC_Os10g34480, built with the web tool RiceFREND (Sato et al., 2013) based on microarray data available from ricefrend.dna.affrc.go.jp. Underlined are suberin candidate genes, selected by amino acid sequence comparison, which were included in *in silico* studies in this work. For annotated functions of the genes see table 8.1.

three genes, which have been selected in this work by amino acid sequence comparison to genes involved in suberisation of *A. thaliana* root tissues, points again to their suggested roles in the suberin pathway in *O. sativa*. These genes are the putative GPAT5 orthologue LOC_Os05g38350, the ABC-transporter LOC_Os03g17350 and the peroxidase like LOC_Os06g16350, see table 8.1.

4.3.2 *CYP86B3* mutants

The mutant lines PFG_4A-02646, PFG_1B-19308 and PFG_2B-30065, here referred to as *cyp86b3-1*, *cyp86b3-2* and *cyp86b3-3*, were positively tested to carry the annotated T-DNA insertions in the intron region of *CYP86B3* or 950 bp upstream of its start codon as visualized in figure 3.5. Stable homozygous seeds of *cyp86b3-1* and its corresponding WT were propagated and selected, whereas of *cyp86b3-2* and *-3* only seeds segregating for the mutation could be produced so far. The results of a competitive PCR genotyping for this exact T-DNA insertion are depicted in figure 8.5 B, indicating 4 WT, 2 heterozygous and 6 homozygous KO plants for *cyp86b3-2*. A PCR genotyping *cyp86b3-3*, see figure 8.5 C resulted in a ratio of 3:1:6 (WT/heterozygous/mutant). A ratio of 1:2:1 according to the Mendelian inheritance was expected from a heterozygous parent in the diploid *O. sativa*, resulting in a segregating set of genes featuring all three identifiable genotypes. Cross- and self-pollination between plants of different genotypes regarding either *cyp86b3-2* or *cyp86b3-3* might have caused the observed ratio of 2:1:3 or 3:1:6 respectively, but the sample number of 12 is obviously to small for a conclusion. Root suberin of the tested *cyp86b3-2* plants was analysed and the results presented in chapter 3.2.4 and visualized in figure 3.9 is in line with the identified genotypes.

Although mutants which were homozygous for *cyp86b3-3* could be identified, no gene KO was caused by the T-DNA insertion. The RT-PCR with primers targeting an intron spanning part of the CDS of *CYP86B3* revealed expression in all samples. Variability of band intensity in figure 3.6 B can be related to template concentration as depicted in figure 3.6 A and was independent of the T-DNA insertion in *cyp86b3-3* as tested by genotyping (see figure 8.5 C). This result proves the expression of *CYP86B3* to be unaffected by the mutation in the promoter region in *cyp86b3-3*. The insertion site of 950 bp upstream of the start codon of *CYP86B3* is obviously located too far away to influence regulatory elements of the promoter. Whereas pGA2715, the T-DNA vector used for mutagenesis of *cyp86b3-1*, carries an enhancer element based on the 35S promoter of the cauliflower mosaic virus, which is used to increase expression of genes down stream of the insertion side, pGA2707, the vector causing the mutation in *cyp86b3-3*, does not (Jeong et al., 2002). Thus, en-

hanced expression of *CYP86B3* in *cyp86b3-3* can neither be expected nor found, as the RT-PCR results in figure 3.6 B revealed (compare WT samples 3 and 6 to the mutant samples 1, 2, 4 and 12). Therefore, *cyp86b3-3* was not subject of further investigation.

4.3.3 Suberin phenotype of *cyp86b3* loss-of-function mutants

Histology

In histological studies aiming at differential developmental effects of the KO in *cyp86b3-1*, the lipophilic polyaromatic fluorochrome Fluorol yellow 088, also named Solvent Green 4, was used to specifically stain lipophilic domains, which were described as the suberin lamellae in endo- and exodermis of roots (Brundrett et al., 1991). The epifluorescence microscopic images are depicted in figure 3.7. The early development of suberin lamellae in comparison to *O. sativa* japonica cv. Azucena examined in previous studies (Ranathunge et al., 2011a) can most likely be attributed to the different cultivar. In the top row of figure 3.7 the outer tangential exodermal cell walls are already stained, giving a continuous signal of faint yellow in a distance of less than 20 mm from the root tip. At maximal 30 mm from the tip the stain of suberin lamellae appears to be even stronger.

However, no differences between staining patterns of endo- and exodermal cell walls in roots of *cyp86b3-1* and WT were discovered. Taking into account that the unchanged aromatic fraction constitutes approx. 90 % of all substances extracted, it is not surprising that conventional staining procedures and microscopic observations in comparison with the WT did not reveal the loss of ω-hydroxylated VLCFA in *cyp86b3-1*.

Likewise, staining of cross sections with Sudan red 7b did not reveal any differences between *cyp86b3-1* and WT roots grown in aerated hydroponics at first sight (data not shown). However it has already been summarised that the lipophilic stain is not sensitive enough to highlight small amounts of developing suberised tissues (Ranathunge et al., 2011b). Nevertheless, this method might be usable for a semi-quantitative direct comparison of lipophilic cell wall embeddings of the same tissue from different lines and stress treatments for screening purpose.

Root development, particularly the formation of aerenchyma and different root zones related to distance from the root tip, was not altered in the mutant as examined by bright field microscopy.

Chemical analysis of suberin

A. thaliana mutant lines with defective *CYP86B1*, named *ralph1* and *ralph2*, were characterised to be lacking the function of a monooxygenase of VLCFA involved in biosynthesis of ω-hydroxy acids of chain length C22 and higher (Compagnon et al., 2009). Loss-of-function mutants of the root-expressed orthologue *CYP86B3* in *O. sativa* were expected to have reduced amounts of very long chain ω-hydroxy acids in root suberin as well. Extraction and chemical analysis of the T-DNA insertion lines *cyp86b3-1* and *cyp86b3-2* were carried out as described in chapter 2.5.2 and results are depicted in figure 3.8 and figure 3.9 respectively.

The analysis revealed that no ω-hydroxy acids of chain length C24 and higher were incorporated in root suberin of the two individual mutant lines lacking CYP86B3. In addition, the ω-hydroxy acid derivative C24 α,ω-diacid could not even be found in traces in the mutants, except for the basal suberin of *cyp86b3-1*.

Suberin monomers from plants which were heterozygous for *cyp86b3-2*, depicted in figure 3.9, were not affected in composition and total amounts in comparison to the WT. Even though results have not yet been proven statistically, the one copy of the allele *CYP86B3* per diploid cell, obviously was sufficient to maintain a transcript level, which did not interfere with the suberin biosynthesis pathway and led to the suberin phenotype of the homozygous WT.

The changes in suberin composition caused by mutation of *CYP86B3* correspond to the chemical phenotype of the KO of its orthologue in *A. thaliana*, where with C22 and C24 all fatty acid derivatives of chain lengths exceeding C20 were affected. Since suberin of *A. thaliana* mainly consists of unsaturated C18 as well as saturated fatty acid derivatives with chain lengths C16 to C24, the impact on total aliphatic suberin was much smaller in the *ralph* mutants. In *O. sativa*, where monomers with chain length from C24 to C30 constitute 85.5 % of the total aliphatic suberin in WT, the impact of the KO was extended to all occurring chain length up to C30. The contrast between the total loss of ω-hydroxy acids C24–C30 in *O. sativa* on one hand and the incomplete reduction of the corresponding substances in *A. thaliana* on the other hand can be related to the number of genes of both species in subclade *CYP86B*, see figure 3.1. Since *OsCYP86B3* is the only representative of *O. sativa* in this subclade, another cytochrome P450 enzyme with redundancy in function and range of substrates is unlikely. However, exactly this was discussed for both lines carrying mutations in either *AtCYP86B1* or *AtCYP86B2* (Diehl, 2008, 2011), presumably resulting in traces of their affected products, which were not found in *O. sativa*.

Compared to basal or whole root suberin, the amount of suberin in apical root parts

is much smaller (when related to either surface area or dry weight). This feature can be ascribed to the portion of young undifferentiated tissue, characterised by the absence of lipophilic cell wall embeddings with only traces of suberin from the future suberin lamellae, which are still in development in the zone of differentiation. This is also responsible for the different amounts of suberin monomers other than very long chain ω-hydroxy acids affected by the mutation, in apical roots of *cyp86b3-1* and WT. The high variability of aliphatic compounds in apical root parts of WT plants indicates a region very sensitive to external factors inducing suberin development, such as physical forces or, more likely, variable oxygen concentrations caused by irregular aeration of the hydroponic culture. Nonetheless, since root tip parts of 2–4 cm length have been analysed, variations in sampling might also be responsible for these significant differences.

In contrast to the analysed root suberin in *cyp86b3-1*, amounts of the individual ω-hydroxy acids were slightly decreasing with chain length in *cyp86b3-2*. This can be attributed to chromatography issues, even though extensive maintenance was carried out, as described under chapter 2.5.4. In these cases especially VLCFA and their derivatives tend to be discriminated with increasing chain length.

Further differences in suberin monomer composition between *cyp86b3-1* and *cyp86b3-2* might be ascribed to diverse extraction methods. Since amounts of the substance class of α-hydroxy acids were highly variable between different studies, and origin of the compounds cannot be clarified as discussed in chapter 4.2, they will be excluded from the following discussion.

ω-Hydroxy acids are the main compounds of the aliphatic suberin in root of *O. sativa*. Hence, both examined mutations of *CYP86B3* led to a strong decrease of total aliphatic suberin, by 74.1 % in basal roots of *cyp86b3-1* and 58.5 % in *cyp86b3-2*. The aliphatic suberin in the mutants featured only C16 ω-hydroxy acid, and C24 α,ω-diacid in basal roots (compare table 8.3 to table 8.4) as well as traces of alcohols and monocarboxylic acids of chain lengths C18 and C24, which were not present in all samples tested. These findings support the widely accepted current model of an aliphatic suberin biosynthesis pathway which was established on the basis of knowledge about suberin monomer composition, biochemical studies and examination of loss-of-function mutants of *A. thaliana* (Molina and Franke, 2013). This model implicates activation of plastid derived fatty acids, elongation of acyl-CoA and subsequent hydroxylation at the ER by chain length specific cytochrome P450 enzymes. In further oxidation steps the resulting ω-hydroxy acids could be converted to α,ω-diacids, as depicted in figure 4.2. An interruption of the process at the first hydroxylation step would explain, why the downstream products are also affected

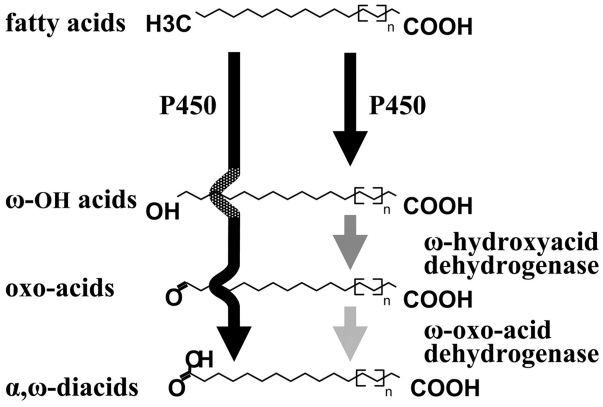

Figure 4.2: Possible pathways for ω-oxidation of fatty acids in *O. sativa* suberin, based on a model for *A. thaliana* from Compagnon et al. (2009). With n = 1 and 5–8.

in the mutants *cyp86b3-1* and *cyp86b3-2* and suggest an accumulation of the substrate of *CYP86B3*, specified as fatty acids in the model (see also figure 1.2).

When *ralph* mutants (*Atcyp86b1*) were investigated, a significant increase of the C22 fatty acid was revealed besides decreased amounts of ω-hydroxylated suberin monomers. Apart from the α-hydroxy acids extracted with the suberin monomers of basal *cyp86b3-1* roots, only the C24 fatty acid was increased in *cyp86b3-2*, significant for $\alpha = 0.1$, which was not found in the samples after cell wall digestion and might therefore be derived rather from the fraction of unbound lipids than the suberin polymer. This was taken as a hint that the mutation of *CYP86B3* could cause changes to the root lipidome, in addition to those identified in the cell wall polyester analysis.

Despite further changes of suberin and similar polyesters in *ralph* mutants, such as the seed coat polyester, no comparable tissues were examined in *O. sativa*. If cuticular wound suberin, bundle sheath cell wall embeddings or grain covering tissues would be affected as well in *cyp86b3* mutants, this would allow general conclusions about the lipid pathway in those tissues featuring the types of cell wall modification mentioned here.

4.3.4 FAME analysis of *cyp86b3-1*

The amounts of some compounds extracted with suberin monomers from basal and whole roots were slightly increased in the KO mutants of *CYP86B3*, depicted in figure 3.8 B and figure 3.9. This increase suggests compensational effects, or more likely, accumulation of metabolic precursors of ω-hydroxylated VLCFA. To test this hypothesis, a total lipid extraction of *cyp86b3-1* whole roots and corresponding WT, grown in aerated hydroponics for 33 d, was carried out according to the method in chapter 2.5.3, with subsequent transesterification and analysis via GC-MS and GC-FID. Amounts of methyl esters of extracted aliphatic lipids are listed in table 8.5 and depicted in figure 3.10. The methodology of

lipid extraction and preparation for GC analysis leads to the standardised methyl esters and TMS esters of the extracts. In case of the suberin analysis all free fatty acids have supposedly been removed before transesterification and the finally extracted methyl esters can be traced back to the depolymerised suberin polyester, whereas the chemical origin of the detected free FAME cannot be determined by this procedure. The methyl esters of very long chain monocarboxylic acids and ω-hydroxy acids presumably derived from the corresponding acyl-CoA which are the precursors of suberin monomers as predicted by suberin pathway models (see figure 1.2). Also possible origins of these FAME are acylglycerol, feruloyl esters and oligoesters of ω-hydroxy acids, serving as suberin building blocks (Pollard et al., 2008). However, glycerol was not quantified and the amount of ferulic acid was only 4.4 % of that of the sum of all ω-hydroxy acids and less than 0.3 % of all aliphatics.

Main components of the extractable lipids were the methyl esters of C18 polyunsaturated fatty acid (52.0±0.4 %, mean and SD of all aliphatic extracts) and C16 fatty acid (24.2±0.2 %), derived from membrane lipids. All VLCFA derivatives of chain lengths C22 and higher reflected the corresponding suberin monomers in composition and amounts per root surface area. Of the substances which were not observed in the course of suberin analysis predominantly monocarboxylic fatty acids were identified in the total lipid fraction of roots. Besides additional compounds from all substance classes with chain lengths shorter than those incorporated in the suberin polyester only minor amounts of unesterified fatty acids and alcohols were found.

The analysis of *cyp86b3-1* revealed a total loss of ω-hydroxy acids in the solvent extractable lipid phase of roots. This reflected the chemical phenotype of the suberin polyester of same plants. According to the suberin biosynthesis model (see figure 1.2), presumed precursors of the ω-hydroxy acids in suberin are monocarboxylic acids of identical carbon chain length, which were identified as the methyl ester of the selfsame after transesterification. These FAME accumulated in the roots of *cyp86b3-1* by amounts nearly equimolar to the loss of the corresponding ω-hydroxy acids in comparison to the WT. This clearly indicates a direct impact of the mutation in *CYP86B3* on ω-hydroxylation of VLCFA in *cyp86b3-1* and points toward the proteins enzymatic function.

Even though a biosynthesis pathway with ω-hydroxylation of shorter acyl-CoA before the elongation to the ω-hydroxylated VLCFA in suberin cannot be ruled out, it seems rather unlikely since FAME of shorter chain lengths did not accumulate in the mutant, see figure 3.10. In this scenario monocarboxylic fatty acids as the precursors of ω-hydroxy acids would have to be either determined for a specific elongation after ω-hydroxylation to re-

sult in the described accumulation of VLCFA or to be elongated by an unspecific elongation complex, which metabolises all accumulating fatty acids independent of their functional groups.

In *A. thaliana* an accumulation of proposed ω-hydroxy acid precursors was shown in the suberin of *ralph* mutants, particularly for the C22 fatty acid. Although solvent extractable esters of monocarboxylic fatty acids accumulated in *cyp86b3-1*, they were not integrated in the root suberin, as they are not part of the native composition in *O. sativa*. Since the export of suberin monomers is not yet understood, one can only speculate whether this might be due to lack of translocation mechanisms for monocarboxylic acids, such as membrane transporters, or their exclusion from suberin building blocks like oligoesters (Pollard et al., 2008).

4.3.5 Stress treatments

Various stress conditions interfering with water relations of plants or known to induce suberisation in roots were used to induce expression of suberin candidate genes or to examine physiological barrier properties in mutants with altered suberin composition. In chapter 3.1.2 microarray based expression of *O. sativa* genes putatively involved in suberin biosynthesis is visualised (figure 3.2) and opposed to tissue specific expression obtained via RT-PCR (figure 3.3), with results considered in chapter 4.1.

Mannitol

Different osmotic stress treatments were chosen to differentially activate genes playing a role in drought response such as genes involved in suberisation. Under treatment with 400 mmol L^{-1} mannitol plants lost turgor completely and formed white crystals mainly on sheaths but also on leaves (not shown). Since plants were not able to maintain cell pressure, rather excretion of the osmolyte than guttation is likely to cause this effect. Even though mannitol solutions with equal osmolality were used before to stress seedlings of *O. sativa* (Jain et al., 2006) and even higher concentrations were applied to *A. thaliana* (Höfer, 2008), 400 mmol L^{-1} of mannitol was considered as too high to trigger a response to water loss without severe additional effects. For this reason, stress response resulting from mannitol treatment was not considered any further.

NaCl

Since it was shown that salt stress strongly induces suberized barriers in roots of dicotyledons (Reinhardt and Rost, 1995) as well as of *O. sativa* (Krishnamurthy et al., 2009), a treatment with 200 mmol NaCl over 2 h was chosen to activate genes potentially related to suberin biosynthesis. The results of this treatment are discussed for the individual suberin candidates in chapter 4.1. The high concentrations of 200 mmol L^{-1} NaCl have been proven to be toxic for the glycophyte *O. sativa*. Even lower concentrations cause typical stress effects as described in detail by Krishnamurthy et al. (2009, 2011) but also increased suberin amounts in roots. A treatment of *O. sativa* cv. Dongjin, hydroponically grown for 19 d, with NaCl in a concentration of 100 mmol L^{-1} for 10 d was chosen to examine the stress tolerance of the mutant altered in suberin composition in comparison to the WT. These conditions led to strongly reduced growth of roots and of green plant organs, also reflected in 40 % smaller leaf dry weights, see figure 3.12, and wilted first and second leaves, as observable in figure 3.11. Anyhow, the salt stress did not reveal any physiological phenotype caused by the absence of C24–C30 ω-hydroxy acids in the root suberin of *cyp86b3-1*.

Stagnant growth conditions

Suberin in the exodermis of *O. sativa* roots is expected to build the main barrier against radial oxygen loss (ROL) (Kotula et al., 2009; Nishiuchi et al., 2012). In this context the role of reduced aliphatic suberin in hypoxic stress tolerance was examined with the mutant *cyp86b3-1* in comparison to WT. The cultivation under stagnant conditions in deoxygenated agar solution for 18 d led to a slower growth rate compared to aerated cultivation and yellowish leaves with fresh weight reduced by 52 %. The root system featured longer adventitious roots of an relatively wide diameter, whereas seminal and thinner roots were less abundant in comparison to control plants. This habit was also described before by Ranathunge et al. (2011a) who found the development of "'bushy-type' root systems with short, but greater number of adventitious roots" under stagnant conditions, with significant larger diameters. The difference in root length as well as the yellowish leaves might be attributed to nutrient starvation in the 0.1 % agar solution, caused by decreased lateral diffusion. Although this effect was not described before when the same technique was applied (Kotula et al., 2009; Ranathunge et al., 2011a), nightly temperatures of about 20–23 °C even led to coagulation of the low concentrated agar restricting not only bulk water flow but also decelerate lateral diffusion of nutrients. Cultivation under stagnant

conditions induces an increase in barrier properties to prevent ROL from the basal root to the surrounding medium (Kotula et al., 2009). This might coincide with an inhibited collateral nutrient absorption, as predicted by Clark and Harris (1981) and Colmer and Bloom (1998) and the already suggested nutrient starvation of the plant.

When growth and developmental responses to the stress treatments were compared between WT and *cyp86b3-1*, no differential phenotype of the KO was discovered. No difference of root systems of the mutant in length, number or diameter of individual roots could be determined under all growth conditions tested. Fresh weights as well as dry weights of aerial parts of *cyp86b3-1* were not different from WT. The values, represented in figure 3.12, allow an estimation of the water content of leaves. With 82.1±0.8 % vs. 81.1±2.1 % the relative water content of WT was not different from that in the mutant after growth under control conditions. Similarly salt stress did not lead to differences with 80.2±1.5 % in WT and 78.9±0.3 % in the mutant. Only after stagnant cultivation relative water content was significantly different for $\alpha = 0.05$ with 76.1±2.7 % in WT compared to control conditions. This was already assessable by observation of the more yellowish leaves mentioned above. Nonetheless, no difference could be found in comparison to *cyp86b3-1* grown under the same conditions where the relative water content was 76.7±1.7 %.

Iron

Kolattukudy (2001) reported that at least some dicotyledonous plants react to Fe deficiency with decreased suberin accumulation in the root, supposedly to facilitate uptake of the essential trace mineral. The effect observed in *Phaseolus vulgaris* can be assigned to regulation rather than direct impact on enzymes involved in suberin metabolism, since peroxidase activity decreased, but activity of Fe dependent enzymes such as ω-hydroxylases did not (Sijmons et al., 1985). Besides the proposed decreased barrier for Fe in tissues less suberised the authors speculate that an later suberisation could support diffusion of reducing compounds needed for iron allocation.

On the other hand excess Fe^{2+} can become an yield limiting factor for most *O. sativa* varieties under stagnant growth conditions (Becker and Asch, 2005). Fe^{2+} leads to leaf bronzing by increased production of radicals and accumulation of polyphenolics. Fe^{2+} from cortex enters the xylem by translocation to the symplast to pass the endodermis, or by apoplastic bypass. An increased conductivity and reduced selectivity for ions could be expected in mutants with affected apoplastic barriers.

No difference of the habitus of *cyp86b3-1* was caused by cultivation in medium containing toxic Fe concentrations in comparison to the WT, conducted by Lin-Bo Wu in the

laboratory of Michael Frei (Institut für Nutzpflanzenwissenschaften und Ressourcenschutz, University of Bonn, personal communication). In the context of these studies root suberin composition of four rice lines with different susceptibilities to high Fe concentrations was analysed but no differential response in suberisation could be related to the treatment (data not shown). These findings highlighted that resistance to Fe stress is more complex and not simply mediated by a diffusion barrier such as a suberised exodermis.

However, Wehler (2013) examined the amounts of macro and micro elements in leaves of field grown mutant plants *cyp86b3-1* and WT by inductively coupled plasma atomic emission spectroscopy. In comparison to the WT only contents of Al and Fe were significantly increased in the mutant by 65.1 % and 66.1 % respectively (p-value < 0.05). Due to a high variance between replicates, the increase of other elements, such as Na (21.3 %, p-value $= 0.116$) and Cu (25.7 %, p-value $= 0.301$) was not significant. The higher contents of metal ions in leaves of *cyp86b3-1* indicate an increased permeability of the apoplastic root barriers for water and particularly solutes. This denotes the role of root suberin as diffusion barrier for ionic solutes such as iron and the impact of the altered suberin in *cyp86b3-1* in particular. In contrast to all tests in the course of this work which were conducted in the laboratory, this was carried out under field conditions. Even though conditions are easier to assess in controlled environments, this gives a hint that physiological phenotypes are more difficult to examine under less competitive artificial growth conditions.

4.3.6 Barrier properties of *cyp86b3-1*

Radial oxygen loss in roots

Most varieties of *O. sativa* develop a higher degree of root porosity and a barrier to radial diffusion of oxygen from the basal root tissue to the medium when grown under stagnant conditions (Colmer et al., 1998; Colmer, 2003). This porosity is derived from aerenchyma formation by programmed cell death and lysis of cell walls in the cortex (Yamauchi et al., 2013) and the reduced ROL comes along with an accumulation of mainly aliphatic suberin along the root (Kotula et al., 2009). Those adaptations of root morphology facilitate the supply of apical cells with oxygen under hypoxic conditions through the root.

To examine the differential barrier characteristics of *cyp86b3-1* and WT roots against ROL, roots were cultivated under the conditions described in chapter 2.2.4 and transferred to a 0.1 % agar solution containing reduced methylen blue. Radial diffusion of oxygen from the aerenchyma to the root surface and medium was visualised by oxidation of the

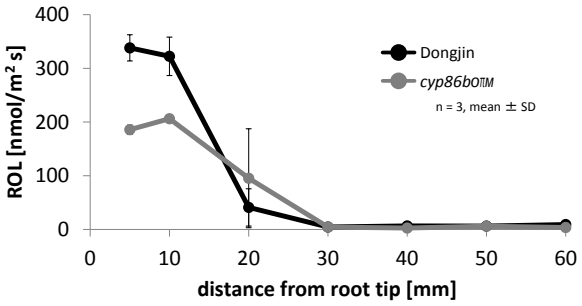

Figure 4.3: ROL measurement of *cyp86b3-1* and Dongjin roots. Roots were grown for 9 d under aerated and subsequently 14 d under stagnant conditions, length: 100–110 mm (unpublished results from Kohtaro Watanabe, in the laboratory of Mikio Nakazono, Laboratory of Plant Genetics and Breeding, Nagoya University, Japan).

beforehand reduced and colourless methylen blue, see figure 3.13.

During development lateral roots break through endodermis and exodermis. Resulting breaches did allow the diffusion of oxygen from root cortex to the medium, regardless of the genotype or treatment applied to the tested plants. Apical parts of roots from all different conditions were also stained. The outermost root tips of plants which were cultivated under aerated conditions, were stained to a lesser extend, though. In those roots, most of the oxygen was either already consumed by the living tissue, or the tip was not sufficiently supplied by lack of aerenchyma.

To assess differences in staining pattern between mutant and WT, distances from the root tips to the end of continuous stain were measured and compared, see figure 3.14. In plants cultivated under stagnant conditions the zone of pronounced ROL in *cyp86b3-1* was 20 % shorter than in the WT. This partially correlates with ROL measured with an oxygen electrode by Kohtaro Watanabe, in the laboratory of Mikio Nakazono (Laboratory of Plant Genetics and Breeding, Nagoya University, Japan). These measured rates of oxygen loss to the medium are displayed as a function of distance from root tip in figure 4.3. ROL is significantly higher at the root apex, 5–10 mm from tip, in WT plants compared to *cyp86b3-1*, the root part still lacking suberin lamellae. However, behind that zone no oxygen diffusion was measurable in both genotypes, which is again in line with the staining experiments of this work. This indicates that the lack of very long chain ω-hydroxy acids in the mutant does not affect the barrier properties of the exodermal suberin lamellae for gases.

Solute uptake

Solute uptake in roots can be studied with the help of various tracers. Besides transport experiments with stains like PTS on basis of the pressure chamber technique (reviewed by Steudle and Peterson (1998) and Zimmermann and Steudle (1998)), photosynthesis inhibitors can be used, which are generally derived from herbicide development. Invasive measurements such as staining experiments can hardly be used for time dependent

examination of solute uptake. In contrast to that, monitoring of photosynthesis activity in presence of specific inhibitors allows for a continuous time dependent non-invasive measurement on the living plant. In this study Metribuzin was used as such a photosynthesis inhibitor, a triazinone with a molecular weight of 214.28 g mol^{-1} and an octanol/water partition coefficient of $logK_{OW} = 1.60$. The molecule is relatively small in comparison to most dyes and the partition coefficient of less than 50 denotes the non-ionic compound to be membrane permeable but still to be a fairly good tracer for bulk flow of water, since it is easily desorbed by the aqueous phase (Shi et al., 2005).

Results of continuous photosynthesis monitoring with a pulse-amplitude modulation fluorometer (PAM) on flag leaves are displayed in figure 3.15. When the inhibitor Metribuzin was applied via hydroponic solution a 20 % faster inhibition of photosynthesis was observed in *cyp86b3-1* compared to the Dongjin background. Since a decrease in photosynthesis activity can be correlated with the uptake of Metribuzin, one can conclude that roots of *cyp86b3-1* exhibit significantly reduced retention properties.

One have to keep in mind, that the plant is a complex structure with various pathways for water and solute transport (Steudle and Peterson, 1998) which results in different factors influencing the time it takes for a compound applied with the medium to reach the site of chlorophyll fluorescence measurement. Driving forces of transport processes are based on concentration gradients and, at least after entering the xylem, on bulk water flow, which depends on transpiration and root pressure. However, in various preliminary studies no correlation between either root surface area or stomatal transpiration rate and the time of half maximal inhibition was found. In order to minimise variation, equal osmotic potential of the medium, temperature and light intensity, as well as distance of point of PAM measurement to root-shoot junction was carefully maintained. The decrease of photosynthetic yield during the lag phase can be referred to the measurement itself, since it was dependent on number of saturating pulses per minute and even occurred in control measurements without Metribuzin, for which it is negligible. Since surface areas of roots, on which solute uptake is linearly dependent, and of green parts, which correlate with transpiration, were not altered in *cyp86b3-1* compared to WT plants, the 13 % faster uptake of Metribuzin into leaves can be attributed to changes of root barrier properties.

The mutation in *CYP86B3* led to a total loss of ω-hydroxy acids C24–C30, which are the main components of aliphatic root suberin in *O. sativa*. However, *cyp86b3-1* plants did not reveal differences in root morphology and habitus. Furthermore, the altered suberin composition did not cause differential susceptibilities to various stresses under controlled conditions. Though, in field trials higher metal ion contents were determined in leaves

of the mutant, indicating decreased retention in roots. The significantly shorter times of half-maximal photosynthesis inhibition after exposition to Metribuzin confirmed the decrease of apoplastic barrier properties in *cyp86b3-1* caused by the altered aliphatic suberin composition.

4.4 Heterologous complementation of *ralph*

The function of CYP86B3 was not only characterized on the basis of two individual KO mutants of *O. sativa* but also examined by heterologous complementation of *A. thaliana* lines, which were mutated in the orthologue gene. In order to express *CYP86B3* heterologously under a native promoter in *ralph* and *ralph*/*horst*, transgenic plants carrying p*Ralph*:CDS *CYP86B3* were generated. Their root suberin composition was analysed and compared to the genetic background, as depicted in figure 3.20 with average absolute amounts in table 8.6 and table 8.7.

Results of this work were in accordance with published suberin phenotypes of *ralph* (Compagnon et al., 2009) and *ralph*/*horst* (Höfer et al., 2008; Diehl, 2011). The decrease or even total loss of C22–C24 ω-hydroxy acids in *ralph* and of all natively occurring chain length including derivatives in *ralph*/*horst* compared to the WT Col-8 was accompanied by an accumulation of the corresponding fatty acids in *ralph*.

α-Hydroxy acids, which amounted to 57 % to the total aliphatic fraction in the double KO but only to 40 % in the WT, had about the same total amounts in all samples, whereas almost all other compounds were affected by the different mutations. In order to collect the total lipid fraction of the examined roots samples were not subjected to cell wall digestion here. As discussed in chapter 4.2 this has an significant effect on the amounts of α-hydroxy acids extracted with suberin monomers.

The heterologous expression of *CYP86B3* from *O. sativa* complemented the *ralph* phenotype in *ralph*::p*Ralph*:CDS *CYP86B3* and *ralph*/*horst*::p*Ralph*:CDS *CYP86B3*, by restoring the amounts of suberin monomers found in Col-8, of C22 and C24 ω-hydroxy acids in particular. However, compounds with chain lengths smaller than C22 were unaffected and stayed reduced in the complemented double KO *ralph*/*horst* in comparison to the WT. The different suberin monomer composition in *O. sativa* and *A. thaliana* heterologously expressing *CYP86B3* can be referred to the limited substrate for the enzyme, since the polyester of *A. thaliana* contains only aliphatic components of chain length up to C24, whereas native suberin of *O. sativa* contains monomers of chain lengths up to C30. Even though α-hydroxy acids with chain length up to C26 are abundant in roots of *A. thaliana*,

only ω-hydroxylated fatty acid derivatives up to C24 were part of the suberin.

These results again give strong evidence to suggest that CYP86B3 acts as ω-hydroxylase of fatty acids with chain length C22 and higher.

5 Summary

Aim of this work was the identification and characterisation of genes involved in the biosynthesis of suberised border tissues and the investigation of the physiological impact of altered suberin composition on apoplastic barrier properties of roots in the globally important crop and model species *O. sativa*.

A number of candidates of different protein classes have been selected by BLAST analyses against *O. sativa* databases using *A. thaliana* sequences known to play key roles in suberin synthesis. Closest related genes were determined by sequence alignments. *In silico* and RT-PCR based expression studies of selected genes confirmed their activity in tissues undergoing suberisation. In the course of this study, CYP86B3 in *O. sativa* could be identified to be the orthologue of RALPH, a ω-hydroxylase of VLCFA in *A. thaliana*.

The knockout mutation of *CYP86B3* did not cause visible growth or development related phenotypes, not even under cultivation conditions provoking osmotic or hypoxic stress adaptation. Although no difference in suberisation could be visualised in histological studies, chemical analysis revealed a complete reduction of ω-hydroxylated fatty acids of carbon chain lengths from C24 to C30 in the knockout mutants *cyp86b3*, resembling the chemical phenotype of aliphatic cell wall polyesters in roots of the *A. thaliana* mutant *ralph*. The interference with the ω-hydroxylation of suberin monomer precursors led to an accumulation of VLCFA of corresponding chain lengths in the total lipid fraction of mutant roots.

In order to examine the impact of the altered suberin composition on solute uptake in *cyp86b3-1*, the photosynthesis inhibitor Metribuzin was applied with the medium and its uptake was monitored via measurement of the photosynthetic yield. The apoplastic tracer was taken up significantly faster into leaves of the mutant in comparison to WT plants.

From these results it becomes evident that not only the suberin composition is altered in *cyp86b3-1* but also barrier properties of the root are significantly impaired by the loss of the suberin monomers C24–C30 ω-hydroxy acids.

The function of CYP86B3 was not only characterized on the basis of two individual KO mutants of *O. sativa* but also examined by the transgenic expression of *CYP86B3* under a

native promoter in *A. thaliana* plants which were mutated in the orthologue gene *CYP86B1*. This heterologous complementation of *ralph* restored the WT suberin phenotype and characterised the cytochrome P450 monooxygenase as ω-hydroxylase of fatty acids with chain lengths of C22 and higher in root suberin of *O. sativa*. So far, *CYP86B3* is the only known plant ω-hydroxylase of VLCFA with chain lengths exceeding C24.

6 Zusammenfassung

Ein Ziel dieser Arbeit war die Identifizierung von Genen mit Beteiligung an der Suberinbiosynthese in Reis auf Grundlage bekannter Suberingene der Modellpflanze Arabidopsis. Ein weiteres Ziel war die Untersuchung von entsprechenden Linien, in welchen diese potentiellen Suberingene per Mutation ausgeschaltet waren. Neben chemisch-analytischer Charakterisierung und Ableiten der biochemischen Funktion der betroffenen Enzyme aus der Monomerzusammensetzung des Suberins, sollten Mutanten vor deren genetischem Hintergrund auf Unterschiede im Wasser- und Ionenhaushalt untersucht werden, um die physiologische Relevanz der veränderten apoplastischen Barrieren zu ermitteln.

Eine Reihe von potentiellen Suberinbiosyntheseenzymen in Reis wurde anhand von Sequenzvergleichen zu bekannten Enzymen in Arabidopsis bestimmt. Die Auswahl wurde mittels *in silico*-Analysen und molekularbiologischen Untersuchungen auf Kandidaten eingeengt, deren Genexpression räumlich und zeitlich mit der Suberinisierung von Zellwänden in der Wurzel korreliert. Im Rahmen dieser Arbeit stellte sich OsCYP86B3 in Reis als ortholog zu AtCYP86B1 (RALPH) in Arabidopsis heraus, einer Cytochrom P450 ω-Hydroxylase von sehr langkettigen Fettsäuren in der Suberinsynthese.

Reismutanten mit Defekt in *OsCYP86B3* entwickelten sich auch unter verschiedenen Stressbedingungen zu Pflanzen, die im Phänotyp nicht vom Wildtyp zu unterscheiden waren. Obwohl histologische Untersuchungen ebenfalls keine morphologischen Unterschiede zwischen Wurzeln von Mutanten und Wildtyp zeigten, insbesondere der Suberinisierung von Endodermis und Exodermis, wurde die Wurzelsuberinzusammensetzung mittels GC-MS chemisch analysiert. Der funktionale Verlust von OsCYP86B3 führte zu einer vollständigen Reduktion von ω-Hydroxysäuren der Kohlenstoffkettenlängen C24 bis C30, was den Suberinphänotyp von Arabidopsismutanten des orthologen *AtCYP86B1* widerspiegelte. Die Analyse von Lipiden, die sich mit organischen Lösungsmitteln aus Wurzelgewebe extrahieren ließen, zeigte eine Akkumulation von Fettsäureestern der Kettenlängen C24 bis C30, den angenommenen biochemischen Vorstufen der betroffenen Suberinmonomere.

Die Funktion von OsCYP86B3 wurde nicht nur an zwei unabhängigen Mutanten in Reis untersucht, sondern darüber hinaus auch mittels heterologer Komplementierung der ent-

sprechenden Mutante in Arabidopsis. Die Expression von *OsCYP86B3* unter dem Promotor des nativen orthologen Gens *AtCYP86B1* in den Mutanten *ralph* und *ralph*/*horst* komplementierte den Suberinphänotyp von *ralph* und stellte die Suberinzusammensetzung des Wildtyps wieder her.

Um den Effekt der veränderten Suberinzusammensetzung in den Reismutanten auf die Barriereeigenschaften der Wurzel gegenüber Wasser und darin gelösten Stoffen zu testen, wurde der Photosyntheseinhibitor Metribuzin verwendet und dessen Transport in die Blätter mittels Messung der Photosyntheserate beobachtet. Die Aufnahme von Metribuzin war signifikant schneller in den Pflanzen mit defektem *OsCYP86B3*, deren Suberinzusammensetzung durch das Fehlen der C24–C30 ω-Hydroxysäuren charakterisiert war.

Mit den Ergebnissen dieser Arbeit konnte OsCYP86B3 als ω-Hydroxylase von Fettsäuren mit Kettenlängen C22 und höher in der Biosynthese aliphatischer Suberinmonomere in Reis identifiziert werden und darüber hinaus die Rolle der produzierten sehr langkettigen ω-Hydroxysäuren an den Barriereeigenschaften von Wurzelgrenzflächen aufgezeigt werden.

7 Lists and References

Bibliography

Abramoff, M., Magalhães, P. J. and Ram, S. J. (2004), 'Image processing with ImageJ', *Biophotonics international* 11(7), 36–42.

Altschul, S. F., Gish, W., Miller, W., Myers, E. W. and Lipman, D. J. (1990), 'Basic Local Alignment Search Tool', *Journal of molecular biology* 215(3), 403–410.

Bailey, T. L. and Elkan, C. (1994), 'Fitting a mixture model by expectation maximization to discover motifs in biopolymers.', *Proceedings / ... International Conference on Intelligent Systems for Molecular Biology ; ISMB. International Conference on Intelligent Systems for Molecular Biology* 2, 28–36.

Bak, S. r., Beisson, F., Bishop, G., Hamberger, B., Höfer, R., Paquette, S. and Werck-Reichhart, D. (2011), 'Cytochromes p450.', *The Arabidopsis book / American Society of Plant Biologists* 9, e0144.

Becker, M. and Asch, F. (2005), 'Iron toxicity in rice—conditions and management concepts', *Journal of Plant Nutrition and Soil Science* 168(4), 558–573.

Beisson, F., Li-Beisson, Y. and Pollard, M. (2012), 'Solving the puzzles of cutin and suberin polymer biosynthesis.', *Current opinion in plant biology* 15(3), 329–37.

Beisson, F., Li, Y., Bonaventure, G., Pollard, M. and Ohlrogge, J. B. (2007), 'The acyltransferase GPAT5 is required for the synthesis of suberin in seed coat and root of Arabidopsis.', *The Plant cell* 19(1), 351–68.

Benveniste, I., Tijet, N., Adas, F., Philipps, G., Salaün, J.-P. P. and Durst, F. (1998), 'CYP86A1 from Arabidopsis thaliana encodes a cytochrome P450-dependent fatty acid omega-hydroxylase.', *Biochemical and biophysical research communications* 243(3), 688–93.

Bernards, M. A. (2002), 'Demystifying suberin', *Canadian Journal of Botany* 80(3), 227–240.

Bernards, M., Summerhurst, D. K. and Razem, F. (2004), 'Oxidases, peroxidases and hydrogen peroxide: The suberin connection', *Phytochemistry Reviews* 3(1/2), 113–126.

Boerjan, W., Ralph, J. and Baucher, M. (2003), 'Lignin biosynthesis.', *Annual review of plant biology* 54, 519–46.

Brundrett, M. C., Kendrick, B. and Peterson, C. a. (1991), 'Efficient lipid staining in plant material with sudan red 7B or fluorol yellow 088 in polyethylene glycol-glycerol.',

Biotechnic & histochemistry: official publication of the Biological Stain Commission 66(3), 111–116.

Cao, P., Jung, K.-H., Choi, D., Hwang, D., Zhu, J. and Ronald, P. C. (2012), 'The rice oligonucleotide array database: an atlas of rice gene expression', *Rice* 5(1), 1–9.

Clark, L. H. and Harris, W. H. (1981), 'Observations on the Root Anatomy of Rice (Oryza sativa L.)', *American Journal of Botany* 68(2), 154–161.

Collard, B. C. Y., Das, A., Virk, P. S. and Mackill, D. J. (2007), 'Evaluation of 'quick and dirty' DNA extraction methods for marker-assisted selection in rice (Oryza sativa L.)', *Plant Breeding* 126(1), 47–50.

Colmer, T. D. (2003), 'Aerenchyma and an Inducible Barrier to Radial Oxygen Loss Facilitate Root Aeration in Upland, Paddy and Deep-water Rice (Oryza sativa L.)', *Annals of Botany* 91(2), 301–309.

Colmer, T. D. and Bloom, A. J. (1998), 'A comparison of NH4+ and NO3- net fluxes along roots of rice and maize', *Plant, Cell and Environment* 21(2), 240–246.

Colmer, T. D., Gibberd, M. R., Wiengweera, a. and Tinh, T. K. (1998), 'The barrier to radial oxygen loss from roots of rice (Oryza sativa L.) is induced by growth in stagnant solution', *Journal of Experimental Botany* 49(325), 1431–1436.

Compagnon, V., Diehl, P., Benveniste, I., Meyer, D., Schaller, H., Schreiber, L., Franke, R. and Pinot, F. (2009), 'CYP86B1 is required for very long chain omega-hydroxyacid and alpha, omega -dicarboxylic acid synthesis in root and seed suberin polyester', *Plant physiology* 150(4), 1831–43.

Curtis, M. D. and Grossniklaus, U. (2003), 'A gateway cloning vector set for high-throughput functional analysis of genes in planta.', *Plant physiology* 133(2), 462–9.

Dethloff, F. (2009), Untersuchungen zur Genfamilie der β-Ketoacyl-CoA-Synthasen unter abiotischen Stressbedingungen in Arabidopsis thaliana, diploma thesis, University of Bonn.

Diehl, P. (2008), Untersuchungen zur Bedeutung von für die Biosynthese aliphatischer Zellwandpolymere in Arabidopsis thaliana, diploma thesis, University of Bonn.

Diehl, P. (2011), Studien zur Aufklärung der Biosynthese apoplastischer Polyester in höheren Pflanzen, PhD thesis, University of Bonn.

Draber, W., Tietjen, K., Kluth, J. F. and Trebst, A. (1991), 'Herbicides in Photosynthesis Research', *Angewandte Chemie International Edition in English* 30(12), 1621–1633.

Drew, M. C. and Lynch, J. M. (1980), 'Soil Anaerobiosis, Microorganisms, and Root Function', *Annual Review of Phytopathology* 18(1), 37–66.

Duan, H. and Schuler, M. A. (2005), 'Differential expression and evolution of the Arabidopsis CYP86A subfamily.', *Plant physiology* 137(3), 1067–81.

Edgar, R. C. (2004), 'MUSCLE: multiple sequence alignment with high accuracy and high throughput', *Nucleic acids research* 32(5), 1792–1797.

Enstone, D. E., Peterson, C. and Ma, F. (2003), 'Root Endodermis and Exodermis: Structure, Function, and Responses to the Environment', *Journal of Plant Growth Regulation* 21(4), 335–351.

Fiebig, A., Mayfield, J. a., Miley, N. L., Chau, S., Fischer, R. L. and Preuss, D. (2000), 'Alterations in CER6, a gene identical to CUT1, differentially affect long-chain lipid content on the surface of pollen and stems.', *The Plant cell* 12(10), 2001–8.

Franke, R. B., Dombrink, I. and Schreiber, L. (2012), 'Suberin goes genomics: use of a short living plant to investigate a long lasting polymer.', *Frontiers in plant science* 3(1), 4.

Franke, R., Briesen, I., Wojciechowski, T., Faust, A., Yephremov, A., Nawrath, C. and Schreiber, L. (2005), 'Apoplastic polyesters in Arabidopsis surface tissues - a typical suberin and a particular cutin', *Phytochemistry* 66(22), 2643–58.

Franke, R., Höfer, R., Briesen, I., Emsermann, M., Efremova, N., Yephremov, A. and Schreiber, L. (2009), 'The DAISY gene from Arabidopsis encodes a fatty acid elongase condensing enzyme involved in the biosynthesis of aliphatic suberin in roots and the chalaza-micropyle region of seeds.', *The Plant journal : for cell and molecular biology* 57(1), 80–95.

Garg, R., Tyagi, A. K. and Jain, M. (2012), 'Microarray analysis reveals overlapping and specific transcriptional responses to different plant hormones in rice.', *Plant signaling & behavior* 7(8), 951–956.

Genty, B., Briantais, J.-M. and Baker, N. R. (1989), 'The relationship between the quantum yield of photosynthetic electron transport and quenching of chlorophyll fluorescence', *Biochimica et Biophysica Acta (BBA) - General Subjects* 990(1), 87–92.

Girard, A.-L., Mounet, F., Lemaire-Chamley, M., Gaillard, C., Elmorjani, K., Vivancos, J., Runavot, J.-L., Quemener, B., Petit, J., Germain, V., Rothan, C., Marion, D. and Bakan, B. (2012), 'Tomato GDSL1 is required for cutin deposition in the fruit cuticle.', *The Plant cell* 24(7), 3119–34.

Graça, J. and Pereira, H. (2000), 'Suberin structure in potato periderm: glycerol, long-chain monomers, and glyceryl and feruloyl dimers.', *Journal of agricultural and food chemistry* 48(11), 5476–83.

Graça, J. and Santos, S. (2007), 'Suberin: a biopolyester of plants' skin', *Macromolecular bioscience* 7(2), 128–35.

Haslam, T. M. and Kunst, L. (2013), 'Extending the story of very-long-chain fatty acid elongation.', *Plant science : an international journal of experimental plant biology* 210, 93–107.

Hattersley, P. W. and Browning, A. J. (1981), 'Occurrence of the suberized lamella in leaves of grasses of different photosynthetic types. I. In parenchymatous bundle sheaths and PCR ("Kranz") sheaths', *Protoplasma* 109(3-4), 371–401.

Heitz, T., Widemann, E., Lugan, R., Miesch, L., Ullmann, P., Désaubry, L., Holder, E., Grausem, B., Kandel, S., Miesch, M., Werck-Reichhart, D. and Pinot, F. (2012), 'Cytochromes P450 CYP94C1 and CYP94B3 catalyze two successive oxidation steps of plant hormone Jasmonoyl-isoleucine for catabolic turnover.', *The Journal of biological chemistry* 287(9), 6296–306.

Höfer, R. (2008), Untersuchungen zur Suberinentwicklung und der Bedeutung von Cytochrom P-450 Monooxygenasen bei der Suberinbiosynthese in Arabidopsis thaliana, PhD thesis, University of Bonn.

Höfer, R., Briesen, I., Beck, M., Pinot, F., Schreiber, L. and Franke, R. (2008), 'The Arabidopsis cytochrome P450 CYP86A1 encodes a fatty acid omega-hydroxylase involved in suberin monomer biosynthesis.', *Journal of experimental botany* 59(9), 2347–60.

Hose, E., Clarkson, D. T., Steudle, E., Schreiber, L. and Hartung, W. (2001), 'The exodermis: a variable apoplastic barrier', *Journal of experimental botany* 52(365), 2245–64.

Hruz, T., Laule, O., Szabo, G., Wessendorp, F., Bleuler, S., Oertle, L., Widmayer, P., Gruissem, W. and Zimmermann, P. (2008), 'Genevestigator v3: a reference expression database for the meta-analysis of transcriptomes.', *Advances in bioinformatics* 2008, 420747.

Jain, M., Nijhawan, A., Tyagi, A. K. and Khurana, J. P. (2006), 'Validation of housekeeping genes as internal control for studying gene expression in rice by quantitative real-time PCR.', *Biochemical and biophysical research communications* 345(2), 646–51.

James, D. W., Lim, E., Keller, J., Plooy, I., Ralston, E. and Dooner, H. K. (1995), 'Directed tagging of the Arabidopsis FATTY ACID ELONGATION1 (FAE1) gene with the maize transposon activator.', *The Plant cell* 7(3), 309–19.

Jeon, J. S., Lee, S., Jung, K. H., Jun, S. H., Jeong, D. H., Lee, J., Kim, C., Jang, S., Yang, K., Nam, J., An, K., Han, M. J., Sung, R. J., Choi, H. S., Yu, J. H., Choi, J. H., Cho, S. Y., Cha, S. S., Kim, S. I. and An, G. (2000), 'T-DNA insertional mutagenesis for functional genomics in rice.', *The Plant journal : for cell and molecular biology* 22(6), 561–570.

Jeong, D.-h., An, S., Kang, H.-g., Moon, S., Han, J.-j., Park, S., Lee, H. S., An, K. and An, G. (2002), 'T-DNA insertional mutagenesis for activation tagging in rice.', *Plant physiology* 130(4), 1636–44.

Joubès, J., Raffaele, S., Bourdenx, B., Garcia, C., Laroche-Traineau, J., Moreau, P., Domergue, F. and Lessire, R. (2008), 'The VLCFA elongase gene family in Arabidopsis thaliana: phylogenetic analysis, 3D modelling and expression profiling.', *Plant molecular biology* 67(5), 547–566.

Kandel, S., Sauveplane, V., Compagnon, V., Franke, R., Millet, Y., Schreiber, L., Werck-Reichhart, D. and Pinot, F. (2007), 'Characterization of a methyl jasmonate and wounding-responsive cytochrome P450 of Arabidopsis thaliana catalyzing dicarboxylic fatty acid formation in vitro.', *The FEBS journal* 274(19), 5116–27.

Kenrick, P. and Crane, P. R. (1997), 'The origin and early evolution of plants on land', *Nature* 389(6646), 33–39.

Kolattukudy, P. E. (1981), 'Structure, Biosynthesis, and Biodegradation of Cutin and Suberin', *Annual Review of Plant Physiology* 32(1), 539–567.

Kolattukudy, P. E. (2001), 'Polyesters in higher plants.', *Advances in biochemical engineering/biotechnology* 71, 1–49.

Kolattukudy, P. E. and Agrawal, V. P. (1974), 'Structure and composition of aliphatic constituents of potato tuber skin (suberin)', *Lipids* 9(9), 682–691.

Kolattukudy, P. P. E. (2002), Suberin from Plants, *in* Y. Doi and A. Steinbüchel, eds, 'Biopolymers, Polyesters I - Biological Systems and Biotechnological Production', 3 edn, Biopolymers, Wiley, chapter 2, pp. 41–68.

Koressaar, T. and Remm, M. (2007), 'Enhancements and modifications of primer design program Primer3', *Bioinformatics (Oxford, England)* 23(10), 1289–91.

Kotula, L., Ranathunge, K., Schreiber, L. and Steudle, E. (2009), 'Functional and chemical comparison of apoplastic barriers to radial oxygen loss in roots of rice (Oryza sativa L.) grown in aerated or deoxygenated solution.', *Journal of experimental botany* 60(7), 2155–67.

Krishnamurthy, P. (2008), Ion transport mechanisms of salt tolerance in rice, Phd thesis, University of Mysore.

Krishnamurthy, P., Ranathunge, K., Franke, R., Prakash, H. S., Schreiber, L. and Mathew, M. K. (2009), 'The role of root apoplastic transport barriers in salt tolerance of rice (Oryza sativa L.).', *Planta* 230(1), 119–34.

Krishnamurthy, P., Ranathunge, K., Nayak, S., Schreiber, L. and Mathew, M. K. (2011), 'Root apoplastic barriers block Na+ transport to shoots in rice (Oryza sativa L.).', *Journal of experimental botany* pp. 1–14.

Kurdyukov, S., Faust, A. and Nawrath, C. (2006), 'The epidermis-specific extracellular BODYGUARD controls cuticle development and morphogenesis in Arabidopsis', *The Plant Cell Online* 18(2), 321–339.

Larkin, M. a., Blackshields, G., Brown, N. P., Chenna, R., McGettigan, P. a., McWilliam, H., Valentin, F., Wallace, I. M., Wilm, A., Lopez, R., Thompson, J. D., Gibson, T. J. and Higgins, D. G. (2007), 'Clustal W and Clustal X version 2.0.', *Bioinformatics (Oxford, England)* 23(21), 2947–48.

Lee, S.-B., Jung, S.-J., Go, Y.-S., Kim, H.-U., Kim, J.-K., Cho, H.-J., Park, O. K. and Suh, M.-C. (2009), 'Two Arabidopsis 3-ketoacyl CoA synthase genes, KCS20 and KCS2/DAISY, are functionally redundant in cuticular wax and root suberin biosynthesis, but differentially controlled by osmotic stress.', *The Plant journal : for cell and molecular biology* 60(3), 462–475.

Li-Beisson, Y. (2011), 'Cutin and Suberin', *eLS* 2011(March).

Li, Y., Beisson, F., Koo, A. J. K., Molina, I., Pollard, M. and Ohlrogge, J. (2007), 'Identification of acyltransferases required for cutin biosynthesis and production of cutin with suberin-like monomers.', *Proceedings of the National Academy of Sciences of the United States of America* 104(46), 18339–44.

Manske, M. (2006), GENtle, a free multi-purpose molecular biology tool, PhD thesis, Universität Köln.

McFarlane, H. E., Shin, J. J. H., Bird, D. a. and Samuels, a. L. (2010), 'Arabidopsis ABCG transporters, which are required for export of diverse cuticular lipids, dimerize in different combinations.', *The Plant cell* 22(9), 3066–75.

Millar, A. A., Clemens, S., Zachgo, S., Giblin, E. M., Taylor, D. C. and Kunst, L. (1999), 'CUT1, an Arabidopsis gene required for cuticular wax biosynthesis and pollen fertility, encodes a very-long-chain fatty acid condensing enzyme.', *The Plant cell* 11(5), 825–838.

Miyamoto, N., Steudle, E., Hirasawa, T. and Lafitte, R. (2001), 'Hydraulic conductivity of rice roots', *Journal of Experimental Botany* 52(362), 1835–46.

Molina, I., Bonaventure, G., Ohlrogge, J. and Pollard, M. (2006), 'The lipid polyester composition of Arabidopsis thaliana and Brassica napus seeds.', *Phytochemistry* 67(23), 2597–610.

Molina, I. and Franke, R. (2013), Biosynthesis of Suberin Polyesters, *in* 'The Arabidopsis book / Acyl-lipid metabolism', Vol. 8, American Society of Plant Biologists, chapter 2.10., pp. 24–26.

Molina, I., Li-beisson, Y., Beisson, F., Ohlrogge, J. B. and Pollard, M. (2009), 'Identification of an Arabidopsis feruloyl-coenzyme A transferase required for suberin synthesis.', *Plant physiology* 151(3), 1317–28.

Nagahashi, G., Thomson, W. W. and Leonard, R. T. (1974), 'The casparian strip as a barrier to the movement of lanthanum in corn roots.', *Science* 183(4125), 670–671.

Naseer, S., Lee, Y., Lapierre, C., Franke, R., Nawrath, C. and Geldner, N. (2012), 'Casparian strip diffusion barrier in Arabidopsis is made of a lignin polymer without suberin.', *Proceedings of the National Academy of Sciences of the United States of America* 109(25), 10101–6.

Nawrath, C., Schreiber, L., Franke, R. B., Geldner, N., Reina-Pinto, J. J. and Kunst, L. (2013), 'Apoplastic diffusion barriers in Arabidopsis', *The Arabidopsis book / American Society of Plant Biologists* 11, e0167.

Nelson, D. R., Ming, R., Alam, M. and Schuler, M. a. (2008), 'Comparison of Cytochrome P450 Genes from Six Plant Genomes', *Tropical Plant Biology* 1(3-4), 216–235.

Nelson, D. R., Schuler, M. A., Paquette, S. M., Werck-Reichhart, D. and Bak, S. r. (2004), 'Comparative genomics of rice and Arabidopsis. Analysis of 727 cytochrome P450 genes and pseudogenes from a monocot and a dicot', *Plant Physiology* 135(June), 756–772.

Nishiuchi, S., Yamauchi, T., Takahashi, H., Kotula, L. and Nakazono, M. (2012), 'Mechanisms for coping with submergence and waterlogging in rice', *Rice* 5(1), 2.

Nosbüsch, D. (2009), Untersuchung des β-Ketoacyl-CoA Synthase-Gens At4g34510 in Arabidopsis thaliana, diploma thesis, University of Bonn.

Ouyang, S., Zhu, W., Hamilton, J., Lin, H., Campbell, M., Childs, K., Thibaud-Nissen, F., Malek, R. L., Lee, Y., Zheng, L., Orvis, J., Haas, B., Wortman, J. and Buell, C. R. (2007), 'The TIGR Rice Genome Annotation Resource: improvements and new features.', *Nucleic acids research* 35(Database issue), D883–7.

Pereira, H. (1988), 'Chemical composition and variability of cork from Quercus suber L.', *Wood Science and Technology* 22(3), 211–218.

Pereira, H. (2013), 'Variability of the Chemical Composition of Cork', *BioResources* 8(2), 2246–56.

Pollard, M., Beisson, F., Li, Y. and Ohlrogge, J. B. (2008), 'Building lipid barriers: biosynthesis of cutin and suberin', *Trends in plant science* 13(5), 236–246.

Ranathunge, K. (2005), The role of the apoplastic transport barriers for radial water and ion uptake in rice (Oryza sativa L.) and corn (Zea mays L.) roots, PhD thesis, Universität Bayreuth.

Ranathunge, K., Lin, J., Steudle, E. and Schreiber, L. (2011a), 'Stagnant deoxygenated growth enhances root suberization and lignifications, but differentially affects water and NaCl permeabilities in rice (Oryza sativa L.) roots', *Plant, cell & environment* 34(8), 1223–40.

Ranathunge, K., Schreiber, L. and Franke, R. (2011b), 'Suberin research in the genomics era–new interest for an old polymer.', *Plant science : an international journal of experimental plant biology* 180(3), 399–413.

Reinhardt, D. and Rost, T. L. (1995), 'Salinity accelerates endodermal development and induces an exodermis in cotton seedling roots', *Environmental and Experimental Botany* 35(4), 563–574.

Sato, Y., Namiki, N., Takehisa, H., Kamatsuki, K., Minami, H., Ikawa, H., Ohyanagi, H., Sugimoto, K., Itoh, J.-I., Antonio, B. a. and Nagamura, Y. (2013), 'RiceFREND: a platform for retrieving coexpressed gene networks in rice.', *Nucleic acids research* 41(Database issue), D1214–21.

Schreiber, L. (1996), 'Chemical composition of Casparian strips isolated from Clivia miniata Reg. roots: evidence for lignin', *Planta* 199(4), 596–601.

Schreiber, L. and Franke, R. (2011), 'Endodermis and exodermis in roots', *eLS* pp. 1–7.

Schreiber, L., Franke, R., Hartmann, K.-D., Ranathunge, K. and Steudle, E. (2005), 'The chemical composition of suberin in apoplastic barriers affects radial hydraulic conductivity differently in the roots of rice (Oryza sativa L. cv. IR64) and corn (Zea mays L. cv. Helix).', *Journal of experimental botany* 56(415), 1427–36.

Schreiber, L., Hartmann, K., Skrabs, M. and Zeier, J. (1999), 'Apoplastic barriers in roots: chemical composition of endodermal and hypodermal cell walls', *Journal of Experimental Botany* 50(337), 1267–1280.

Schuler, M. a., Duan, H., Bilgin, M. and Ali, S. (2006), 'Arabidopsis cytochrome P450s through the looking glass: a window on plant biochemistry', *Phytochemistry Reviews* 5(2-3), 205–237.

Schuler, M. A. and Rupasinghe, S. G. (2010), Comparisons Between Oryza and Arabidopsis P450s, *in* 'Advances in Botanical Research, Band 60', Advances in botanical research, Elsevier Science, chapter Molecular, pp. 288–291.

Schuler, M. a. and Werck-Reichhart, D. (2003), 'Functional genomics of P450s.', *Annual review of plant biology* 54, 629–67.

Serra, O., Soler, M., Hohn, C., Franke, R., Schreiber, L., Prat, S., Molinas, M. and Figueras, M. (2009), 'Silencing of StKCS6 in potato periderm leads to reduced chain lengths of suberin and wax compounds and increased peridermal transpiration.', *Journal of experimental botany* 60(2), 697–707.

Shi, T., Schönherr, J. and Schreiber, L. (2005), 'Accelerators increase permeability of cuticles for the lipophilic solutes metribuzin and iprovalicarb but not for hydrophilic methyl glucose', *Journal of agricultural and food chemistry* 53(7), 2609–15.

Shiono, K., Ogawa, S., Yamazaki, S., Isoda, H., Fujimura, T., Nakazono, M. and Colmer, T. D. (2011), 'Contrasting dynamics of radial O2-loss barrier induction and aerenchyma formation in rice roots of two lengths.', *Annals of botany* 107(1), 89–99.

Sijmons, P. C., Kolattukudy, P. E. and Bienfait, H. F. (1985), 'Iron Deficiency Decreases Suberization in Bean Roots through a Decrease in Suberin-Specific Peroxidase Activity.', *Plant physiology* 78(1), 115–20.

Soler, M., Serra, O., Molinas, M., Huguet, G., Fluch, S. and Figueras, M. (2007), 'A genomic approach to suberin biosynthesis and cork differentiation.', *Plant physiology* 144(1), 419–31.

Steudle, E. and Peterson, C. a. (1998), 'How does water get through roots?', *Journal of Experimental Botany* 49(322), 775–788.

Tamura, K., Peterson, D., Peterson, N., Stecher, G., Nei, M. and Kumar, S. (2011), 'MEGA5: molecular evolutionary genetics analysis using maximum likelihood, evolutionary distance, and maximum parsimony methods.', *Molecular biology and evolution* 28(10), 2731–39.

Thomas, R., Fang, X., Ranathunge, K., Anderson, T. R., Peterson, C. a. and Bernards, M. a. (2007), 'Soybean root suberin: anatomical distribution, chemical composition, and relationship to partial resistance to Phytophthora sojae.', *Plant physiology* 144(1), 299–311.

Todd, J., Post-Beittenmiller, D. and Jaworski, J. G. (1999), 'KCS1 encodes a fatty acid elongase 3-ketoacyl-CoA synthase affecting wax biosynthesis in Arabidopsis thaliana.', *The Plant journal : for cell and molecular biology* 17(2), 119–130.

Turner, J. W., Hartman, B. E. and Hatcher, P. G. (2013), 'Structural characterization of suberan isolated from river birch (Betula nigra) bark', *Organic Geochemistry* 57(4), 41–53.

Untergasser, A., Cutcutache, I., Koressaar, T., Ye, J., Faircloth, B. C., Remm, M. and Rozen, S. G. (2012), 'Primer3 - new capabilities and interfaces', *Nucleic acids research* 40(15), e115.

Ureshi, A.-n., Matuda, S., Ohashi, E., Onishi, K., Takamure, I. and Kato, K. (2012), 'The rice RCN1/OsABCG5 mutation is associated with root de-velopment in response to nutrient shortage', *Plant Root* 6, 28–35.

Wang, H., Qi, M. and Cutler, a. J. (1993), 'A simple method of preparing plant samples for PCR', *Nucleic acids research* 21(17), 4153–4.

Watanabe, K., Nishiuchi, S., Kulichikhin, K. and Nakazono, M. (2013), 'Does suberin accumulation in plant roots contribute to waterlogging tolerance?', *Frontiers in plant science* 4(6), 178.

Wehler, R. D. (2013), Physiological and analytical characterization of rice varieties under drought conditions, master thesis, University of Bonn.

Xiao, F., Goodwin, S. M., Xiao, Y., Sun, Z., Baker, D., Tang, X., Jenks, M. a. and Zhou, J.-M. (2004), 'Arabidopsis CYP86A2 represses Pseudomonas syringae type III genes and is required for cuticle development.', *The EMBO journal* 23(14), 2903–13.

Yamauchi, T., Shimamura, S., Nakazono, M. and Mochizuki, T. (2013), 'Aerenchyma formation in crop species: A review', *Field Crops Research* 152(10), 8–16.

Yang, W., Pollard, M., Li-Beisson, Y., Beisson, F., Feig, M. and Ohlrogge, J. (2010), 'A distinct type of glycerol-3-phosphate acyltransferase with sn-2 preference and phosphatase activity producing 2-monoacylglycerol.', *Proceedings of the National Academy of Sciences of the United States of America* 107(26), 12040–5.

Yang, W., Simpson, J. P., Li-Beisson, Y., Beisson, F., Pollard, M. and Ohlrogge, J. B. (2012), 'A land-plant-specific glycerol-3-phosphate acyltransferase family in Arabidopsis: substrate specificity, sn-2 preference, and evolution', *Plant physiology* 160(2), 638–52.

Yasuno, N., Takamure, I., Kidou, S.-i., Tokuji, Y., Ureshi, A.-n., Funabiki, A., Ashikaga, K., Yamanouchi, U., Yano, M. and Kato, K. (2009), 'Rice shoot branching requires an ATP-binding cassette subfamily G protein.', *The New phytologist* 182(1), 91–101.

Yeats, T. H., Martin, L. B. B., Viart, H. M.-F., Isaacson, T., He, Y., Zhao, L., Matas, A. J., Buda, G. J., Domozych, D. S., Clausen, M. H. and Rose, J. K. C. (2012), 'The identification of cutin synthase: formation of the plant polyester cutin.', *Nature chemical biology* 8(7), 609–11.

Yu, D., Ranathunge, K., Huang, H., Pei, Z., Franke, R., Schreiber, L. and He, C. (2008), 'Wax Crystal-Sparse Leaf1 encodes a beta-ketoacyl CoA synthase involved in biosynthesis of cuticular waxes on rice leaf', *Planta* 228(4), 675–85.

Zeier, J. and Schreiber, L. (1998), 'Comparative investigation of primary and tertiary endodermal cell walls isolated from the roots of five monocotyledoneous species: chemical composition in relation to fine structure', *Planta* (206), 349–361.

Zimmermann, H., Hartmann, K., Schreiber, L. and Steudle, E. (2000), 'Chemical composition of apoplastic transport barriers in relation to radial hydraulic conductivity of corn roots (Zea mays L.)', *Planta* 210(2), 302–311.

Zimmermann, H. and Steudle, E. (1998), 'Apoplastic transport across young maize roots: effect of the exodermis', *Planta* 206(1), 7–19.

List of Figures

List of Tables

8 Supplemental

8.1 *In silico* studies

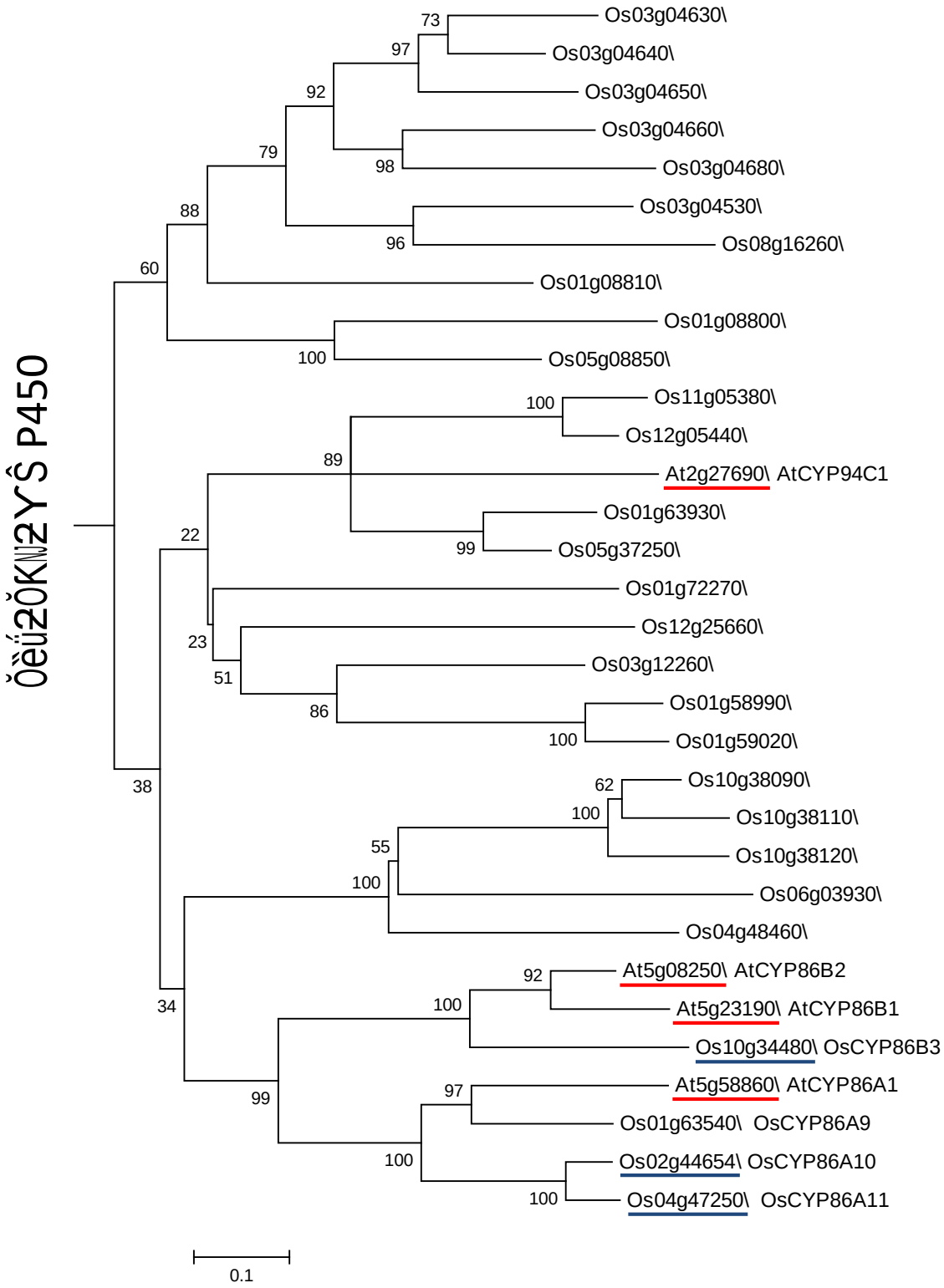

Figure 8.1: Neighbor-joining phylogram of protein sequences from members of the cytochrome P450 protein family with bootstrap values. *A. thaliana* proteins used initially for blastp analysis are underlined in red and closest related suberin candidates in *O. sativa* in blue.

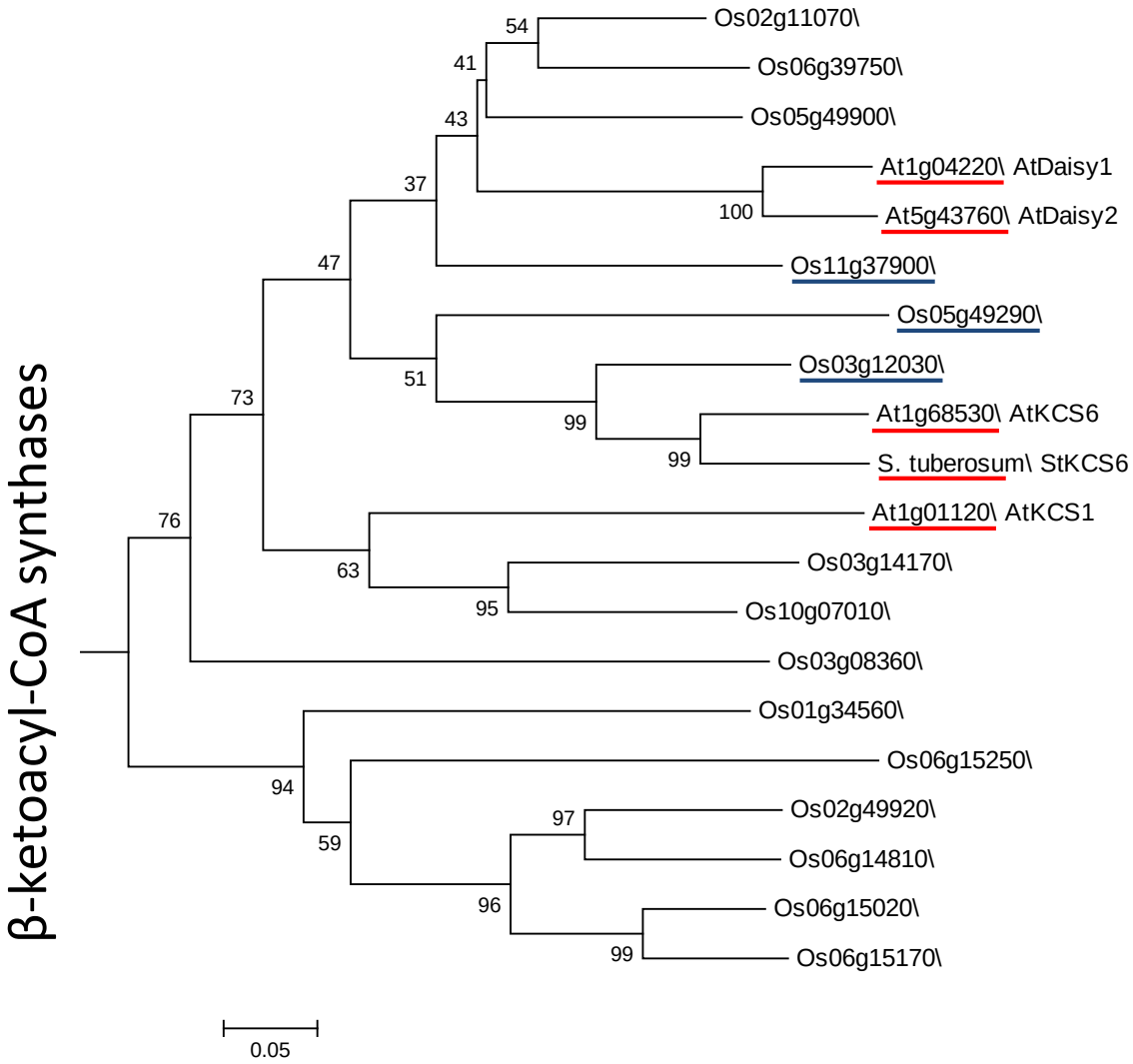

Figure 8.2: Neighbor-joining phylogram of protein sequences from members of the β-ketoacyl-CoA synthase protein family with bootstrap values. *A. thaliana* proteins used initially for blastp analysis are underlined in red and closest related suberin candidates in *O. sativa* in blue.

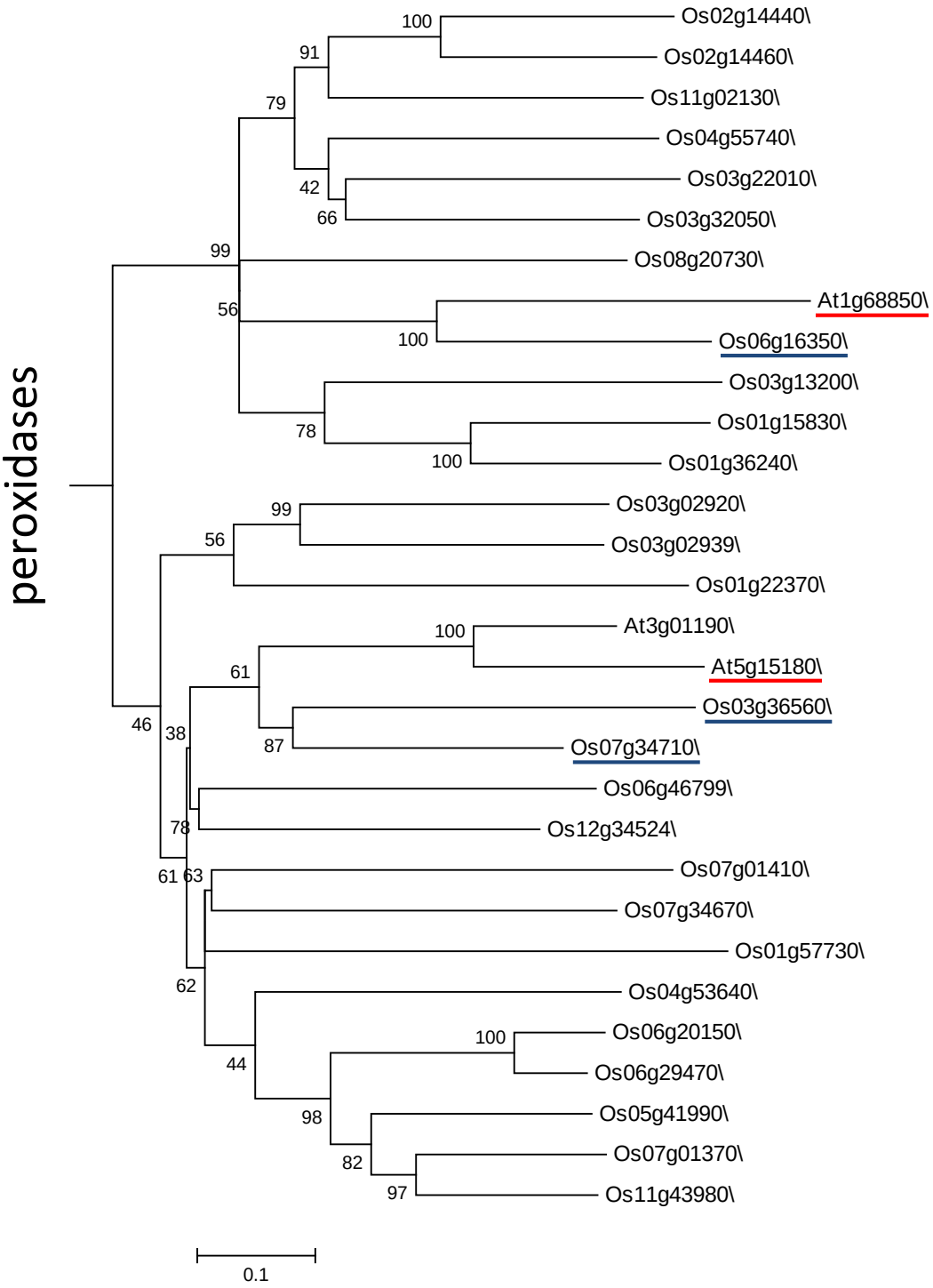

Figure 8.3: Neighbor-joining phylogram of protein sequences from members of the peroxidase protein family with bootstrap values. *A. thaliana* proteins used initially for blastp analysis are underlined in red and closest related suberin candidates in *O. sativa* in blue.

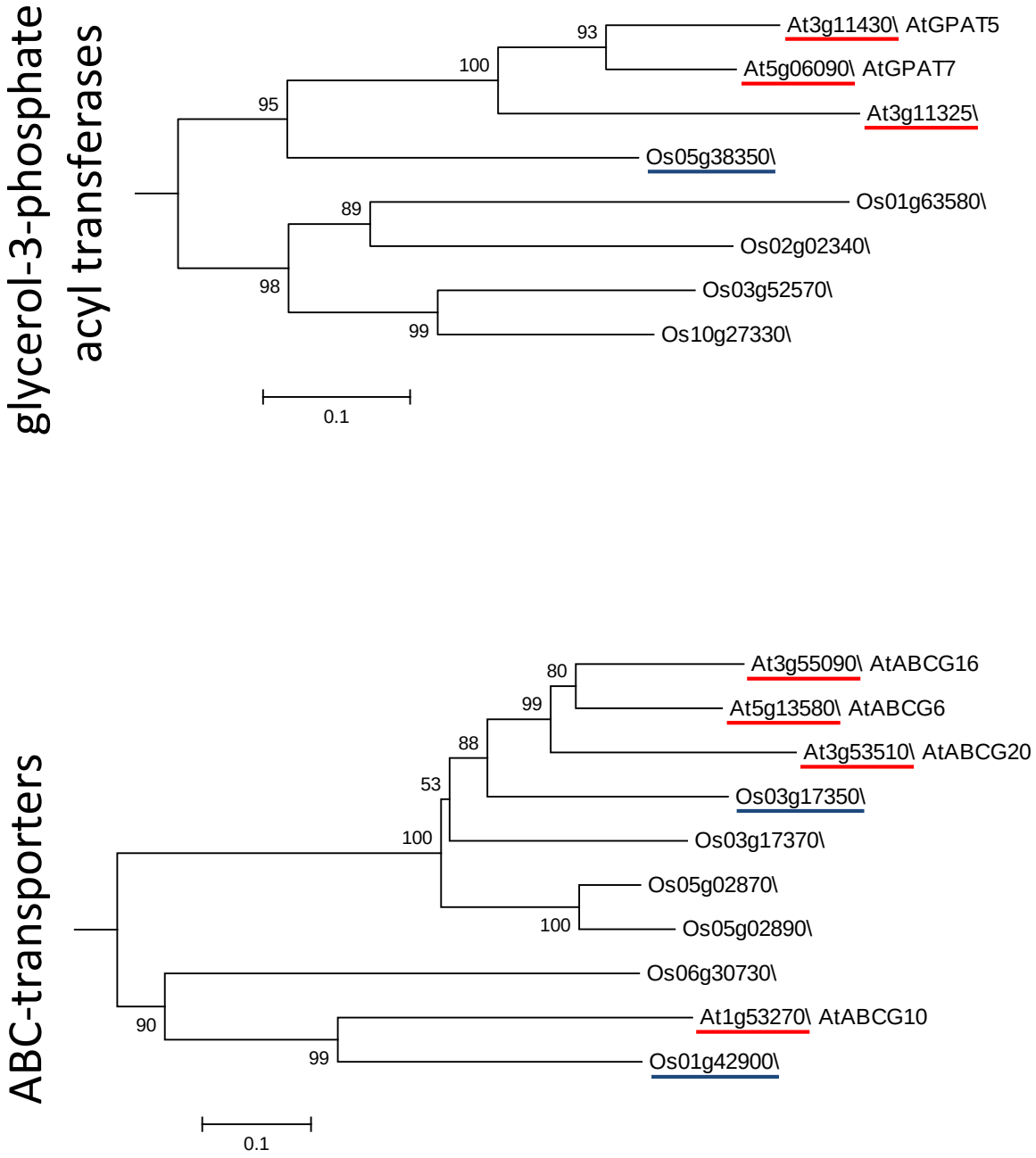

Figure 8.4: Neighbor-joining phylogram of protein sequences from members of the families glycerol-3-phosphate acyltransferases and ABC-transporters with bootstrap values. *A. thaliana* proteins used initially for blastp analysis are underlined in red and closest related suberin candidates in *O. sativa* in blue.

Table 8.1: Annotations of genes co-expressed with *CYP86B3* in *O. sativa* as visualised in the co-expression network in figure 4.1, built with the web tool RiceFREND (Sato et al., 2013) based on microarray data. With No. indicating the hierarchy in the network. Underlined are suberin candidate genes, as selected by amino acid sequence comparison, which were included in *in silico* studies in this work.

No.	LocusID	Description
0	LOC_Os10g34480	Similar to Cytochrome P450-like protein (CYP86B1)
1	LOC_Os05g38350	Similar to Glycerol-3-phosphate acyltransferase 5 (EC 2.3.1.15) (AtGPAT5)
1	LOC_Os10g37400	Protein of unknown function DUF538 family protein
2	LOC_Os03g57970	Plant lipid transfer/seed storage/trypsin-alpha amylase inhibitor domain containing protein
2	LOC_Os05g49900	Similar to Fatty acid elongase 1-like protein
2	LOC_Os05g50100	Conserved hypothetical protein
2	LOC_Os07g40830	Conserved hypothetical protein
2	LOC_Os07g40890	Conserved hypothetical protein
3	LOC_Os01g42380	PDR-like ABC transporter (PDR3 ABC transporter)
3	LOC_Os02g36870	Protein of unknown function DUF962 family protein
3	LOC_Os02g43660	Plastocyanin-like domain containing protein
3	LOC_Os03g04120	Similar to Adenosine monophosphate binding protein 1 AMPBP1
3	LOC_Os03g17350	ABC transporter related domain containing protein
3	LOC_Os03g57980	Plant lipid transfer/seed storage/trypsin-alpha amylase inhibitor domain containing protein
3	LOC_Os04g30490	Multi antimicrobial extrusion protein MatE family protein
3	LOC_Os04g51520	Similar to Xyloglucan endotransglycosylase (Fragment)
3	LOC_Os05g01030	Similar to Potential phospholipid-transporting ATPase 7 (EC 3.6.3.1) (Aminophospholipid flippase 7)
3	LOC_Os05g15630	Protein of unknown function DUF588 family protein
3	LOC_Os06g11450	Conserved hypothetical protein
3	LOC_Os06g16350	Similar to Peroxidase 11 precursor (EC 1.11.1.7) (Atperox P11) (ATP23a/ATP23b)
3	LOC_Os07g40860	Conserved hypothetical protein
3	LOC_Os07g40870	Similar to Surface protein PspC
3	LOC_Os07g48229	Similar to Vacuolar sorting receptor 1 precursor (AtVSR1) (Epidermal growth factor receptor-like protein 1) (AtELP1) (AtELP) (BP80-like protein b) (AtBP80b) (Spot 3 protein)
3	LOC_Os10g03400	Cellular retinaldehyde binding/alpha-tocopherol transport family protein

8.2 Genotyping

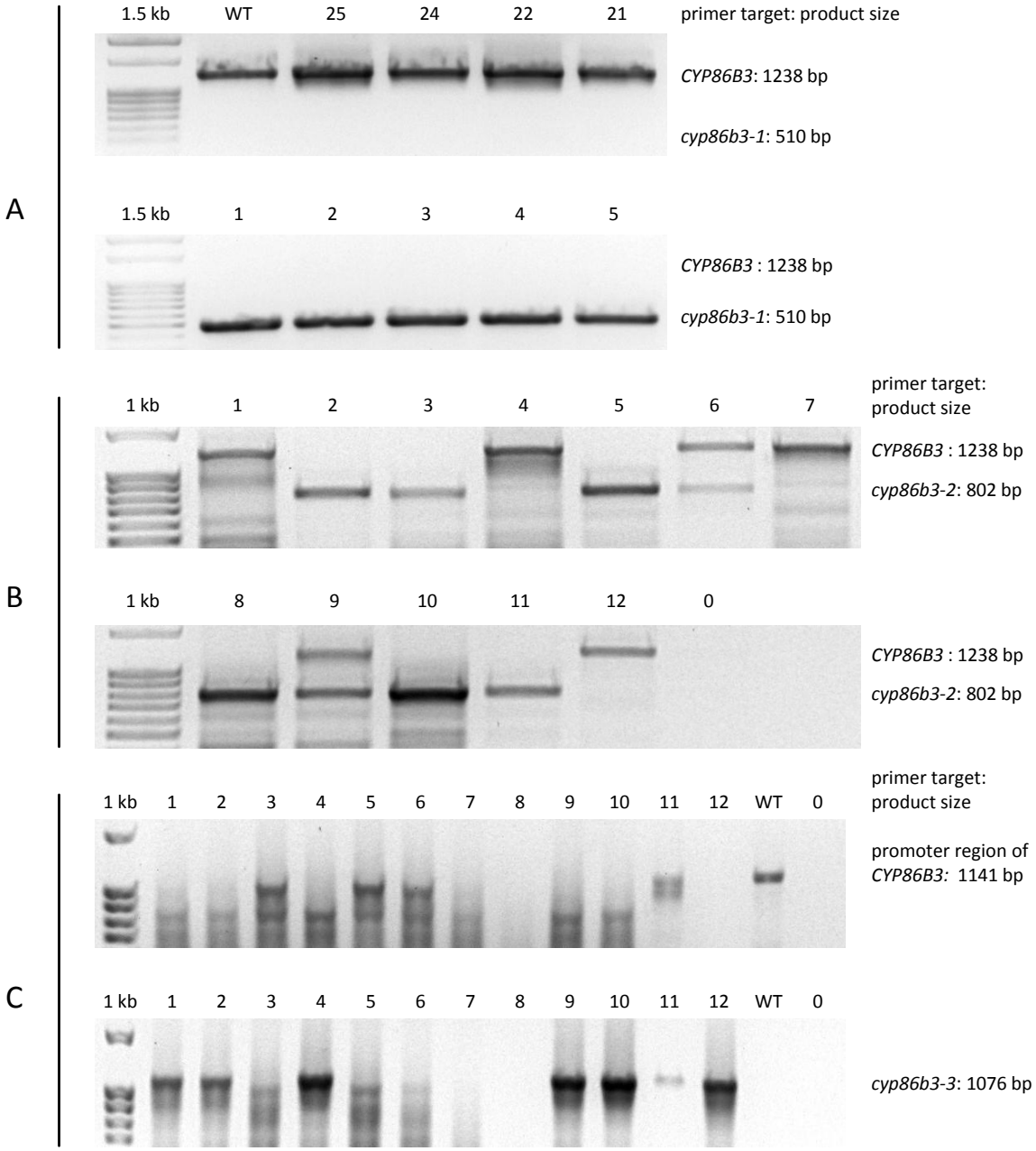

Figure 8.5: Genotyping of PFG T-DNA insertion mutants in LOC_Os10g34480 (*CYP86B3*). Competitive PCR with primer combinations for intron insertion: LS590, LS591 and LS592 (A) or LS593 (B) respectively. Primer combinations for promoter insertion: LS709 and LS708 (C, upper line) or LS594 (C, lower line) respectively. With 1 kb and 1.5 kb: depicted top band of the 100 bp DNA-ladder, extended; numbers: DNA template of respective plants; WT: positive control (Dongjin DNA); 0: negative control (H_2O_{HPLC}).

8.3 Result tables of chemical analyses

Table 8.2: Apical root suberin composition of homozygous KO plants *cyp86b3-1* and their Dongjin background (WT). Values reflect amounts of suberin monomers arranged according to substance class and carbon chain length in arithmetic means of four replicates from individual plants with standard deviation (SD) per root surface area. Sampling of the most apical 2–4 cm from root tip without laterals was conducted after cultivation in aerated hydroponics for 33 d. With OH: primary alcohol; -OH: hydroxy acid; numbers: carbon chain length; *t*-test: unpaired *t*-test with two-tailed distribution, significant differences are underlined. For the diagram see figure 3.8 A.

monomers	**WT** [$\mu g\,cm^{-2}$±SD]	***cyp86b3-1*** [$\mu g\,cm^{-2}$±SD]	***t*-test** α= 0.01
ALIPHATICS	**0.649±0.100**	**0.168±0.085**	**0.000**
alcohols	**0.020±0.010**	**0.018±0.010**	**0.790**
OH 18	0.020±0.010	0.018±0.010	0.790
α,ω-diacids	**0.005±0.002**	**0.000±0.000**	**0.003**
diacid 24	0.005±0.002	0.000±0.000	0.003
ω-OH acids	**0.405±0.083**	**0.013±0.007**	**0.000**
ω-OH 16	0.041±0.006	0.013±0.007	0.001
ω-OH 24	0.031±0.003	0.000±0.000	0.000
ω-OH 26	0.102±0.013	0.000±0.000	0.000
ω-OH 28	0.207±0.057	0.000±0.000	0.000
ω-OH 30	0.024±0.009	0.000±0.000	0.002
α-OH acids	**0.219±0.029**	**0.138±0.071**	**0.078**
α-OH 20	0.049±0.024	0.029±0.016	0.233
α-OH 24	0.074±0.025	0.048±0.026	0.206
α-OH 26	0.097±0.028	0.060±0.031	0.131
AROMATICS	**5.478±1.577**	**2.396±1.487**	**0.029**
coumaric	2.485±0.741	1.050±0.654	0.027
ferulic	2.993±0.836	1.346±0.835	0.032
TOTAL SUBERIN	**6.127±1.488**	**2.565±1.563**	**0.016**

Table 8.3: Basal root suberin composition of homozygous KO plants *cyp86b3-1* and their Dongjin background (WT). Values reflect amounts of suberin monomers arranged according to substance class and carbon chain length in arithmetic means of five replicates from individual plants with standard deviation (SD) per root surface area. Sampling of the basal 3–6 cm from root-shoot junction was conducted after cultivation in aerated hydroponics for 33 d. With -OH: hydroxy acid; numbers: carbon chain length; *t*-test: unpaired *t*-test with two-tailed distribution, significant differences are underlined. For the diagram see figure 3.8 B.

monomers	**WT** [$\mu g\,cm^{-2}$±SD]	***cyp86b3-1*** [$\mu g\,cm^{-2}$±SD]	***t*-test** α= 0.01
ALIPHATICS	**2.083±0.665**	**1.560±0.241**	**0.137**
α,ω-diacids	**0.029±0.019**	**0.022±0.008**	**0.468**
diacid 24	0.029±0.019	0.022±0.008	0.468
ω-OH acids	**1.662±0.541**	**0.415±0.082**	**0.001**
ω-OH 16	0.280±0.103	0.415±0.082	0.050
ω-OH 24	0.145±0.039	0.000±0.000	0.000
ω-OH 26	0.494±0.131	0.000±0.000	0.000
ω-OH 28	0.686±0.256	0.000±0.000	0.000
ω-OH 30	0.058±0.024	0.000±0.000	0.001
α-OH acids	**0.392±0.109**	**1.123±0.169**	**0.000**
α-OH 20	0.025±0.006	0.034±0.028	0.514
α-OH 24	0.130±0.028	0.423±0.070	0.000
α-OH 26	0.237±0.078	0.666±0.123	0.000
AROMATICS	**15.360±4.425**	**20.084±8.628**	**0.308**
coumaric	8.141±2.196	11.963±3.948	0.095
ferulic	7.219±2.230	8.121±5.497	0.743
TOTAL SUBERIN	**17.443±5.073**	**21.644±8.643**	**0.376**

Table 8.4: Root suberin composition of homozygous KO plants *cyp86b3-2* and their Dongjin background (WT). Values reflect amounts of suberin monomers arranged according to substance class and carbon chain length in arithmetic means of four (WT) and three (*cyp86b3-2*) replicates from individual plants with standard deviation per root surface area. Sampling was conducted after cultivation in aerated hydroponics for 27 d. With acid: monocarboxy fatty acid; OH: primary alcohol; -OH: hydroxy acid; numbers: carbon chain length; SD: standard deviation; *t*-test: unpaired *t*-test with two-tailed distribution, significant differences are underlined. For the diagram see figure 3.9.

monomers **apical**	**WT** [$\mu g\,cm^{-2}$±SD]	***cyp86b3-2*** [$\mu g\,cm^{-2}$±SD]	***t*-test** α= 0.01
ALIPHATICS	**1.861±0.217**	**1.472±0.342**	**0.149**
acids	**0.039±0.005**	**0.088±0.032**	**0.053**
acid 24	0.039±0.005	0.088±0.032	0.053
alcohols	**0.053±0.013**	**0.040±0.015**	**0.305**
OH 18	0.031±0.015	0.014±0.006	0.086
OH 24	0.022±0.001	0.026±0.017	0.712
α,ω-diacids	**0.006±0.006**	**0.000±0.000**	**0.090**
diacid 24	0.006±0.006	0.000±0.000	0.090
ω-OH acids	**0.600±0.073**	**0.162±0.045**	**0.000**
ω-OH 16	0.177±0.039	0.162±0.045	0.660
ω-OH 24	0.164±0.016	0.000±0.000	0.000
ω-OH 26	0.149±0.016	0.000±0.000	0.000
ω-OH 28	0.088±0.045	0.000±0.000	0.010
ω-OH 30	0.022±0.012	0.000±0.000	0.011
α-OH acids	**1.163±0.177**	**1.182±0.274**	**0.919**
α-OH 20	0.041±0.003	0.048±0.017	0.527
α-OH 22	0.054±0.011	0.062±0.010	0.347
α-OH 23	0.092±0.022	0.080±0.011	0.375
α-OH 24	0.521±0.048	0.580±0.137	0.515
α-OH 25	0.198±0.043	0.189±0.027	0.751
α-OH 26	0.257±0.058	0.223±0.083	0.574
AROMATICS	**24.412±11.746**	**20.949±3.683**	**0.593**
coumaric	15.567±7.771	13.014±2.687	0.558
ferulic	8.844±3.975	7.935±1.017	0.670
TOTAL SUBERIN	**26.273±11.956**	**22.421±3.353**	**0.556**

Table 8.5: Root free fatty acid methyl esters (FAME) of homozygous KO plants *cyp86b3-1* and their Dongjin background. Total lipid extract of ground roots, grown in aerated hydroponics for 33 d, arranged according to substance class and carbon chain length with number of double bonds if applicable. Values reflect arithmetic means of three (WT) and four (*cyp86b3-1*) replicates from individual plants with standard deviation in $\mu g\,cm^{-2}$ per root surface area. With FAME: free fatty acid methyl ester; TMS: trimethylsilyl; ω-OH: ω-hydroxy; α-OH: α-hydroxy; C-numbers: carbon chain length; *t*-test: unpaired *t*-test with two-tailed distribution, significant differences are underlined. For the diagram see figure 3.10.

aliphatics	**WT** [$\mu g\,cm^{-2}$±SD]	***cyp86b3-1*** [$\mu g\,cm^{-2}$±SD]	***t*-test** α= 0.01
acid methyl esters	**7.156±3.512**	**7.722±3.256**	**0.834**
acid methyl ester C14	0.023±0.005	0.020±0.008	0.565
acid methyl ester C16	2.489±0.466	2.030±0.858	0.446
acid methyl ester C17	0.048±0.006	0.042±0.017	0.605
acid methyl ester C18	0.156±0.025	0.133±0.056	0.540
acid methyl ester C18:3/2	3.917±3.225	4.350±1.814	0.828
acid methyl ester C19	0.008±0.002	0.010±0.004	0.356
acid methyl ester C20	0.049±0.007	0.056±0.027	0.659
acid methyl ester C20:1	0.034±0.004	0.029±0.014	0.610
acid methyl ester C20:2	0.015±0.003	0.009±0.004	0.074
acid methyl ester C22	0.032±0.004	0.033±0.015	0.978
acid methyl ester C23	0.065±0.009	0.055±0.023	0.538
acid methyl ester C24	0.178±0.024	0.240±0.111	0.398
acid methyl ester C26	0.086±0.002	0.333±0.146	0.035
acid methyl ester C28	0.050±0.006	0.335±0.141	0.019
acid methyl ester C30	0.007±0.006	0.046±0.020	0.026
acid TMS esters	**0.149±0.037**	**0.143±0.054**	**0.868**
acid TMS ester C16	0.043±0.014	0.042±0.017	0.923
acid TMS ester C18	0.024±0.004	0.026±0.011	0.782
acid TMS ester C18:1	0.017±0.004	0.016±0.006	0.865
acid TMS ester C18:3/2	0.065±0.017	0.059±0.021	0.680
alcohols	**0.048±0.009**	**0.061±0.026**	**0.456**
alcohol C18	0.005±0.002	0.005±0.002	0.801
alcohol C20	0.004±0.000	0.005±0.002	0.502
alcohol C22	0.002±0.000	0.004±0.002	0.375
alcohol C24	0.014±0.001	0.021±0.008	0.276
alcohol C26	0.012±0.001	0.012±0.005	0.970
alcohol C28	0.010±0.008	0.015±0.008	0.465

Continued on next page.

Continuation of Root FAME of homozygous KO plants *cyp86b3-1* and their Dongjin background.

aliphatics	**WT** [$\mu g\,cm^{-2}$±SD]	***cyp86b3-1*** [$\mu g\,cm^{-2}$±SD]	***t*-test** α= 0.01
ω-OH acid methyl esters	**0.445±0.040**	**0.027±0.013**	**0.000**
ω-OH acid methyl ester C20	0.014±0.002	0.019±0.010	0.499
ω-OH acid methyl ester C22	0.007±0.001	0.008±0.004	0.557
ω-OH acid methyl ester C24	0.046±0.017	0.000±0.000	0.002
ω-OH acid methyl ester C26	0.241±0.008	0.000±0.000	0.000
ω-OH acid methyl ester C28	0.136±0.015	0.000±0.000	0.000
α-OH acid methyl esters	**0.477±0.069**	**0.429±0.210**	**0.723**
α-OH acid methyl ester C16	0.011±0.002	0.012±0.007	0.783
α-OH acid methyl ester C18	0.007±0.001	0.007±0.004	0.873
α-OH acid methyl ester C20	0.081±0.014	0.070±0.036	0.623
α-OH acid methyl ester C22	0.025±0.006	0.021±0.011	0.596
α-OH acid methyl ester C23	0.081±0.011	0.081±0.035	0.999
α-OH acid methyl ester C24	0.186±0.025	0.148±0.076	0.453
α-OH acid methyl ester C25	0.037±0.002	0.047±0.021	0.439
α-OH acid methyl ester C26	0.049±0.011	0.043±0.022	0.705
TOTAL FAME	**8.275±3.560**	**8.381±3.556**	**0.970**

Table 8.6: Root suberin composition of *A. thalina* WT Col-8, KO *ralph* and the corresponding line complemented with CDS *CYP86B3*. Values reflect amounts of suberin monomers arranged according to substance class and carbon chain length in arithmetic means of four replicates from individual plants (three for Col-8, one for *ralph*::p*Ralph*:CDS *CYP86B3*) with standard deviation per dw. Significant differences to values in next column to the left are underlined ($\alpha = 0.01$, unpaired t-test with two-tailed distribution). With acid: monocarboxy fatty acid; alcohol: primary alcohol; α,ω-diacid: α,ω-dicarboxylic acid; -OH: -hydroxy; numbers: carbon chain length. For the diagram see figure 3.20 A.

SUBERIN MONOMERS	**Col-8** [$\mu g\,mg^{-1}$±SD]	***ralph*** [$\mu g\,mg^{-1}$±SD]	**complemented** [$\mu g\,mg^{-1}$] n = 1
acids	**0.707±0.076**	**1.068±0.059**	**1.202**
acid C18	0.030±0.002	0.037±0.006	0.078
acid C20	0.100±0.008	0.130±0.007	0.089
acid C22	0.428±0.064	0.706±0.053	0.856
acid C24	0.149±0.023	0.194±0.007	0.180
alcohols	**0.252±0.029**	**0.342±0.024**	**0.217**
alcohol C18	0.101±0.009	0.127±0.010	0.119
alcohol C20	0.106±0.015	0.156±0.018	0.000
alcohol C22	0.045±0.009	0.060±0.013	0.099
α,ω-diacids	**0.650±0.033**	**0.698±0.113**	**1.044**
α,ω-diacid C16	0.035±0.009	0.037±0.014	0.085
α,ω-diacid C18	0.094±0.016	0.122±0.006	0.141
α,ω-diacid C18:1	0.479±0.037	0.503±0.111	0.769
α,ω-diacid C20	0.042±0.011	0.036±0.012	0.048
ω-OH acids	**1.778±0.071**	**1.436±0.108**	**1.718**
ω-OH acid C16	0.235±0.011	0.239±0.014	0.214
ω-OH acid C18	0.059±0.007	0.052±0.032	0.124
ω-OH acid C18:1	0.955±0.081	1.013±0.055	0.927
ω-OH acid C20	0.120±0.036	0.114±0.008	0.090
ω-OH acid C22	0.364±0.015	0.018±0.015	0.310
ω-OH acid C24	0.046±0.003	0.000±0.000	0.052
α-OH acids	**2.320±0.343**	**2.173±0.087**	**1.768**
α-OH acid C16	0.082±0.014	0.073±0.005	0.060
α-OH acid C20	0.155±0.136	0.054±0.037	0.252
α-OH acid C22	0.261±0.045	0.253±0.017	0.170
α-OH acid C23	0.074±0.026	0.062±0.005	0.091
α-OH acid C24	1.191±0.067	1.230±0.056	0.729
α-OH acid C24:1	0.261±0.012	0.286±0.022	0.132
α-OH acid C25	0.114±0.093	0.030±0.043	0.247
α-OH acid C26	0.184±0.012	0.186±0.013	0.087
TOTAL SUBERIN	**5.707±0.183**	**5.716±0.131**	**5.950**

Table 8.7: Root suberin composition of *A. thalina* WT Col-8, double KO *ralph*/*horst* and the corresponding line complemented with CDS *CYP86B3*. Values reflect amounts of suberin monomers arranged according to substance class and carbon chain length in arithmetic means of four replicates from individual plants with standard deviation per dw. Significant differences to values in next column to the left are underlined ($\alpha = 0.01$, unpaired t-test with two-tailed distribution). With acid: monocarboxy fatty acid; alcohol: primary alcohol; α,ω-diacid: α,ω-dicarboxylic acid; -OH: -hydroxy; numbers: carbon chain length. For the diagram see figure 3.20 B.

SUBERIN MONOMERS	**Col-8** [µg mg^{-1}±SD]	***ralph*/*horst*** [µg mg^{-1}±SD]	**complemented** [µg mg^{-1}±SD]
acids	**0.707±0.076**	**0.711±0.063**	**0.571±0.079**
acid C18	0.030±0.002	0.038±0.005	0.070±0.055
acid C20	0.100±0.008	0.108±0.009	0.064±0.010
acid C22	0.428±0.064	0.411±0.064	0.316±0.105
acid C24	0.149±0.023	0.154±0.025	0.120±0.021
alcohols	**0.252±0.029**	**0.295±0.019**	**0.239±0.021**
alcohol C18	0.101±0.009	0.127±0.006	0.084±0.010
alcohol C20	0.106±0.015	0.117±0.013	0.112±0.006
alcohol C22	0.045±0.009	0.051±0.013	0.043±0.029
α,ω-diacids	**0.650±0.033**	**0.182±0.028**	**0.214±0.033**
α,ω-diacid C16	0.035±0.009	0.037±0.008	0.073±0.037
α,ω-diacid C18	0.094±0.016	0.010±0.020	0.000±0.000
α,ω-diacid C18:1	0.479±0.037	0.135±0.019	0.141±0.025
α,ω-diacid C20	0.042±0.011	0.000±0.000	0.000±0.000
ω-OH acids	**1.778±0.071**	**0.384±0.034**	**0.572±0.182**
ω-OH acid C16	0.235±0.011	0.070±0.005	0.072±0.008
ω-OH acid C18	0.059±0.007	0.015±0.018	0.022±0.025
ω-OH acid C18:1	0.955±0.081	0.294±0.017	0.245±0.080
ω-OH acid C20	0.120±0.036	0.005±0.006	0.020±0.015
ω-OH acid C22	0.364±0.015	0.000±0.000	0.193±0.121
ω-OH acid C24	0.046±0.003	0.000±0.000	0.019±0.028
α-OH acids	**2.320±0.343**	**2.124±0.045**	**1.837±0.379**
α-OH acid C16	0.082±0.014	0.071±0.002	0.071±0.024
α-OH acid C20	0.155±0.136	0.076±0.028	0.143±0.078
α-OH acid C22	0.261±0.045	0.241±0.033	0.206±0.041
α-OH acid C23	0.074±0.026	0.063±0.006	0.068±0.057
α-OH acid C24	1.191±0.067	1.189±0.024	1.001±0.223
α-OH acid C24:1	0.261±0.012	0.277±0.020	0.209±0.070
α-OH acid C25	0.114±0.093	0.030±0.023	0.042±0.032
α-OH acid C26	0.184±0.012	0.177±0.005	0.097±0.066
TOTAL SUBERIN	**5.707±0.183**	**3.695±0.158**	**3.433±0.621**

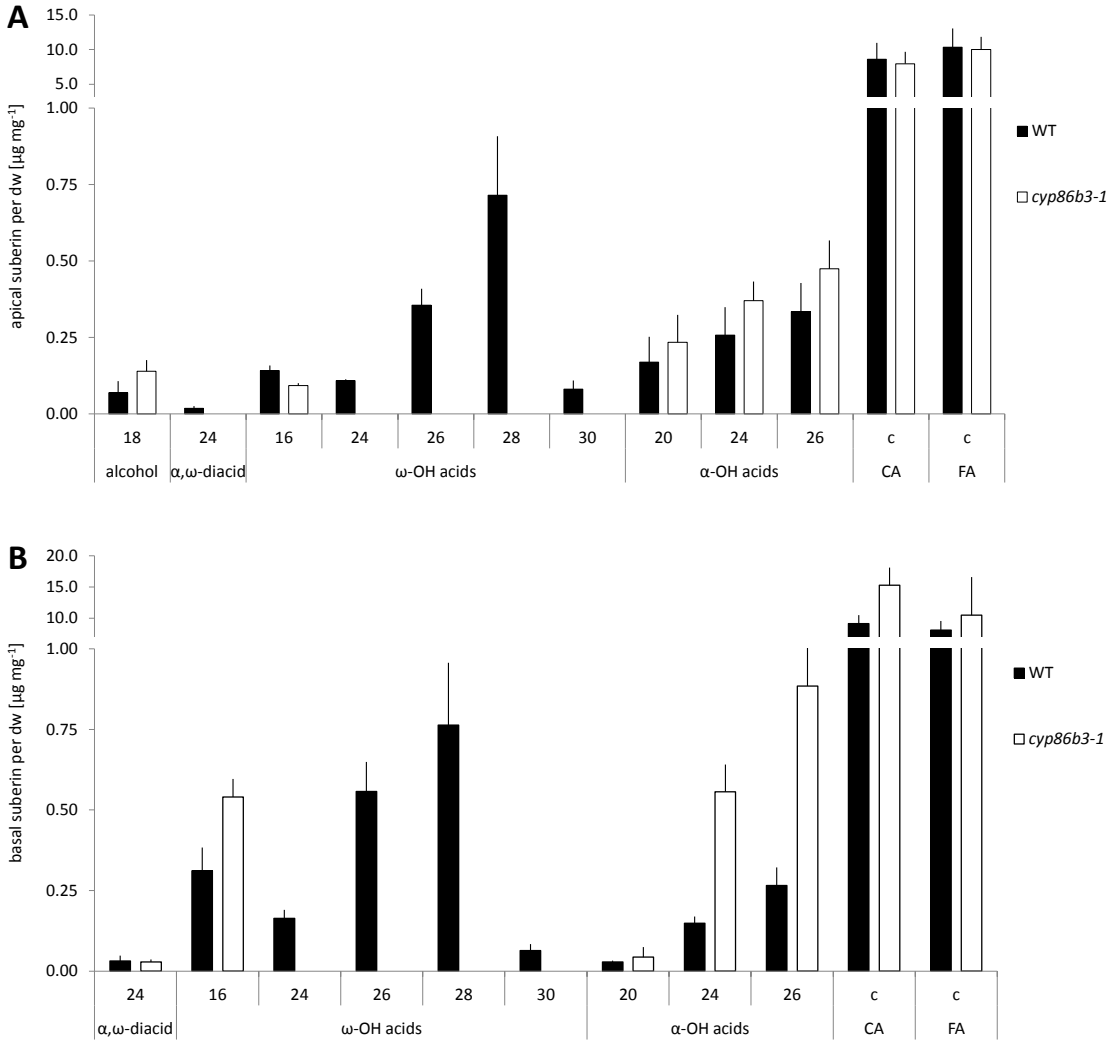

Figure 8.6: Apical (A) and basal (B) root suberin composition of homozygous KO plants *cyp86b3-1* and their Dongjin background. Chemical transesterification and subsequent GC-FID analysis revealed a complete loss of ω-hydroxy acids with chain length of C24 and higher in *cyp86b3-1*. Depicted are amounts of suberin monomers arranged according to substance class and carbon chain length. Bars reflect arithmetic means of four (A) and five (B) replicates respectively from individual plants with 95 % CI in µg mg^{-1} dw. Sampling of the most apical 2-4 cm from root tip without laterals (A) and the basal 3-6 cm from root-shoot junction (B) was conducted after cultivation in aerated hydroponics for 33 d. With dw: dry weight; α,ω-diacid: α,ω-dicarboxylic acid; ω-OH: ω-hydroxy; α-OH: α-hydroxy; c: cyclic/aromatic substance; CA: coumaric acid; FA: ferulic acid. For the suberin amounts of *cyp86b3-1* related to root surface area see figure 3.8.

Acknowledgment

Special thanks go to

- my thesis advisor Prof. Dr. Lukas Schreiber, who received me in the pleasant atmosphere of his work group, for his support and advice as well as the opportunity and freedom to work on this topic
- my second advisor Dr. Rochus Franke for his support, countless helpful suggestions on lab issues and valuable discussions far beyond those
- Prof. Dr. Gynheung An and Dr. Jongjin Park (Plant Functional Genomics Institute at POSTECH University, Pohang, Korea) who kindly provided the T-DNA insertion lines examined in this work
- Prof. Dr. Mikio Nakazono (Laboratory of Plant Genetics and Breeding, Nagoya University, Japan) and his work group, especially
  Nishiuchi Shunsaku for the generation of transgenic rice lines and
  Kohtaro Watanabe who kindly measured ROL in *cyp86b3-1*
- Prof. Dr. Michael Frei (Institut für Nutzpflanzenwissenschaften und Ressourcenschutz, University of Bonn) for help with plant cultivation and
  Lin-Bo Wu in his work group for help with propagation and examination of iron stress response of *cyp86b3-1*
- Dr. Alexander Fleck (Institut für Pflanzenernährung, Leibniz Universität Hannover) for propagation of above mentioned lines
- all current and former members of the work group Ecophysiology for all their help, for taking me as I am and for being just who they are!
  particularly Dr. Kosala Ranathunge for introducing me to hydroponic cultures, root pressure probe, rice, roots, physiology and for lots of fun inside and outside the office,
  Dr. Katsuhiro Shiono for his help regarding *in silico* and wet lab research on rice,
  Sheron, Patrik and Daniela who introduced me to chemical analysis and molecular biological work
- Kati, who was my first tutor in this work group and finally married me, for proofreading of this work, for everything there was, is and will be and for what to describe would turn this work into a love letter.

Thank you!